Thermal management of the thermochemical Cu-Cl cycle linked with industrial processes for hydrogen production

By

Haris Ishaq

A Thesis Submitted in Partial Fulfilment
of the Requirements for the degree of
Master of Applied Science
in
Mechanical Engineering

Faculty of Engineering and Applied Science
University of Ontario Institute of Technology

Oshawa, Ontario, Canada

Abstract

This thesis study develops, analyzes and evaluates three integrated systems using process heats available in industrial applications for hydrogen production via copper-chlorine (Cu-Cl) cycle. The first system consists of single- and multi-stage reheat Rankine cycles, a four-step thermochemical Cu-Cl cycle, and a hydrogen compression system. Systems 2 consists of a thermochemical four-step hydrogen production Cu-Cl cycle, a hydrogen compression system and a multi-stage reheat Rankine cycle. System 3 contains single- and multi-stage reheat Rankine cycles, a thermochemical hydrogen production Cu-Cl cycle, a hydrogen compression system and a reverse osmosis desalination unit. Both Aspen Plus and Engineering Equation Solver software packages are employed for system analysis, modeling and performance assessment. The overall system energy and exergy efficiencies are found to be 39.8% and 40.5% for the first system, 32.7% and 32% for the second system, and 48.6% and 40.2% for the third system.

Keywords: Hydrogen production; thermal management; energy conversion; Cu-Cl cycle; heat recovery; Rankine cycle

Acknowledgments

I would like to express my most profound gratitude to my supervisor Professor Dr. Ibrahim Dincer and my co-supervisor Professor Dr. Greg Naterer for their admirable and exemplary guidance, tolerance and counseling. They provided me with the extraordinary and exceptional atmosphere for research.

I would like to thank my colleagues at UOIT for their assistance and support especially the people in my research room ACE3030B who helped me during the preparation of this thesis, especially Osamah Siddiqui, Ahmed Hasan, Maan Al-Zareer, Muhammad Izzat, Dr. Farrukh Khalid, Abdullah AlZahrani, Arda Yapicioglu, Huseyin Karasu and Murat Demir. I would also like to thank some of my close friends Bilal Umer, Osamah Siddiqui, Asad Ali and Muhammad Inam for their support during a hard time. A special thanks to my uncle Shahid Islam who always supported me in any manner.

I would like to express my gratitude to my parents and brothers for their never-ending support, inspiration, and encouragement throughout my life.

Table of Contents

List of Tables

List of Figures

Nomenclature

A	area (m^2)
Ėn	energy rate (kW)
ex	specific exergy (kJ/kg)
Ėx	exergy rate (kW)
$\dot{E}x_{dest}$	exergy destruction (kW)
h	specific enthalpy (kJ/kg)
HHV	higher heating value (kJ/kg)
LLV	lower heating value (kJ/kg)
$\dot{m}$	mass flow rate (kg/s)
n	number of moles
P	pressure (kPa)
Q	heat (kJ)
$\dot{Q}$	heat rate (kW)
R	gas constant (kJ/kmol K)
s	specific entropy (kJ/kg K)
$\dot{S}_{gen}$	Entropy generation rate (kW/K)
T	temperature (°C)
V	Volume
$\dot{W}$	Power or work rate (kW).

Greek letters

η	energy efficiency
ρ	density (kg/m^3)
ψ	exergy efficiency

Subscripts

0	ambient conditions
B#	block name in Aspen Plus
C	compressor
Cu-Cl	copper-chlorine cycle

Comp compressor

ch chemical

H_2 hydrogen

i input

ov overall

O_2 oxygen.

RC Rankine cycle

RO reverse osmosis

W work

Subscripts

ch chemical

d destruction

en energy

ex exergy

p pump

ph physical

Acronyms

CSPA Canadian Steel Producers Association

Cu-Cl Copper-Chlorine cycle

EAF Electric Arc Furnace

EES Engineering Equation Solver

HCS Hydrogen Compression System.

HEX Heat Exchanger

HPT High-Pressure Turbine

IEA International Energy Agency.

ITC International Technologies Consultants

LPT Low-Pressure Turbine

MSRC Multistage Reheat Rankine Cycle

RC Rankine Cycle

RO Reverse Osmosis

Chapter 1: Introduction

Energy is a key resource in wealth generation and economic development of countries. Major growth in the population and economic development is occurring around the world. Energy demand and availability are the two key factors which play an important part in bringing economic development.

1.1 Energy Needs and Challenges

The energy demand is increasing very quickly. Energy supply from different sources in past 25 years can be seen in Figure 1.1. The resources which covers this increase in energy demand are facing excessive challenges and also resulting in quick depletion of these resources. The major part of the energy demand is set to be covered by the fossil fuels, and this is the exact reason for faster depletion of fossil fuels. The main drawback while using fossil fuel is the emissions produced which results in many environmental problems and global warming [1]. With the deficiency of efficiently available fossil fuel resources and the environmental problems connected with it, some other sources like renewable energy sources are required which are viable and environmentally benign as well.

The main reason behind industrial and academic research efforts is global warming [2]. This has much importance regarding environmental impacts, which is somehow connected to social sustainability and economic sustainability [3].

Many methods like integrated power plants and running power plant at full capacity are being used to increase energy production efficiency through fossil fuels. Due to the variation in energy demands in day and night times, fixing a full capacity for the power plant will not be a suitable and practical solution if energy storage system is not being used.

Hydrogen receives a benefit of working as both energy carrier and energy storage system [5], and efficiency can be increased by operating the power plant at full capacity if excess energy is stored [6].

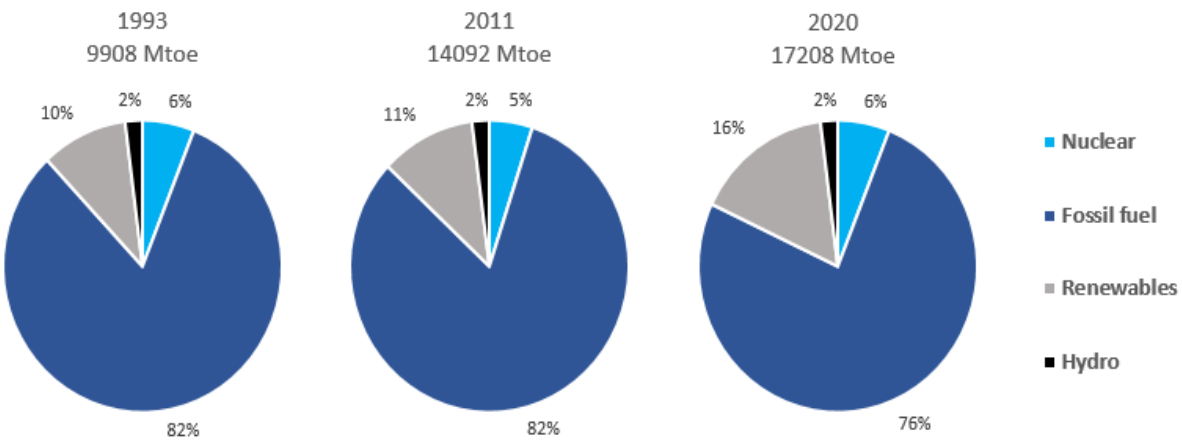

Figure 1.1 Energy supply by different sources (data from [4]).

Muradov and Veziroglu [7] worked the different methods to produce hydrogen as a green path from fossil fuels. Electrolysis is one of the leading methods, Cu-Cl cycle is also one of the encouraging and promising processes for hydrogen production. Producing hydrogen through one step from heat while skipping the intermediate step of converting heat into electricity is one of the leading advantages of hydrogen production through the thermochemical cycle. Hydrogen is produced from fossil fuels through many processes like biomass gasification, steam methane reforming, and coal gasification. Coal plays a vital role in the most abundant Fossil fuel worldwide in power production. Coal gasification is often coupled with power producing combined cycles. Presently, the higher portion of hydrogen is produced from coal worldwide [8].

The CO_2 emissions by blast furnace gases are plotted and compared in Figure 1.2. This emission data excludes the emissions during power generation. The highest relative amounts of CO_2 emissions occur in the iron and steel sectors, and also non-metallic mineral sector which accounts for 27% each. Then the chemical and petrochemical sector have 16% of the CO_2 emissions. The CO_2 emissions from various industrial sectors are shown in Figure 1.2.

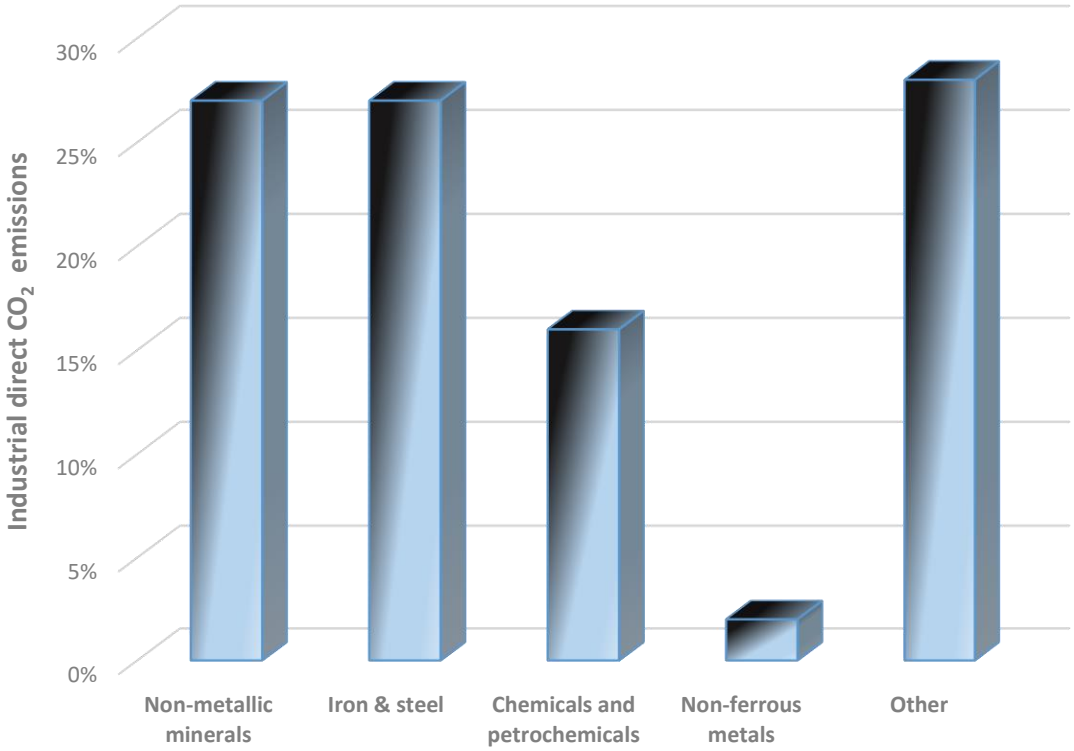

Figure 1.2 CO_2 emissions from blast furnace gas used by the iron and steel industry (data from [9]).

1.2 Waste heat sources

In this thesis, the terminology of "waste heat" will refer to exhaust gas streams from industrial processes which are emitted, to a lesser or greater extent, to the environment. Often a portion of this exhaust heat is recovered, in whole or in part, through other internal processes so that the temperature of the gas stream is reduced significantly before it is released to the environment. These internal recovery processes vary among different industrial processes, depending on the overall plant efficiency. Recent advances in energy conservation have significantly improved the efficiency of heat recovery processes in industry. Nevertheless, there are still significant remaining exhaust heat streams at the upper limits of temperature in the Cu-Cl cycle which are emitted to the environment as waste heat. In this thesis, it will be assumed that the exhaust gas streams from the industrial processes are primarily used for three integrated systems involving hydrogen, electricity and fresh water production.

The energy usage of different industries is described in Figure 1.3 in past 25 years. Steel, cement and glass industries occupy a huge part of total energy requirements, and these industries are also providing with the high amount of materials production. Currently, the leading industries with respect to the waste heat source temperatures are steel, cement and glass industries [10–13].

1.2.1 Steel Industry

Steel is considered as the basic building block worldwide. Many industries and appliances like automobiles, oil pipelines, appliances, buildings and bridges use steel as a base material. Steel manufacturing exists for centuries, and the steel making process continues to develop. Steel is produced by many ways in furnaces by melting different ores like scrap metal, iron ore or other additives. The molten metal from the furnace is solidified into partially finished shapes before being rolled in different shapes like beams, rod, sheets, wire, and tubing. Using scrap metal for making steel is the cheapest method. Many sources like automobiles, household appliances, and old bridges provide with the steel scrap which is then placed in a furnace, the extreme heat in furnace melts the scrap into molten steel [11].

1.2.2 Cement industry

Cement is synthesized by the controlled chemical composition of limestone, clays, silica, iron ore and slag. A rock-like substance is formed when this controlled composition is heated at very high temperatures which are then grounded into fine powder. Different processes are performed and started from quarry the mixture of raw materials and rocks are crushed after quarrying To manufacture the cement [14]. This is distributed into several stages. In the first step, rocks are crushed to 6 inches of maximum size. Then hammer mills reduce the rock size to 3 inches or less. This crushed rock is then mixed with other materials like fly ash and then entered in the cement kiln. These ingredients are then heated up to about 1500 degrees Celsius in the cement kiln. The finely grounded slurry is then fed into the top end. This slurry is then converted into clinker by passing through the kiln. Clinker is then entered in different coolers to obtain the handling temperature. The cooling of clinkers produces heated which is entered to the kilns, and this process saves fuel. After

passing through the cooling section, these clinkers are grinded and mixed with the small composition of limestone and gypsum. Cement then becomes ready for transport [10].

1.2.3 Glass industry

The glass manufacturing techniques are differentiated on the basis of manufacturing scale and scope and different specifications like specific product quality and ultimate compositions required. So glass manufacturing process is widely divided into two sections of the batch, and continuous process and both of these methods can be used for manufacturing common glasses like soda lime silicate glass and borosilicate. Glass quality basically depends upon many processing factors such as flexibility in design, volume, cost, and speed. The advantage of continuous processing is that raw material is continuously fed into the furnace which makes the production continuous [15,16].

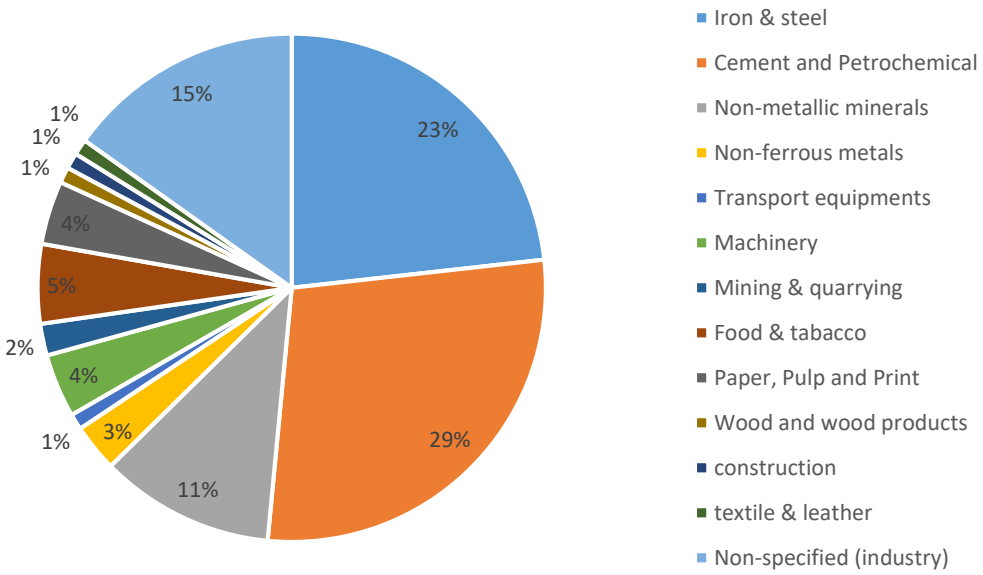

Figure 1.3 Energy usage of different industries (data from [12]).

1.3 Motivation

The various energy challenges which we are facing currently have some expectations from hydrogen to become a solid fuel and overcome these energy challenges. The main advantage behind this is because when hydrogen is oxidized, it does not eject the greenhouse gases and with this environmentally benign method, global warming is

controlled, and living species are not affected. Hydrogen can be used as a clean energy carrier and fuel as well if it is obtained through clear energy source. Some industries such as steel, cement, and glass are consuming a huge portion of total energy requirements and playing an important role in materials production while some flue gases are emitted by these industries. These exhaust gases are at very high temperatures and sometimes contains some emissions as well. Therefore, producing hydrogen from clean energy sources to solve the environmental issues and recovering the waste heat to produce hydrogen from clean energy methods is the motivation of this research. Three energy systems are introduced and analyzed during this research which should be able to produce clean hydrogen by recovering the industrial waste heat and environment friendly as well.

1.4 Objectives

In this study, a complete analysis of copper-chlorine cycle integrated with a different system is presented. The thermodynamic analysis and simulations of the systems proposed in this study are performed in Aspen Plus simulation software and Engineering Equation Solver (EES). The specific objectives of this study are presented as follows:

- To develop three different configurations of integrated systems for hydrogen production through the copper-chlorine cycle and power production. These proposed systems produce clean hydrogen by the thermochemical Cu-Cl cycle. The significant components of proposed systems are a waste heat source, thermochemical copper-chlorine cycle, multistage Rankine cycle and supporting systems.
- To develop the model of three proposed systems using Aspen Plus as simulation software. The mathematical modeling of some systems is performed in Engineering Equation Solver (EES).
- To validate the results of subsystems of the proposed systems with previously published data.
- To investigate the detailed energy and exergy analyses on each of the newly proposed systems: for each proposed systems, performing complete energy and exergy analyses; by thermodynamic analysis, determine the energy and exergy efficiencies of all three proposed system and subsystems; calculating the exergy

efficiencies and exergy destruction rates of each component of all three proposed systems.

- To determine the performance assessment of all three proposed systems in terms of energy and exergy efficiencies. The exergy efficiencies and exergy destruction rates are calculated for all components of each system, and overall performance is also measured.
- To perform comprehensive parametric studies on the systems and evaluating the proposed systems by varying different working conditions to see their effects on the proposed systems.

The waste heat sources used to develop the systems consider waste heat sources from the different industrial group (steel, cement and glass industries).

For the modeling, developing and simulating the proposed systems, the simulation software Aspen Plus and Engineering Equation Solver (EES) are used in this thesis. In this thesis, the proposed systems are realistic and applicable to the designs developed in the literature.

Chapter 2: Literature Review

This chapter describes the comprehensive literature review on hydrogen production from thermochemical copper-chlorine cycle and industrial waste heat sources. Hydrogen is produced by clean energy method which can be stored, used for industries, used for storage and can also be used for filling the fuel tank of hydrogen-fueled vehicles. Produced hydrogen can be used for many purposes such as: for electricity production; it can be used in fuel cells; can be used to produce heat by combusting it; can also be used in the production of some other fuels like ammonia.

2.1 Use of steel industry waste heat

Canada's primary steel production is represented by Canadian Steel Producers Association (CSPA) at the national level. The steel sector is one of the largest industries of Canada which generates more than $8 billion of sales and $3 billion exports per year and provides employment to almost 35000 employees [11]. The primary focus of this study is producing steel and forming hot rolled products. Twelve steel-production plants of Canada consisting of eight electric arc furnace (EAF) plants and four integrated plants are considered in this study and production of these plants in 2002 was 14.9 million tonnes [11]. These were some of the primary objectives of this report such as: introducing a methodology for efficiency benchmark determination of Canadian steel producers; propose some new technologies for making the process more energy efficient; provide with the energy-intensity benchmark collection, and present a technology penetration and benchmarks comparison of plants. Various industrial waste heat sources like steel, cement, and glass industries are available for waste heat recovery. In this study, a very useful product hydrogen and power is produced by using these industrial waste heat or flue gases. Many studies are presented for the waste heat recovery, reheat blast furnace, steel industry heat treatment and utilizing waste heat [17–23]. Gerdau Steel mill in North America is one of the top three largest mini-mills in North America as a steel recycler and steel producer. Flue gas temperature from Gerdau steel industry is 810 ℃, and it has the available heat content of 7876.18 kW [24]. The total manufacturing capacity of Gerdau Long Steel North America (GLSNA) is almost 12 million tons per year.

Arzbaechar et al. [25] considered a study on industrial waste heat recovery. The industries are using a tremendous amount of energy described in Figure 1.3 while some significant amount of energy is wasted in different forms like air streams, flue gases and exhaust gases in the form of heat. Waste heat can be defined as the energy associated with different waste streams of heat like exhaust gases leaving the industry and entering into the environment. These waste heat streams then mix up with atmospheric air and sometimes it causes environmental pollution as well. Even though recovering full available waste heat is not technically feasible, but there is still plenty of room available to improve the efficient use of energy. Greenhouse gases (GHG) can also be diminished by recovering industrial waste heat [25]. The fundamental source of industrial waste heat is the exhaust gases ejected from heating equipment like boilers and furnaces. These high-grade sources of waste-heat can easily be used for preheating. The results from different studies are extracted in this paper to identify the industrial waste heat sources [25].

Luo Siyi and Feng Yu [26] presented a paper on the waste heat recovery from the blast furnace slag which is the main by-product of the steel industry. This waste heat from blast furnace slag goes through endothermic reaction and produces hydrogen-rich gas. In this study, the effect of different parameters like mass ratio, feed moisture, slag temperature and particle size on the gas characteristics and product is evaluated. It was concluded that the blast furnace slag temperature significantly affected the distribution of pyrolysis products. Zhang et al. [27] presented a study that the energy consumption of steel industry can be reduced and use of energy can be more efficient by making use of waste heat from blast furnace slag. On the basis of dry slag granulation technology, integrating air Brayton cycle was proposed for this waste heat recovery. Air Brayton cycle finite time thermodynamic model is established in this study its performance is analyzed while being operated with waste heat recovery and it was concluded that 11.98% of recovery efficiency could be achieved.

Margo et al. [28] proposed a new energy based recovery system by integrating the steel industry waste heat with phase change materials. An auxiliary section is introduced between the steam generators, and phase change materials which supply with the auxiliary

heat required for off gas thermal content and result is concluded. The fluid flowing inside the tubes extracts the heat from phase change materials by heat transfer.

Zhang et al. [29] proposed some new techniques of heat recovery from steel industry molten slag. Quenching water is the most common technique used for heat recovery, but this technique is failed to recover slag sensible heat. Some of the physical heat recovery methods like air blast, mechanical crushing and some chemical heat recovery methods like coal gasification, methane reforming are proposed and investigated. The current research, challenges, working principle and future prospects of waste heat recovery techniques are presented. The technologies presented in this study considers cooling slag particles and heat recovery rate as well which plays a vital role in the viable development of steel industry.

2.2 Use of cement slag waste heat

Waste heat recovery from cement industry blast furnace slag usually faces some contradictions by the requirement of generating amorphous slag to use it for cement production [30]. The slag from cement blast furnace has resemblance with lava and have the high composition of lime, silica, and alumina. Numerous studies are conducted to recover the slag waste heat, cement strength enhancement, reuse of fly ask slag, hydraulic cement blinder production and utilizing the waste heat [31–38]. In the previous few decades, various processes for recovering the waste heat in the form of fuel, heat, and electricity have been introduced. The Barati et al. [39] presented a study on waste heat recovery from molten slag. The high temperature range 1200-1600 ℃ of slag presents some opportunities to recover the waste heat. Presently, the work is being done of three different technologies for recovering slag waste heat. The recovery as hot steam is best developed it has the recovery efficiency of 65%. The other two technologies thermoelectric power generation and chemical energy conversion as fuel are arising as research areas of heat recovery. It is concluded that for the discussed two methods, two-step process with produce high efficiency considering minimum technical risk.

One attempt for the granulation and blast furnace heat recovery was presented by NKK utilizing a twin–drum technology [40]. In this technique, slag is drained in between the two drums. When these drums rotate outside, a slag coating is dragged and frozen on

the drums. The boiler gets the heat for steam generation through the heat achieved by the coolant inside the two drums. This study conducted large-scale trials at Fukuyama Works and resulted in 40% of heat recovery. A water stream is passed through the molten granulated slag which converts this water into the steam and this steam is then linked with the thermochemical Cu-Cl cycle [30].

Liu et al. [41] investigated the performance perimeter of granulated cement slag. The most common technique which is used for slag heat recovery is water quenching, and slag is used in cement production after water quenching. The result was concluded that slag distribution of dry granulation has maximum resemblance with the slag obtained from quenching. Qin et al. [42] developed a system for waste heat recovery. The slag which is the primary by-product of the blast furnace is a source of waste heat, and many technologies have been developed to utilize this vast quantity of sensible heat. A new system for recovering and utilizing the waste heat from slag based on granulation of molten slag and pyrolyzing circuited board was proposed in this study and feasibility was verified by the experiments performed for pyrolyzation and dry granulation. Pyrolysis reaction results in chemical energy and an extensive number of combustible gases by converting hot blast furnace slag energy.

Vilaplana et al. [43] presented a study on laboratory scale cement production from ladle furnace. Various compositions of cement and clinker were synthesized on a laboratory scale, and cement with great Alite composition was obtained by varying silica and alumina ratios. It was concluded that producing cement from ladle furnace slag did not impact severely on mineralogical characteristics. Some of the physical properties like volume expansion and compressive strength were affected positively but a litter more setting time was needed. The final result of this study suggested that this technique can be used for cement production to decrease the intensive utilization of energy, raw materials, and carbon emissions.

Neto et al. [44] presented a study on modification of basic oxygen furnace slag for the purpose of making it a suitable additive in cement formulations. Two modified samples of re-melted basic oxygen furnace slag of 300 kg additives were manufactured on pilot-scale. Cement samples were manufactured by 25% composition of modified slag and

remaining 75% composition of ordinary cement which resulted in the lower expansion of 0.1% and higher compressive strength than 40 MPa.

2.3 Use of glass melting furnace waste heat

A report [45] on the feasibility study of glass manufacturing plant was presented by International Technologies Consultants (ITC) for assessing the establishment of Manitoba glass manufacturing plant. This report presented a compilation of data acquired government sources, consumers and glass industries including the economic, technical and marketing information. The Several studies are conducted on the waste heat recovery from glass melting furnace, solid waste residue incineration, glass melting for immobilization of nuclear waste, heat transfer in a reverberatory furnace, glass furnace energy benchmarking, waste glass processing, power generation from waste heat and waste heat utilization [46–54]. Some of the desired parameters were specified by the client such as: recognize the significant raw materials and see their local availability; installation of approved plant location and size; structure definition and glass industry direction; calculate the current and future float glass demand; assessment of total cost and expected a profit of proposed plant. Kumar et al. [16] presented a case study on the waste heat recovery from glass sector. In this case study, it was shown that glass industry is one of the largest commercial energy consumers and the primary source of this energy is coal-based. More then 75% of the total energy is used in glass melting furnace, and plenty of heat is being released in the form of flue gas which has the high heat potential and opportunity of heat recovery with a very high temperature of 1300-1500 ℃ and preheating the combustion air was one of the solutions suggested for reducing energy consumption.

Costa et al. [55] presented the experimental results of the industrial regenerative oil-fired furnace for producing glass containers. The data presented as a result included the gas with specific concentrations of CO_2, CO, O_2, and NO_x. The results declared: about 1690 ℃ as flame park temperature; about 1520 ℃ exhaust gas temperature and 0.1% CO exhaust level. Unfortunately, a minimal amount of experimental data is currently available because of difficulty in measuring and controlling such high flames, so validation of the proposed mathematical model is practically not possible for glass melting furnace. Dzyuzer et al. [56] presented a new technique for evaluating fume heat recovery efficiency. Glass melting

furnaces with high capacity are strongly trending in container glass production because of being economically efficient. The capacity selected for this analysis was 450 tons a day of glass melting furnace which attained the fume temperature of about 1450-1500 ℃. The regime parameters and structural regenerator needed to reach an air temperature of 1300°C are determined.

Sokolov et al. [57] examined the usage of hot glass heat supported by glass melting furnace. High energy consumption and high energy losses are the most critical problem of glassmaking furnace. Many techniques are proposed regarding this issue, and some methods have successfully adopted by industries for enhancing the energy efficiency. The use of hot glass heat in furnace channels for glass container production was examined in this paper, and this is made possible by the help of circulating furnace gases technique. The total fuel consumption can be reduced by utilizing molten glass heat for natural gas steam conversion and used to heat up the furnace melting part, and this technique reduces 5% of total fuel consumption. Yazawa et al. [58] investigated the glass melting process without any process changes for the thermoelectric energy recovery through waste heat available in glass melting furnace. The pellets of melting glass require high furnace temperature about 1500 ℃ for the purpose of glass shaping processes which results in an immense quantity of exergy which is currently being destroyed. Among variations of thermal paths, the fireports are identified as the best potential for the lowest cost. By partially replacing the refractory wall in thickness with a thermoelectric generator, heat loss is kept at the current 9 kW/m2. High temperature gradient around thermoelectric generator needs cooling water heat sink, and its cost is included in the overall cost analysis.

2.4 Thermochemical Cu-Cl hydrogen production cycle

Global warming and pollution are the two primary environmental hazards which are being faced by humankind, and both of these are linked with our dependence on fossil fuels. Various alternatives are available, but hydrogen fuel proposes the maximum benefits regarding the reduction of greenhouse gases and pollutant emissions and diversified supply as well. Most of the hydrogen available on earth is in an H_2O form which is entirely oxidized form, and 460 kJ/mol of energy is required to break hydrogen and oxygen bond in water. Numerous technologies for hydrogen production are available for producing

hydrogen are named as natural gas steam reforming, water electrolysis through different sources like solar, wind and nuclear, coal gasification and water splitting by thermochemical Cu-Cl cycle. Thermochemical Cu-Cl cycles based on the different number of steps and different techniques are also studied and examined [59–72].

Wang et al. [73] presented a study on a new thermochemical Cu-Cl cycle for producing hydrogen accompanying the requirements of reduced excess steam. The thermochemical Cu-Cl water-splitting is one of the most commonly used methods for hydrogen production. The heat requirements for various steps Cu-Cl cycles and their design features, heat grade and heat quantity regarding waster requirements are investigated in this paper. Naterer [74] presented a study on second law viability for hydrogen production from thermochemical Cu-Cl cycle to upgrade the waste heat with heat pumps. Low-grade waste heat usually has low-temperature heat and limited practical applications. The low-grade waste heat is upgraded in this study by exposing this heat to very high-temperature exothermic reactors of ammonia/salt through chemical heat pumps. The electricity can be produced by utilizing this partially recovered waste heat by the heat engine, and this electricity is further used to operate compressors to enhance the vapor pressure in heat pumps and heat is supplied to the Cu-Cl cycle processes requiring high temperature. Second Law analysis and COP result for a heat pump are examined and presented.

Orhan et al. [75] presented a study and analyzed various Cu-Cl cycles to study several design schemes containing its components to examine performance improvement potential. The factors that determine the number and useful grouping of steps for new design schemes are analyzed. A thermodynamic analysis is performed, and a parametric study is conducted for different configurations, and factors are analyzed which determine the active and suitable group of steps for design scheme. The result related to the implementation of these design schemes and their potential benefits is discussed. The Cu-Cl cycle reaction steps are tabulated in Table 2.1. It can be seen that maximum temperature is of decomposition step where oxygen is produced, and the temperature is 500 ℃ [72]. Naterer et al. [71] presented a paper on recent advances in Canada on nuclear-based hydrogen production by thermochemical Cu-Cl cycle. This study includes reactor developments with the integration of Cu-Cl cycle, advanced materials, reliability,

thermochemical properties, safety, and integration of hydrogen plants with a nuclear power plant in Canada during off-peak hours. As a part of Generation IV International Forum, a Canadian consortium is developing some permissive technologies for hydrogen production. Figure 2.1 shows the schematic diagram of the four-step thermochemical Cu-Cl cycle.

Table 2.1 Four-step Cu-Cu cycle reactions [72].

Step	Name	Reaction	Temperature range (°C)
1	Hydrogen production	$2CuCl(aq) + 2HCl(aq) \rightarrow H_2(g) + 2CuCl_2(aq)$	<100
2	Drying	$CuCl_2(aq) \rightarrow CuCl_2(s)$	<100
3	Hydrolysis	$2CuCl_2(s) + H_2O(g) \rightarrow Cu_2OCl_2(s) + 2HCl(g)$	400
4	Oxygen production	$Cu_2OCl_2(s) \rightarrow 0.5\ O_2(g) + 2CuCl(l)$	500

Wang et al. [76] described a study on various steps hydrogen production thermochemical Cu-Cl cycles and their comparison. The thermochemical Cu-Cl cycles are a very promising cycle for hydrogen production by splitting water. The factors that conclude the effective and suitable group of steps are examined [77–82]. In hydrolysis step, water requirement does not depends on hydrolysis steps individually but depends on the combination of hydrolysis step and drying and hydrogen can be produced by electrolysis of $CuCl_2$ or by chlorination of Cu by HCl and the principal advantages and disadvantages regarding a number of steps were also discussed. Ferrandon et al. [83] investigated the hydrolysis step of the thermochemical Cu-Cl cycle to produce Cu_2OCl_2 and HCl through a spray reactor. A spray reactor is designed by Argonne National Laboratory in which $CuCl_2$ aqueous solution is atomized, and counter of co-current flow of Ar/steam is injected into the heated zone. A significant yield of Cu_2OCl_2 is obtained in counter-current design instead of co-current flow, but a small amount of $CuCl_2$ remained unreacted, and the reason behind it was decomposition of Cu_2OCl_2 instead of $CuCl_2$. Jaber et al. [84] proposed a method for increasing the efficiency of thermochemical Cu-Cl cycle through recovering heat by molten CuCl. This study focuses on the heat transfer between air and droplets of CuCl in the counter-current heat exchanger, and it is analyzed. The thermal management

of thermochemical cycle is a critical point and efficiency can be improved exceptionally if all heat is recycled inside the system. A spray column contacting directly with a heat exchanger is examined for heat recovery in this paper. It was concluded that complete heat recovery could be achieved by the heat exchanger with the defined specification of 0.13 m diameter, 0.6 m height and 0.5 and 1 mm droplet diameter and results are presented.

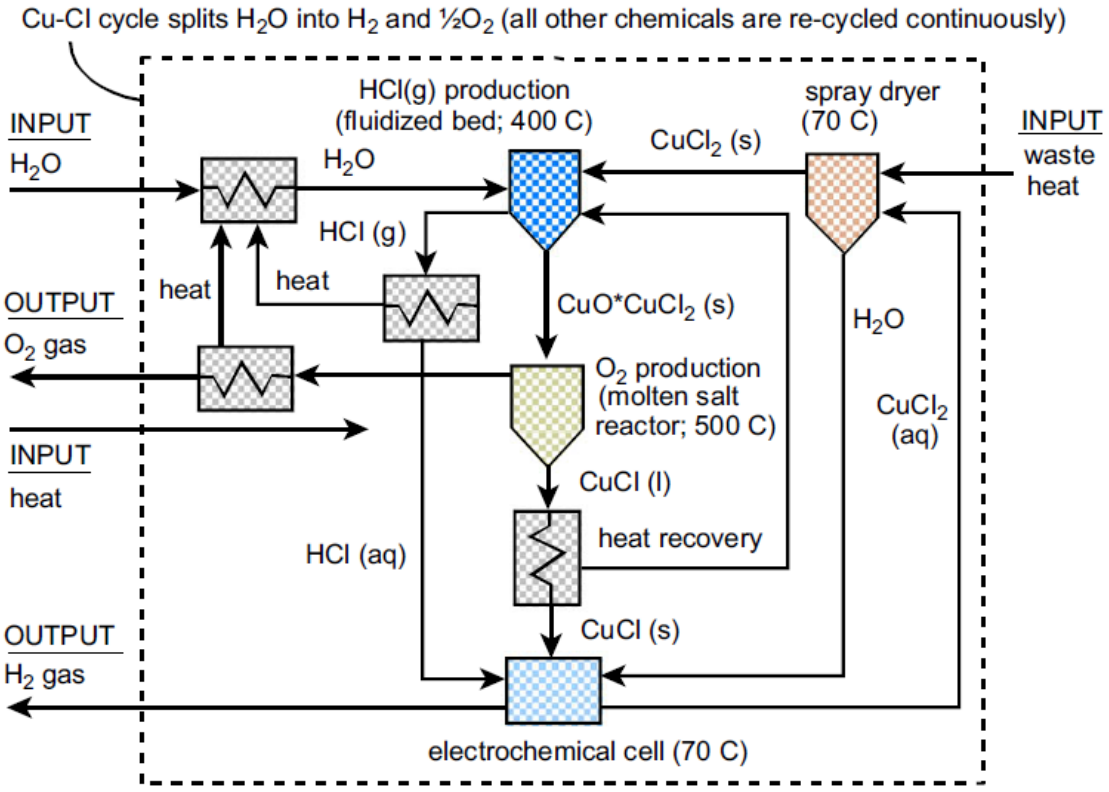

Figure 2.1 Illustration of the four-step thermochemical Cu-Cl cycle [71].

Al-Zareer et al. [85] proposed a novel system consisting of a supercritical water-cooled nuclear reactor supplying heat to the thermochemical Cu-Cl cycle, multistage hydrogen compression system and a combined cycle. This proposed system contains a multistage hydrogen compression system, and hydrogen is produced through a thermochemical Cu-Cl cycle by using a chemical combination of copper with chlorine. Aspen Plus is the simulation software used for modeling and energy, and exergy analysis is carried out of the proposed integrated system. Cetinkaya et al. [64] presented a comprehensive life cycle assessment on different hydrogen production methods which are

named as natural gas steam reforming, water electrolysis through solar and wind sources, coal gasification and thermochemical CuCl cycle and each method were compared in terms of energy equivalents and CO_2 emissions. In this paper, a case study of hydrogen fueling station in Canada is presented and compared with the resources hydrogen available near the fueling station. Regarding CO_2 emissions, thermochemical Cu-Cl hydrogen production cycle using solar and wind sources are found advantageous as compared to other methods.

Dincer and Naterer [68] presented a paper and discussed some new hydrogen production methods which have been investigated experimentally and theoretically at UOIT. This study also examined the recent approaches in thermochemical Cu-Cl cycle and advantages of combining electrolysis with the thermochemical Cu-Cl cycle for hydrogen production. A bunch of activities performed at UOIT helped in developing an innovative system for hydrogen production through electrolysis to thermochemical Cu-Cl cycles and some other integrated cycles for hydrogen production via solar-light. It was concluded that both photochemical and thermochemical cycles proposed auspicious potential for viable hydrogen production. Naterer et al. [86] presented a study on thermochemical Cu-Cl cycle and discussed the hydrogen production by the decomposition of copper oxychloride (Cu_2OCl_2). Heat transfer takes place in Cu-Cl cycle in various endothermic and exothermic reactions. This study emphasises on heat requirements of Cu-Cl cycle steps in order to recover the maximum heat which results in reducing the heat supply and finally overall efficiency of the cycle is improved. This study also analyzes the copper oxychloride thermal design which decomposes to produce molten CuCl and oxygen gas.

2.5 Reverse osmosis desalination unit

Siddiqui and Dincer [87] conducted a study to analyze and design a system integrating desalination, hydrogen production, and electricity generation based on solar tower integration. A desalination reverse osmosis unit is integrated into the proposed system. The energy and exergy analysis is conducted to evaluate the proposed system and its performance. A parametric study is conducted by varying some operating conditions and properties to see its effect on system efficiencies. The study concluded some significant results about the integrated solar based system and reversed osmosis unit performance. Reverse osmosis desalination is integrated with the system in order to recover the low

temperature heat. The heat released by the condenser is used by a reverse osmosis desalination unit to increase the sea water temperature produces fresh water for a community.

Khalid et al. [88] proposed a system integrating gas turbine-modular helium reactor (GT-MHR), and for generating steam, waste heat is used. A parametric study is conducted by varying different parameters like seawater feed inlet temperature, recovery ratio, the inlet temperature of turbine and compression ratio to see their effect on RO process efficiencies, electricity generation, and overall system. The analysis concluded that electricity generation process exergy efficiency is increased by utilizing reactor waste heat.

Islam et al. [89] presented a system integrating solar energy and reverse osmosis unit. The thermodynamic analysis is also performed for performance evaluation. The proposed system contains hydrogen production, heating, cooling, and electricity. Homogeneous charge compression ignition (HCCI) engine is included to overcome the additional electricity demand. By burning in HCCI engine, the significant portion of cost related to the transportation and storage of hydrogen is diminished. The low-cost PV panels are cooled by the recovered waste heat from organic Rankine cycle and HCCI engine for increasing efficiency. The parametric study is conducted by varying the operating parameters to see the effects on system efficiencies.

The overall energy demand is continuously rising and the major part of the energy demand is set to be covered by the fossil fuels. The main reasons for the research on the other sources are diminishing fossil fuel sources, global warming and CO_2 gas emissions. Hydrogen is clean energy carrier and can be used as fuel as well unless it is produced through the clean method. The thermochemical Cu-Cl cycle is one of the most commonly used methods for clean hydrogen production. Produced hydrogen can be used for many purposes such as: for electricity production; it can be used in fuel cells; can be used to produce heat by combusting it; can also be used in the production of some other fuels like ammonia.

2.6 Knowledge gaps and future research needs

Th literature review revealed gaps in past studies regarding waste heat recovery from various industrial sources. There is a significant heat recovery potential in numerous industrial processes. This thesis will examine the waste heat from various industries to operate the thermochemical Cu-Cl cycle for hydrogen production and some other useful outputs such as electricity, fresh water and heating. The key focus of this research is on the industrial waste heat recovery for the production of defined useful outputs. Waste heat from the three prominent industries - steel, cement and glass production - is recovered and integrated with the thermochemical Cu-Cl cycle for hydrogen production and some other useful outputs as well.

Chapter 3: System Description

Three sustainable systems are modeled in this thesis and analyzed energetically and exergetically. Hydrogen production by clean method thermochemical Cu-Cl cycle is the primary purpose of modeled systems along with additional products like electricity and fresh water without impacting the environment, and the source of input for these systems is the industrial waste heat from steel, cement and glass industry. Hydrogen is clean energy carrier and can be used as fuel as well unless it is produced through the clean method and carbon-free hydrogen. This chapter is distributed into three subsections covering each system.

3.1 System 1 - Steel furnace waste heat

In System 1, the input heat source is the steel industrial waste heat being released from a steel heating furnace as flue gas. This system provides the useful outputs like hydrogen, electricity and heating. The major focus of the system is on hydrogen production. The flue gas is emitted at a high temperature of 790℃ while in the thermochemical Cu-Cl cycle, 550℃ of temperature is required. Thus, additional heat is utilized to produce electric power which is not only required to meet the system requirements, but also to provide an additional useful output of electric power. The produced hydrogen proceeds toward the multistage hydrogen compression for the purpose of storing hydrogen at high pressure. The hydrogen gas is released at 500℃ which is then used to operate a multistage reheat Rankine cycle. The heat emitted from the condenser is used for heating purposes. Figure 3.1 presents the schematic diagram of system 1 being operated on the exhaust heat from steel heating furnace. System 1 has steel industrial waste heat recovery, thermochemical Cu-Cl cycle, one single stage and one multistage reheating Rankine cycle. Description of Major steps and cycles is given below.

- **Steel heating furnace exhaust gas**

This exhaust gas is used as the input source for system 1. At state 1, this exhaust gas enters the heat exchangers and partially transfers its heat to the water in heat exchanger 1. Then this exhaust heat in entered in heat exchanger 2 to evaporate the water into steam and to

provide the heat to the thermochemical Cu-Cl cycle. This flue gas contains 26.9 MBtu/hr (7,877 kW) of available heat with a temperature of around 810 ℃ [24]. This exhaust gas is then released to the environment by utilizing is heat, and it provides enough heat to operate Cu-Cl cycle for hydrogen production.

- **Steam Rankine cycle**

The exhaust gas ejected from the steel heating furnace is at the temperature around 810 ℃, and 550 ℃ is the temperature required for operating Cu-Cl cycle, so the additional heat is used to operate a Rankine cycle with this heat. So this heat is transfer to the water coming in the stream 41 and after heating up, this water leave as superheating steam towards the turbine.

- **Thermochemical Cu-Cl cycle**

The thermochemical Cu-Cl cycle considered in this thesis is a four-step Cu-Cl cycle, and the research is being conducted on this cycle at UOIT clean energy research laboratory. This Cu-Cl cycle consists of four different steps named as hydrolysis, decomposition (Oxygen production) step, electrolysis (Hydrogen production step) and drying. The hydrolysis reaction is carried out at 400 ℃ temperature which produces copper oxychloride (Cu_2OCl_2). This copper oxychloride decomposes in cuprous chloride (CuCl) and oxygen gas (O_2) at 500 ℃ temperature. Then aqueous cuprous chloride (CuCl) and aqueous HCl reacts in electrolyzer at 25 ℃ to produce hydrogen gas (H_2) and aqueous cupric chloride ($CuCl_2$). Hydrogen gas is separated, and aqueous cupric chloride is passed through the dryer at 80 ℃ to circulate the solid cupric chloride.

- **Multistage hydrogen compression**

The cuprous chloride reacts with the aqueous HCl in electrolyzer to produce hydrogen gas. This hydrogen gas is then proceeding towards the multistage compression system [2]. The compression of hydrogen is always required in order to store or use for various purposes. Produced hydrogen from Cu-Cl cycle in compressed in three stage compression system with the help of three compressors and three intercoolers which helps in storing this hydrogen gas at high pressure.

- **Multistage reheat Rankine cycle**

The copper oxychloride (Cu_2OCl_2) is decomposed to produce cuprous chloride, and hydrogen gas and reaction temperature is about 500 ℃. Produced oxygen gas at a temperature of 500 ℃ proceeds towards the multistage Rankine cycle for electricity production. This oxygen gas transfers its heat to the water through a heat exchanger which circulates in multistage reheat Rankine cycle to produce electricity, and this electricity can also be used to operate the compressors.

The Aspen Plus model of proposed system 1 is explained according to the Figure 3.2 and Figure 3.3. Figure 3.2 represents the Aspen Plus model of Rankine cycle, thermochemical Cu-Cl cycle, hydrogen compression system and multistage reheat Rankine cycle. Waste heat stream S1 from steel heating furnace enters into the heat exchanger B1and transfer its heat to the other two streams S3 and S10, stream S10 is being used for electricity production in Rankine cycle and in stream S3, water is converted into steam and this steam is used in CuCl cycle not only as water but also to supply the heat to hydrolysis and decomposition reactors.

The flue gas from the blast furnace is linked with the proposed system through a heat exchanger. The flue gas is entered into the heat exchanger B1 through the stream S1 to heat up the water for thermochemical hydrogen production CuCl cycle and Rankine cycle. The heat of the flue gas is then transferred to the other streams. The Stream S4 then leads towards the thermochemical Cu-Cl cycle, and stream S5 leads towards the Rankine cycle turbine.

One stream S5 which is being converted into superheated steam by waste heat enters into the turbine B2 to produce the electricity. Block B3 is being used as a condenser and block B4 is the pump which is used to increase the water pressure which is working fluid in Rankine cycle. Stream S4 leaves the heat exchanger at 550 ℃ and splits into two streams S6 and S8. The stream S13 enters into the heat exchanger B6 to maintain 550 ℃ temperature, and from block B6, it enters into the hydrolysis reactor B8 having the temperature of 400 ℃.

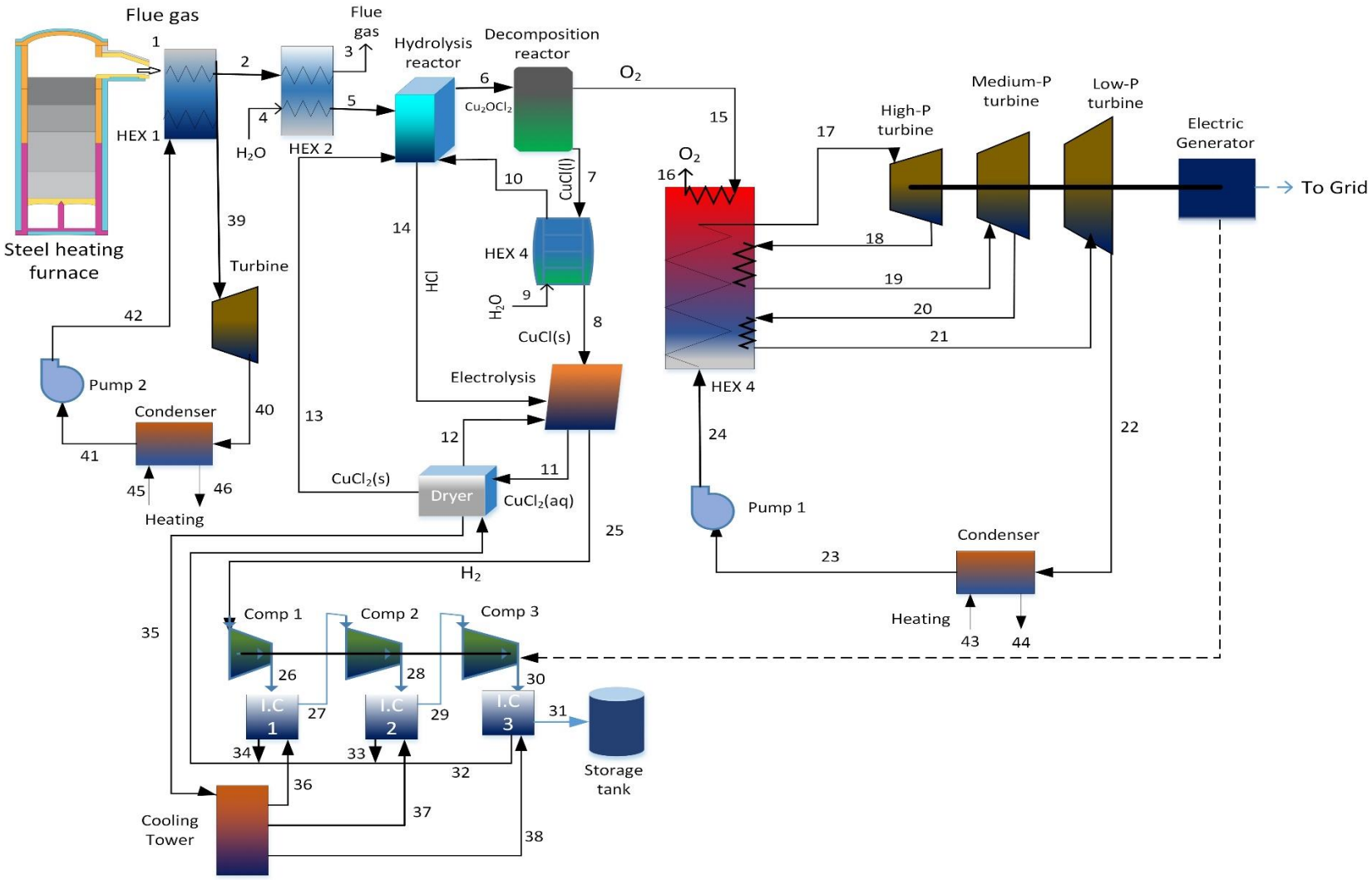

Figure 3.1 System 1 schematic diagram for hydrogen production from thermochemical Cu-Cl cycle utilizing steel industrial waste heat.

One more stream S29 containing $CuCl_2$ enters into the hydrolysis reactor, and this reactor produces copper oxychloride and HCl gas. This mixture then enters into the separator B9 via stream S15 and this block B9 separates Cu_2OCl_2 in S16 stream and HCl in S17 stream. The copper oxychloride enters into the heat exchanger B10 to maintain the temperature of 500 ℃, and then this stream proceeds towards block B11. The second stream from splitter enters into the heat exchanger B7 to maintain the temperature of 550 ℃, and then this stream S12 is also entered into the decomposition reactor B11 to provide with the required heat.

The block B11 decomposes the copper oxychloride into cuprous chloride and oxygen gas. The mixture of these to components enters into the separator B12 via stream S20 which separates oxygen gas in stream S21 and aqueous cuprous chloride in stream S22. The aqueous cuprous chloride then enters the heat exchanger B13 to recover the available heat and then enter into the block B14 which is working as an electrolyzer. The stream S17 enters into the heat exchanger B15 to recover the additional heat, and this stream enters into the electrolysis reactor B14. The electrolysis reaction occurs in reactor B14, and it produces aqueous cupric chloride and hydrogen gas. The electrolyzer consumed 55 kJ of electricity for one mole of hydrogen [90]. The mixture of these two components then proceeds towards the separator B16. The block B16 separates the hydrogen gas from aqueous cupric chloride through stream S26, and stream S27 contains aqueous cupric chloride. This aqueous $CuCl_2$ proceed towards the heat exchanger B17 to maintain the temperature. Then this aqueous cupric chloride is transferred to the dryer B18. The dryer is used to separate water from cupric chloride and to circulate the cupric chloride to continue the cycle. Water is separated through the stream S30, and cupric chloride is entered into the hydrolysis reactor via S29 stream. The thermochemical Cu-Cl cycle steps are tabulated in Table 3.1.

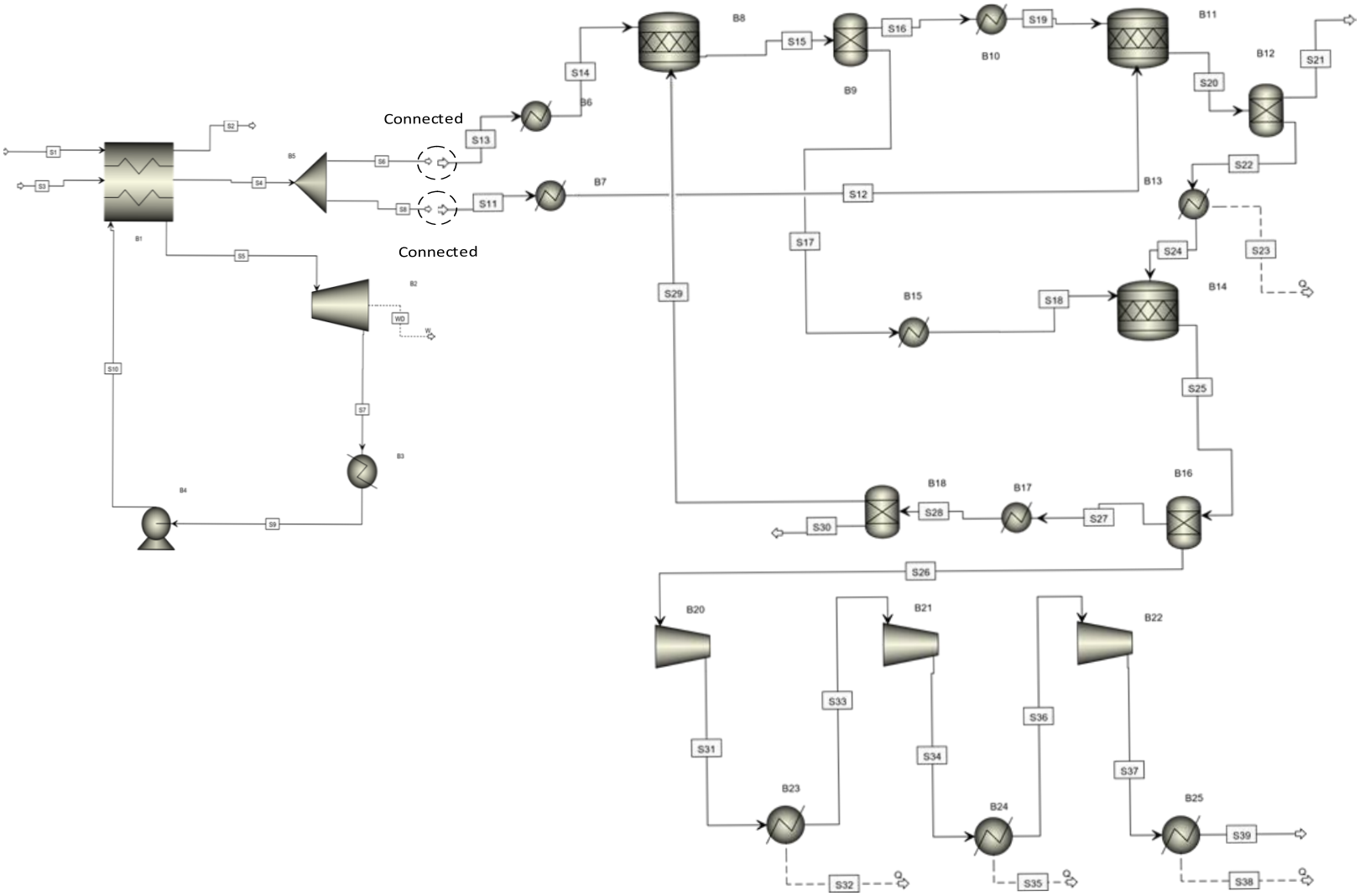

Figure 3.2 The flow sheet of Aspen Plus simulation and modeling of system 1 Rankine cycle, thermochemical Cu-Cl cycle, multistage hydrogen compression and multistage reheat Rankine cycle.

Hydrogen is then entered into the multistage compression system. The hydrogen gas separated through the separator B16 then enters into the first compressor B20. This block increases its pressure, and as a result, its temperature is also increased. After that, this stream proceeds towards first intercooler B23. This intercooler cools the hydrogen gas at the same temperature as compressor input by releasing the heat. This hydrogen gas is then introduced to the second compressor B21 via S33 stream, and this compressor compresses the hydrogen gas furthermore and then enters into the second intercooler B24 to reach the same inlet temperature again. Hydrogen gas then proceeds to the third stage of the compression system. The third compressor B22 increases its pressure till 750 bar for storage, and third intercooler B25 releases its temperature and proceed this gas towards the storage tank. The heat recovered from intercoolers B23 B24 and B25 is used to provide the additional heat to the dryer B18 and after transferring heat to the dryer, stream comes back to the cooling tower. The rigid tank provided the compressed hydrogen with the protection, transportation ease and stored which is one of the advantages of compressed hydrogen.

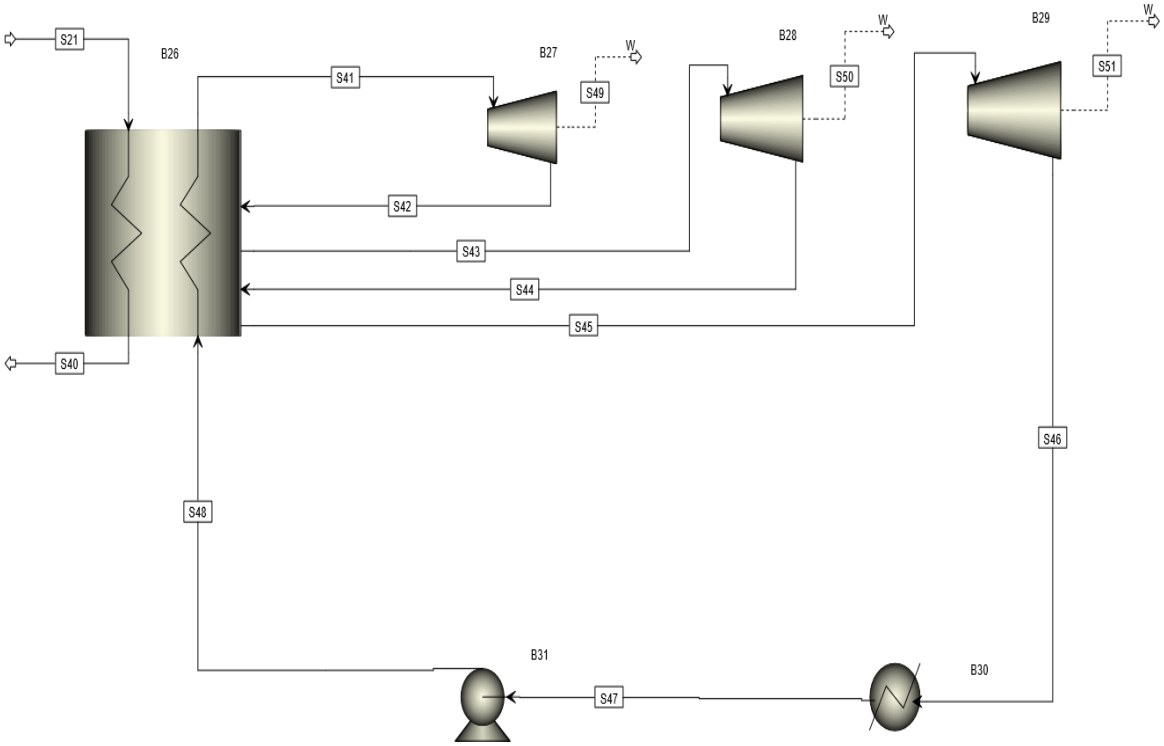

Figure 3.3 Aspen Plus model of system 1 multistage reheat Rankine cycle

Table 3.1 Reactions of the four-step thermochemical Cu-Cl cycle and operating conditions.

Step	Reactor name	Reaction	Temperature range (°C)
1	Hydrogen production reactor	$2CuCl(aq) + 2HCl(aq) \rightarrow H_2(g) + 2CuCl_2(aq)$	<100
2	Water separation by drying or crystallization	$CuCl_2(aq) \rightarrow CuCl_2(s)$	<100
3	Hydrolysis reactor	$2CuCl_2(s) + H_2O(g) \rightarrow Cu_2OCl_2(s) + 2HCl(g)$	400
4	Oxygen production reactor	$Cu_2OCl_2(s) \rightarrow 0.5\ O_2(g) + 2CuCl(l)$	500

The storage tank pressure can be in the range 350-750 bar, depending upon the required size of storage tank [91]. Hydrogen can be stored in two ways either by compressing or liquefying. The first method is used in this thesis which is compressing hydrogen with the help of multistage compression system to reach high pressures for the storage of gas cylinders. The compressed hydrogen storage pressure can be in the range 350-750 bar depending upon the required size of the storage tank which will vary from 0.043 to 0.025 m^3/kg of hydrogen [91].

The Aspen Plus model of multistage Rankine cycle of proposed system 1 is shown and explained according to the Figure 3.3. The oxygen gas from decomposition reactor moves towards the heat exchanger B26 where heat is transferred from oxygen gas to the water circulating in the multistage Rankine cycle, and this heat is used to operate the multistage Rankine cycle. One stream S41 leaves the heat exchanger with superheated steam and enters into the first turbine B27 where this superheated steam is expanded to produce electricity. The outlet stream from the first turbine enters into the heat exchanger B26 for reheating and then transferred to the second turbine B28. The stream S43 expands in B28 to produce electricity and outlet of this block B28 re-enters the heat exchanger B26 for reheating purpose. After reheating, this stream then enters to the third turbine B29 where it expands for the third time to provide with electricity. The outlet of the third turbine leads towards the condenser B30 via S46 stream and then it moves towards the pump B31 in order to increase the fluid pressure. The significant parameters of proposed system 1 are tabulated in Table 3.2.

Table 3.2 Significant parameters of the integrated system including single stage and multistage Rankine cycles, Cu-Cl cycle, and hydrogen compression system.

Component	Parameter	Value
Rankine cycle	The temperature of input flue gas stream	810℃
	The temperature of stream S4 entering Cu-Cl cycle	550℃
	Turbine B2 discharge pressure	0.75 bar
	Rankine cycle operating pressure	5 MPa
	Inlet flue gas mass flow rate	9.21 kg/s
Cu-Cl cycle	Hydrolysis reactor B8 temperature	400℃
	Hydrolysis reactor B8 pressure	1 bar
	Oxygen production reactor B11 temperature	500℃
	Oxygen production reactor B11 pressure	1 bar
	Electrolysis reactor B14 temperature	25℃
	Electrolysis reactor B14 pressure	1 bar
	Electrolysis reactor B14 energy requirement	55.0 kJ/mol H_2
	Dryer B18 operating temperature	80℃
	Dryer B18 operating pressure	1 bar
Multistage hydrogen compression	Number of compression stages	3 stages
	The pressure ratio of the first compressor B20	5
	The pressure ratio of the second compressor B21	5
	The pressure ratio of the third compressor B21	30
	Rankine cycle connected to intercoolers	
	Hydrogen final pressure	750 bar
Multistage Rankine cycle	Multistage Rankine cycle operating pressure	150 bar
	Oxygen gas stream S21 inlet temperature in heat exchanger B26	500℃
	The discharge pressure of turbine B27	37.9 bar
	The discharge pressure of turbine B28	9.26 bar
	The discharge pressure of turbine B29	0.1 bar

3.2 System 2 - Cement slag waste heat

In System 2, the input heat source is the waste heat from cement slag from blast furnace as exhaust gas and this system provides with the useful outputs like hydrogen, electricity and heating. The major focus of this thesis is on hydrogen production. Cement slag has a temperature of 1,300℃ but there are some limitations for heat recovery because of the solidification temperature of particulates in the gas stream and cement slag requires rapid

cooling. The system is developed to produce hydrogen, electricity and heating as major outputs. The produced hydrogen proceeds toward multistage hydrogen compression for the purpose of storing hydrogen at high pressure. The hydrogen gas is released at 500℃ which is then used to operate a multistage reheat Rankine cycle. The heat emitted from the condenser is used for the heating purposes. Figure Figure 3.4 presents the schematic diagram of system 2 being operated on the waste heat from blast furnace cement slag. System 2 has cement slag waste heat recovery, thermochemical Cu-Cl cycle, one single stage and one multistage reheating Rankine cycle. Significant steps and cycles of integrated system 3 are explained below.

- **Cement slag waste heat**

Cement slag waste heat is used as the input source for system 2. Cement slag exits at 1500 ℃ temperature from the blast furnace and many studies have conducted on recovering this waste heat [30]. The whole amount of heat cannot be recovered from cement slag because of the solidification of slag. If heat is recovered before reacting the slag solidification temperature, then it does not affect the original industrial process because cement industry also passes this slag through cooling towers and the solidification temperature of cement slag is 650 ℃ [92]. From the annual production of St. Marys Cement plant Canada, the total heat available before reaching solidification temperature is calculated as 13516.38 kW. So the waste heat from cement slag is recovered just to operate Cu-Cl cycle for hydrogen production.

- **Cu-Cl cycle**

The thermochemical cycle which is used in this thesis is a four-step Cu-Cl cycle. This thermochemical cycle consists of four steps; hydrolysis reaction, decomposition reaction (oxygen production), electrolysis reaction (hydrogen production) and drying process. The hydrolysis reaction is carried out at 400 ℃ temperature which produces copper oxychloride. This copper oxychloride decomposes in cuprous chloride and oxygen gas at 500 ℃ temperature. Then aqueous cuprous chloride and aqueous HCl reacts in electrolyzer at 25 ℃ to produce hydrogen gas and aqueous cupric chloride. Hydrogen gas is separated, and aqueous cupric chloride is passed through the dryer at 80 ℃ to circulate the solid cupric chloride, and the details are tabulated in Table 3.3.

- **Multistage reheat Rankine cycle**

The oxygen gas produced from the decomposition of copper oxychloride (Cu_2OCl_2) is usually at around 500 ℃. So instead of releasing this high-temperature gas to the atmosphere, the available heat is used to operate multistage Rankine cycle for electricity production. This oxygen gas transfers its heat to the water through a heat exchanger which circulates in multistage reheat Rankine cycle to produce electricity, and this electricity can also be used to operate the compressors.

- **Multistage hydrogen compression system**

Hydrogen can be stored in two ways either by compressing or liquefying. The first method is used in this thesis which is compressing hydrogen with the help of multistage compression system to reach high pressures for the storage of gas cylinders. The storage tank pressure can be in the range 350-750 bar, depending upon the required size of the storage tank, so hydrogen produced by electrolysis is passed through multistage hydrogen compression system to make it easier to store it through compression method at a high pressure of 750 bar [93].

The Aspen Plus model of integrated system 2 is explained according to the Figure 3.5. Figure 3.5 represents the Aspen Plus model of the thermochemical Cu-Cl cycle for hydrogen production, multistage hydrogen compression, and multistage reheat Rankine cycle. Waste heat from the blast furnace of cement slag is used to convert water into steam, and this steam is used in CuCl cycle not only as water but also to supply the heat to hydrolysis and decomposition reactors. Water is converted into steam and enter in Cu-Cl cycle at 550 ℃ to utilize as water and to overcome the heat requirement as well.

The main parameters of system 2 are described in table 3.4. The stream S1 enters into the heat exchanger B1 to maintain 550 ℃ temperature, and from block B1, it enters into the hydrolysis reactor B2 having the temperature of 400 ℃. One more stream S26 containing $CuCl_2$ enters into the hydrolysis reactor, and this reactor produces copper oxychloride and HCl gas. This mixture then enters into the separator B3 via stream S3 and this block B3 separates Cu_2OCl_2 in S5 stream and HCl in S6 stream. The copper oxychloride enters into the heat exchanger B4 to maintain the temperature of 550 ℃, and

then this stream proceeds towards block B5 which is decomposition reactor. The second water stream S8 converted into steam through waste heat enters into the heat exchanger B6 to maintain the temperature of 550 ℃, and then this stream S9 is also entered into the decomposition reactor B5 to provide with the required heat. The block B5 decomposes the copper oxychloride into cuprous chloride and oxygen gas. The mixture of these to components enters into the separator B7 via stream S10 which separates oxygen gas in stream S11 and aqueous cuprous chloride in stream S12. The aqueous cuprous chloride then enters the heat exchanger B8 to recover the available heat and then enter into the block B9 which is electrolysis reactor. The stream S6 enters into the heat exchanger B10 to recover the additional heat and this stream also enters into the electrolysis reactor B9. The electrolysis reaction occurs in reactor B9, and it produces aqueous cupric chloride and hydrogen gas. The electrolyzer consumes 55 kJ of electricity for one mole of hydrogen [90]. The mixture of these two components then proceeds towards the separator B11. The block B11 separates the hydrogen gas from aqueous cupric chloride through stream S19, and stream S20 contains aqueous cupric chloride. This aqueous $CuCl_2$ proceed towards the heat exchanger B12 to maintain the temperature.

Table 3.3 The reactions of the four-step Cu-Cl cycle.

Step	Chemical reaction	Temperature range (℃)
1	$2CuCl(aq) + 2HCl(aq) \rightarrow H_2(g) + 2CuCl_2(aq)$	<100
2	$CuCl_2(aq) \rightarrow CuCl_2(s)$	<100
3	$2CuCl_2(s) + H_2O(g) \rightarrow Cu_2OCl_2(s) + 2HCl(g)$	400
4	$Cu_2OCl_2(s) \rightarrow 0.5\ O_2(g) + 2CuCl(l)$	500

Then this aqueous cupric chloride is transferred to the dryer B15. The dryer is used to separate water from cupric chloride and to circulate the cupric chloride to continue the cycle. Water is separated through the stream S27, and cupric chloride is entered into the hydrolysis reactor via S26 stream. Hydrogen is then moved towards the multistage compression system. The hydrogen gas separated through the separator B11 then enters into the first compressor B20. This compressor increases its pressure, and as a result, its temperature is also increased. After that, this stream proceeds towards first intercooler B23. This intercooler cools the hydrogen gas at the same temperature as compressor input by

releasing the heat. This hydrogen gas is then introduced to the second compressor B21 via S35 stream, and this compressor compresses the hydrogen gas furthermore and then enters into the second intercooler B24 to reach the same inlet temperature again. Hydrogen gas then proceeds to the third stage of the compression system. The third compressor B22 increases its pressure till 750 bar for storage, and third intercooler B25 releases its temperature and proceed this gas towards the storage tank. The heat obtained from intercoolers is used to supply the heat to the dryer B15 instead of providing it with some external heat, and after transferring heat to the dryer, the stream comes back to the cooling tower. The rigidity of tank provided the compressed hydrogen with the protection, transportation ease and stored which is one of the advantages of compressed hydrogen. Hydrogen can be stored in two ways either by compressing or liquefying. The first method is used in this thesis which is compressing hydrogen with the help of multistage compression system to reach high pressures for the storage of gas cylinders. The compressed hydrogen storage pressure can be in the range 350-750 bar depending upon the required size of the storage tank which will vary from 0.043 to 0.025 m^3/kg of hydrogen [91].

The oxygen gas from decomposition reactor enters into the heat exchanger B13 where heat is transferred from oxygen gas to the water circulating in the multistage Rankine cycle, and this heat is used to operate the multistage Rankine cycle. One stream S15 leaves the heat exchanger with superheated steam and enters into the first turbine B14 where this superheated steam is expanded to produce electricity.

The outlet stream from the first turbine enters into the heat exchanger B13 for reheating and then enters to the second turbine B16. The stream S23 expands in B16 to produce electricity and outlet of this block B16 re-enters the heat exchanger B13 for reheating purpose. After reheating, this stream then enters to the third turbine B17 where it expands for the third time to provide with electricity.

The outlet of the third turbine leads towards the condenser B19 via S28 stream and then it moves towards the pump B18 in order to increase the fluid pressure. The multistage reheat Rankine cycle is operated at 150 bar pressure.

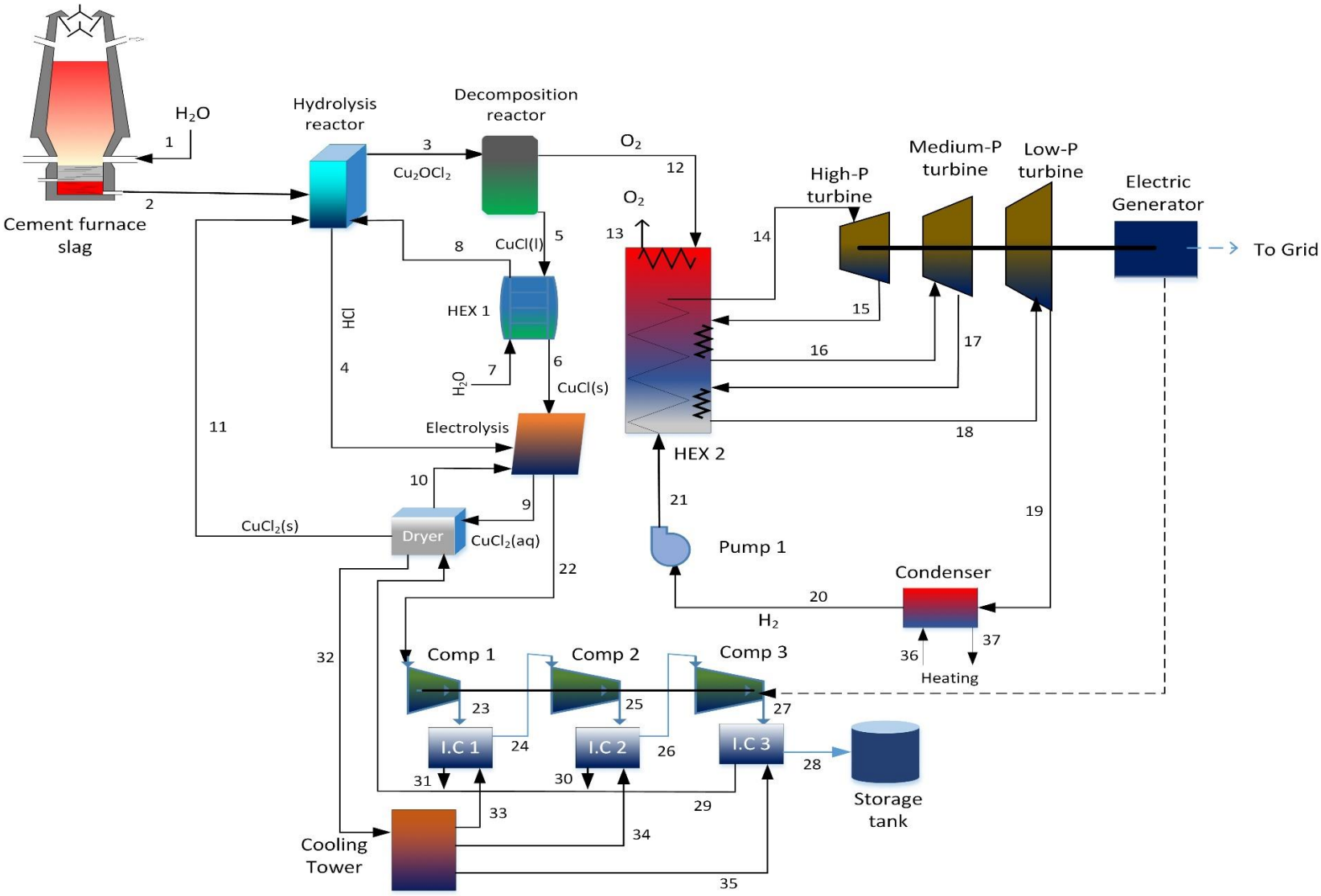

Figure 3.4 System 2 schematic diagram for hydrogen production from thermochemical Cu-Cl cycle utilizing cement slag waste heat.

Table 3.4 Main parameters of the second integrated system.

Component	Parameter	Value
	Inlet flue gas mass flow rate	31.71 kg/s
Cu-Cl cycle	Hydrolysis reactor B2 operating temperature	400℃
	Hydrolysis reactor B2 operating pressure	1 bar
	Oxygen production reactor B5 temperature	500℃
	Oxygen production reactor B5 pressure	1 bar
	Electrolysis reactor B9 operating temperature	25℃
	Electrolysis reactor B9 operating pressure	1 bar
	Electrolysis reactor B9 electrical energy requirement	55.0 kJ/mol H_2
	Dryer B15 operating temperature	80℃
	Dryer B15 operating pressure	1 bar
Multistage compression	Number of compression stages	3 stages
	The pressure ratio of the first compressor B20	5
	The pressure ratio of second compressor B21	5
	The pressure ratio of the third compressor B21	30
	Rankine cycle connected to intercoolers	
	Hydrogen final pressure	750 bar
Multistage Rankine cycle	Multistage Rankine cycle operating pressure	150 bar
	Oxygen gas inlet temperature in heat exchanger B13	500℃
	The discharge pressure of turbine B14	37.9 bar
	The discharge pressure of turbine B16	9.26 bar
	The discharge pressure of turbine B17	0.1 bar

3.3 System 3 - Glass melting furnace waste heat

In System 3, the glass industrial waste heat is used as the input heat source which is being released from glass melting furnace as exhaust gas and this system provides with the useful outputs like hydrogen, electricity and fresh water. The major focus of the system was on hydrogen production. The flue gas is emitted at a high temperature of 1127℃ while in the thermochemical Cu-Cl cycle, a 550℃ temperature is required. Thus, the additional heat is utilized to produce electric power which is not only enough to overcome the system requirements, but also it provides an additional useful output of electric power. The additional low temperature heat available through the condenser is used to produce fresh water through a Reverse Osmosis (RO) desalination unit for a community of 1,500 houses.

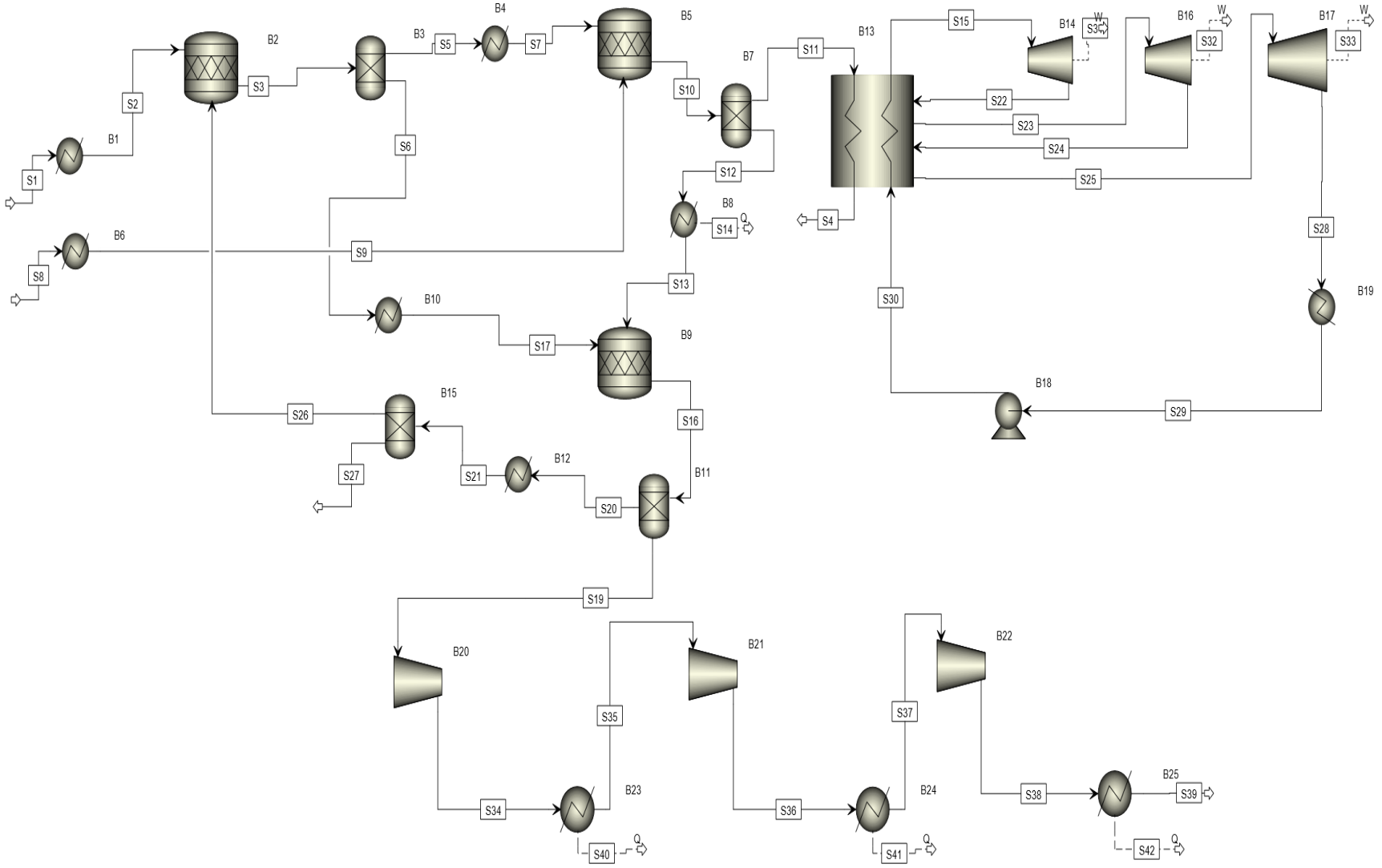

Figure 3.5 The Aspen Plus simulation and modeling flow sheet of system 2 containing Cu-Cl cycle, multistage reheat Rankine cycle and multistage hydrogen compression.

The produced hydrogen proceeds toward multistage hydrogen compression for the purpose of storing hydrogen at a high pressure and the hydrogen chloride gas is released at 400℃ which is then used to operate a multistage reheat Rankine cycle. The heat emitted from the condenser is used for heating purposes. Figure 3.6 presents the schematic diagram of system 3 being operated on the exhaust heat from glass melting furnace. System 2 has glass industrial waste heat recovery, hydrogen production Cu-Cl cycle, one single stage and one multistage reheating Rankine cycle and Reverse osmosis unit. Description of Major steps and cycles is provided below.

- **Glass melting furnace exhaust gas**

Many case studies are presented on the waste heat recovery from glass sector. One case study showed that glass industry is one of the largest commercial energy consumers and the primary source of this energy is coal-based. More then 75% of the total energy is used in glass melting furnace and plenty of heating is being wasted in the form of flue gas with very high temperature of 1500-1800 K and exhaust gas temperature is about 1500 K so preheating the combustion air was one of the solutions suggested for reducing energy consumption, and the amount of heat available for recovery is 7,857 kW [16, 58]. This exhaust gas temperature is about 1127℃, and this waste heat is used to operate Rankine cycle initially because 1127℃ temperature is very high and 550 ℃ temperature is required in Cu-Cl cycle. So additional heat is utilized to operate Rankine cycle.

- **Steam Rankine cycle**

The exhaust gas ejected from the glass melting furnace is at temperature 1400 K (1127 ℃) while the temperature required to operate Cu-Cl cycle is 550 ℃. So the additional heat available in the exhaust heat from glass industry is used to operate the Rankine cycle. The electricity produced from the Rankine cycle can quickly overcome the electricity required by the integrated system.

- **Thermochemical Cu-Cl cycle**

This Cu-Cl cycle used in this thesis consists of four different steps named as hydrolysis, decomposition, electrolysis, and drying and there four reactions and some of their operating conditions are described below.

Step 1: Hydrolysis reactor, the principal requirement of hydrolysis reactor is to maintain the temperature of around 400 ℃ [62].

$$2CuCl_2(s) + H_2O(g) \rightarrow Cu_2OCl_2(s) + 2HCl(g) \quad (3.1)$$

Step 2: The decomposition of copper oxychloride takes place in this reaction to produce cuprous chloride and oxygen gas. The principal requirement of this reaction is to maintain decomposition reactor at around 500 ℃.

$$Cu_2OCl_2(s) \rightarrow 0.5\ O_2(g) + 2CuCl(l) \quad (3.2)$$

Step 3: In this step, aqueous $CuCl_2$ is dried at the temperature of about 80 ℃ to separate the aqueous cupric chloride from water.

$$CuCl_2(aq) \rightarrow CuCl_2(s) \quad (3.3)$$

Step 4: The cuprous chloride reacts with HCl in electrolyzer to produce hydrogen gas in this step, and this step is carried out at the temperature between 25 ℃ and 35 ℃.

$$2CuCl(aq) + 2HCl(aq) \rightarrow H_2(g) + 2CuCl_2(aq) \quad (3.4)$$

- **Multistage reheat Rankine cycle**

The hydrogen chloride (HCl) gas rejected from hydrolysis reactor offer much heat to recover because this stream is at 400 ℃ and this stream is required to enter into the electrolysis reactor where electrolysis is taking place at average ambient temperature 25 ℃. So this additional heat is recovered by passing it through a heat exchanger where this HCl gas transfers its temperature to the water stream which is used as a working fluid in multistage reheat Rankine cycle.

- **Hydrogen compression system**

The hydrogen gas produced in electrolyzer is separated with the help of a separator, and then this is entered into the hydrogen compression system [91]. Because hydrogen can be stored either in liquefied form or in compressed form and compression technique is being used in this thesis. By passing through multistage compression, the pressure of the hydrogen gas increased from 1 bar to 750 bar, and this temperature limit depends upon the storage tank size specification [94].

- **Reverse osmosis unit**

The reverse osmosis unit integrated with the proposed system 3 is designed to produce 17.4 kg/s of fresh water having the salinity of 450 PPM. The 29 kg/s of sea water is supplied to achieve the 17.4 kg/s of fresh water, through the condenser. The low-pressure pump pumps thee sea water from ambient pressure to 650 kPa. Then this saline water is proceeding towards the filter which removes suspended particles. Then good quality water containing small quantity is split by three- way valve and the significant and remaining quantity of water is proceed to the chemical chamber for chemical treatment. Based on osmotic pressure design, the pressure of this water is enhanced till 6000 kPa through high pressure pump. Some of the design parameters are tabulated in Table 3.5.

The simulation model of the third integrated system in Aspen Plus is shown in Figure 3.7, 3.8 and 3.9. Figure 3.7 is representing the Rankine cycle which is used to utilize the additional heat and to supply the power required by the integrated system. Figure 3.8 represents the Aspen plus simulation model of Cu-Cl cycle, and hydrogen compression system and Figure 3.9 explains the multistage reheat Rankine cycle integrated with the third system.

The exhaust gas from glass melting furnace contains 1127 ℃ of temperature and the flow rate of 6.37 kg/s. The temperature required for operating Cu-Cl cycle is 550 ℃. So the additional heat is utilized to operate the Rankine cycle, and the electricity produced by this Rankine cycle is used to supply the required necessary power to the electrolyzer and compressors. The exhaust gas from the blast furnace is linked with the proposed system through a heat exchanger B1. The exhaust gas is entered into the heat exchanger through the stream S1 to heat up the water for thermochemical hydrogen production CuCl cycle and Rankine cycle. The heat of the exhaust gas is then transferred to the other streams. The Stream S4 then leads towards the thermochemical Cu-Cl cycle, and stream S5 leads towards the Rankine cycle turbine.

The Aspen Plus model presented in Figure 3.7 shows that the exhaust gas from glass melting furnace enters into the heat exchanger B1 through S1 stream. This heat exchanger B1 transfers the exhaust gas heat to the S4 water stream which leaves the heat exchanger at 550 ℃ and to the stream S5 by converting the working fluid (water) of

Rankine cycle into the superheated state. Exhaust gas leaves the heat exchanger B1 via stream S2 containing 90 ℃ temperature.

The stream S5 enters into the turbine in superheated state and then expands in the turbine to produce electricity. This Rankine cycle is operated at 5 MPa pressure. The turbine outlet stream passes through the condenser B3 where the temperature is set up as 70 ℃. Sea water also passes through this condenser to obtain the temperature of 40 ℃. From condenser, stream leads towards the pump B4 via stream S9 which increases its pressure and circulates the water again. The stream S4 split into two streams each stream containing 550 ℃ temperature.

Table 3.5 Operating parameters of reverse osmosis unit [89].

Parameter	**Value**	**Unit**
Product water flow rate	17.4	kg/s
Sea water salinity	35000	PPM
Product water salinity	450	PPM
Sea water temperature	25	℃
Efficiency of high and low pressure pump	85%	
Membrane recovery ratio	60%	

Figure 3.8 shows that stream S13 supplies heat to the hydrolysis reactor through heat exchanger B6 and stream S11 provides the decomposition reactor with the heat required by heat exchanger B7. The steam enters into the hydrolysis reactor B8 via stream S15, and one more stream S17 enters into the hydrolysis reactor containing cupric chloride. In hydrolysis reactor, $CuCl_2$ reacts with water at 400 ℃ to produce copper oxychloride and HCl gas. A mixture of these two components reaches to the separator B9 which separates Cu_2OCl_2 from HCl. The hydrogen chloride gas leaves through stream S17 at 400 ℃, and this high temperature heat is utilized to operate multistage reheat Rankine cycle (Figure 3.9) and again enters into the electrolyzer at 25 ℃ temperature.

The copper oxychloride leaves through the stream S16 and enters into the heat exchanger B10 where the temperature is maintained at 550 ℃. Copper oxychloride then enters into the decomposition reactor B11 where it is decomposed at 500 ℃ in cuprous chloride (CuCl) and oxygen gas (O_2). This mixture leads towards the separator B12 via stream S20 which separates oxygen gas containing 500 ℃ in S21 stream and cuprous chloride via S22 stream. Some heat is recovered from the cuprous chloride through heat

exchanger B13 and then entered into the electrolyzer via stream S24. Heat available in oxygen gas stream is recovered and used in Cu-Cl cycle again. In electrolysis reactor, CuCl reacts with HCl to produce aqueous cupric chloride ($CuCl_2$), and hydrogen gas and electrolyzer requires 55 kW of power for 1 mole of hydrogen production.

The mixture of cupric chloride and hydrogen gas is transferred to the separator B16 which separates the hydrogen gas in S26 stream and aqueous cupric chloride in the S27 stream. Aqueous cupric chloride then leads towards the heat exchanger B17 to maintain the temperature. By passing through the heat exchanger, aqueous cupric chloride enters into the dryer B18 which requires 80 ℃ of temperature and this heat is provided by the heat recovered from the multistage intercoolers. Dryer B18 separates hydrogen gas in stream S30, and solid cupric chloride is circulated in the cycle via stream S29 towards hydrolysis reactor.

The heat exchanger B26 behaves as a boiler for multistage reheat Rankine cycle, and this cycle operates at 150 bar pressure. Heat from HCl is transferred to the water in B26 which is converted into superheated steam. This superheated steam enters into the first turbine B27 via stream S41 where it expands to generate power. The discharge pressure of turbine is set up as 37.9 bar from the literature review, and outlet stream enters into the heat exchanger B26 again for reheating purpose. After reheating at the same temperature, superheating steam enters into the second turbine B28 where it expands again to produce power. The discharge pressure of the second turbine is 9.26 bar [95]. The outlet of the second turbine is reheated again in B26 and fed into the third turbine B29. The third turbine also expands the superheated stream and outlet moves towards the condenser B30. From condenser, water moves towards the pump 31 which increases its pressure and circulates it into the cycle.

Figure 3.9 represents the multistage reheat Rankine cycle. A stream S17 enters into the heat exchanger B26 via stream S17 and leave at the average temperature 25 ℃ which is shown in Figure 3.8 entering in the electrolyzer to utilize the temperature of HCl gas. Figure 3.6 represents the schematic diagram of reverse osmosis unit and the analysis for reverse osmosis unit is conducted in Engineering Equation solver.

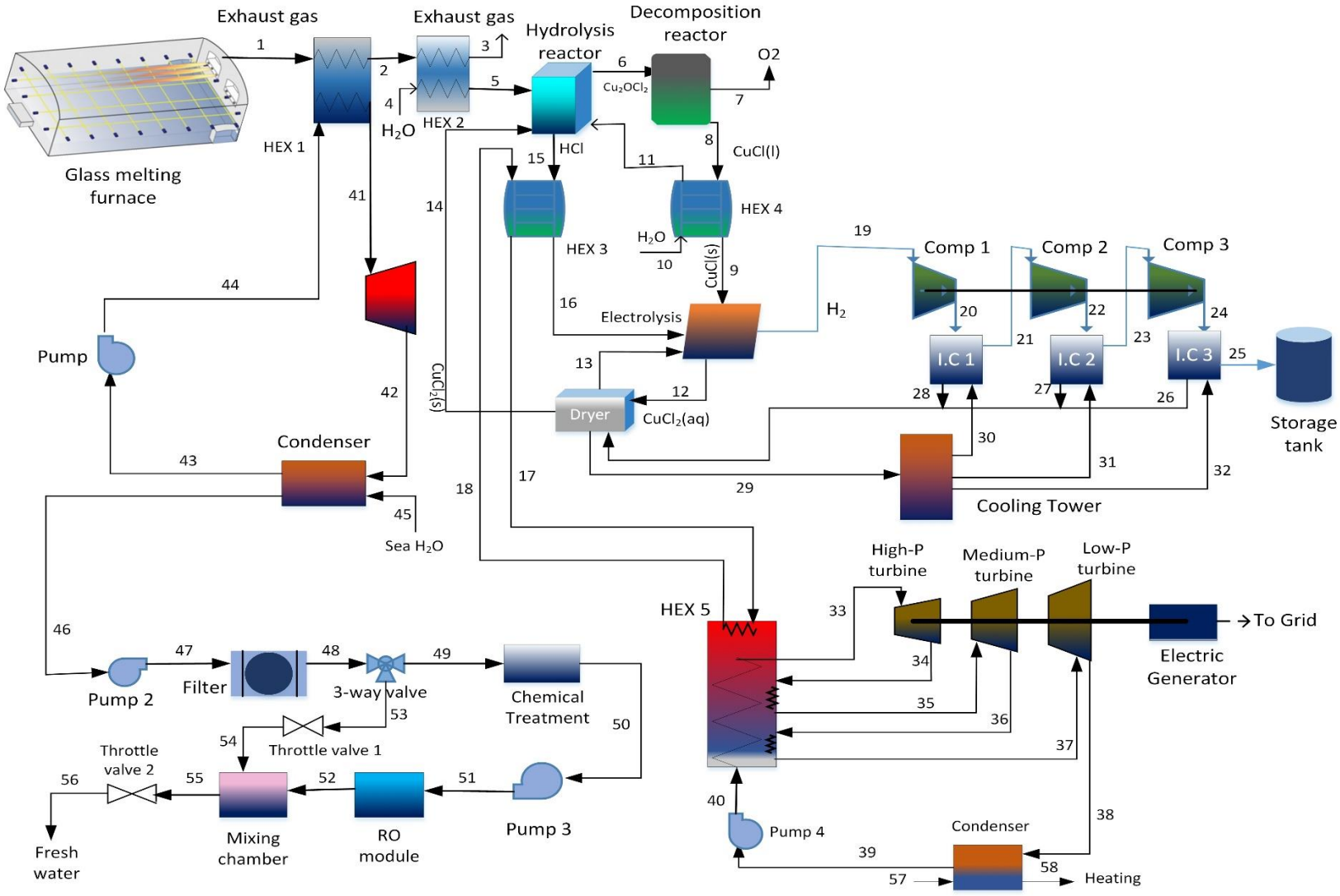

Figure 3.6 System 3 schematic diagram for hydrogen production from thermochemical Cu-Cl cycle utilizing glass industrial waste heat.

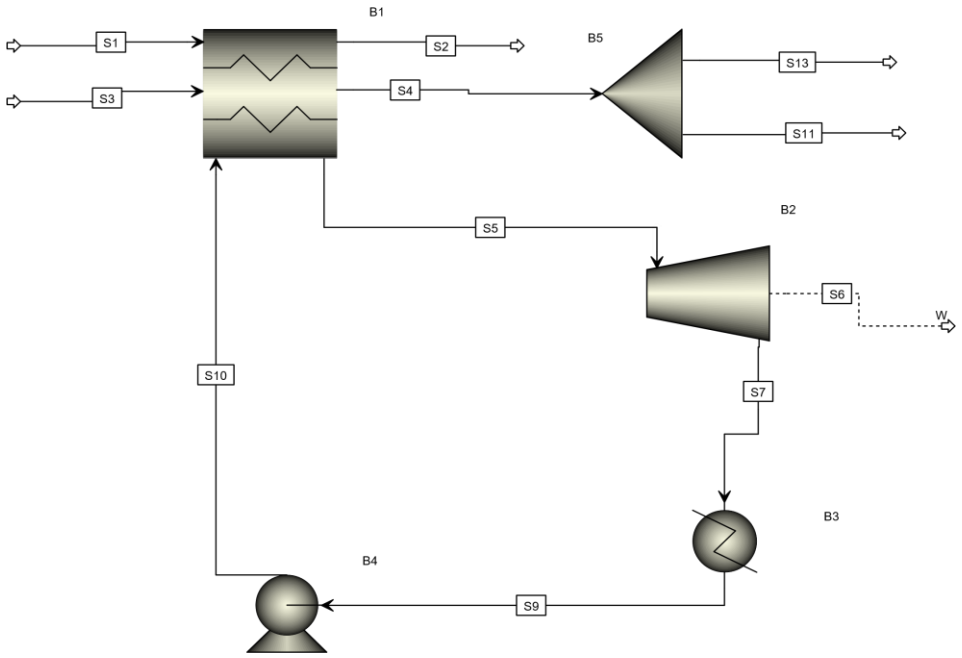

Figure 3.7 Aspen Plus model of the Rankine cycle integrated into system 3.

The reverse osmosis unit integrated with the proposed system 3 is designed to produce 17.4 kg/s of fresh water having the salinity of 450 PPM, and the salinity of sea water is 35000 PPM and to achieve 17.4 kg/s of fresh water, 29 kg/s of sea water is supplied through the condenser. With this mass flow rate, fresh water can be supplied to a community of 1500 houses. The pressure of low pressure pump is set 650 kPa and pressure of high pressure pump is given as 6000 kPa. The significant parameters of system three are presented in Table 3.6.

The membrane recovery ratio is taken as 60% and to operate this mass flow rate, low pressure turbine consumes 18.42 kW of work, and high pressure turbine absorbs 181 kW of work. Figure 3.6 is used for the reference of subscripts for reverse osmosis unit. Sea water enters into the condenser for heating purpose and then moves towards the pump 2 which increases its pressure. Then it passes through the filter which removes the suspended particles. Then three-way valve separates small amount of good quality water and sends it directly to the mixing chamber through the throttle valve 1 while remaining significant part moves into the chemical pre-treatment cycle where chemical treatment is conducted. Water then leads towards the high pressure pump and then by passing through RO module, leads towards the mixing chamber where both water streams mix up, and fresh water is separated by the second throttle valve.

Table 3.6 Significant parameters of the third integrated system where the subscripts of the reverse osmosis unit components and streams are referenced in Figure 3.6.

Component	Parameter	Value
Rankine cycle	The temperature of input flue gas stream	1127℃
	The temperature of stream S4 entering Cu-Cl cycle	550℃
	Turbine B2 discharge pressure	0.1 bar
	Rankine cycle operating pressure	5 MPa
	Inlet flue gas mass flow rate	6.37 kg/s
Cu-Cl cycle	Hydrolysis reactor B8 operating temperature	400℃
	Hydrolysis reactor B8 operating pressure	1 bar
	Oxygen production reactor B11 operating temperature	500℃
	Oxygen production reactor B11 operating pressure	1 bar
	Electrolysis reactor B14 operating temperature	25℃
	Electrolysis reactor B14 operating pressure	1 bar
	Electrolysis reactor B14 electrical energy requirements	55.0 kJ/mol H_2
	Dryer B18 operating temperature	80℃
	Dryer B18 operating pressure	1 bar
Multistage compression	Number of compression stages	3 stages
	The pressure ratio of the first compressor B20	5
	The pressure ratio of second compressor B21	5
	The pressure ratio of the third compressor B21	30
	Rankine cycle connected to intercoolers	
	Hydrogen final pressure	750 bar
Multistage Rankine cycle	Multistage Rankine cycle operating pressure	150 bar
	HCl stream S17 inlet temperature in heat exchanger B26	400℃
	The discharge pressure of turbine B27	37.9 bar
	The discharge pressure of turbine B28	9.26 bar
	The discharge pressure of turbine B29	0.1 bar
Reverse Osmosis unit	Fresh water flow rate	17.4 kg/s
	Operating temperature	45℃
	Membrane recovery ratio	60%
	$\dot{W}_{Pump\ 2}$	18.42 kW
	$\dot{W}_{Pump\ 3}$	181 kW
	$\eta_{pump\ 2}$	0.85
	$\eta_{pump\ 3}$	0.85

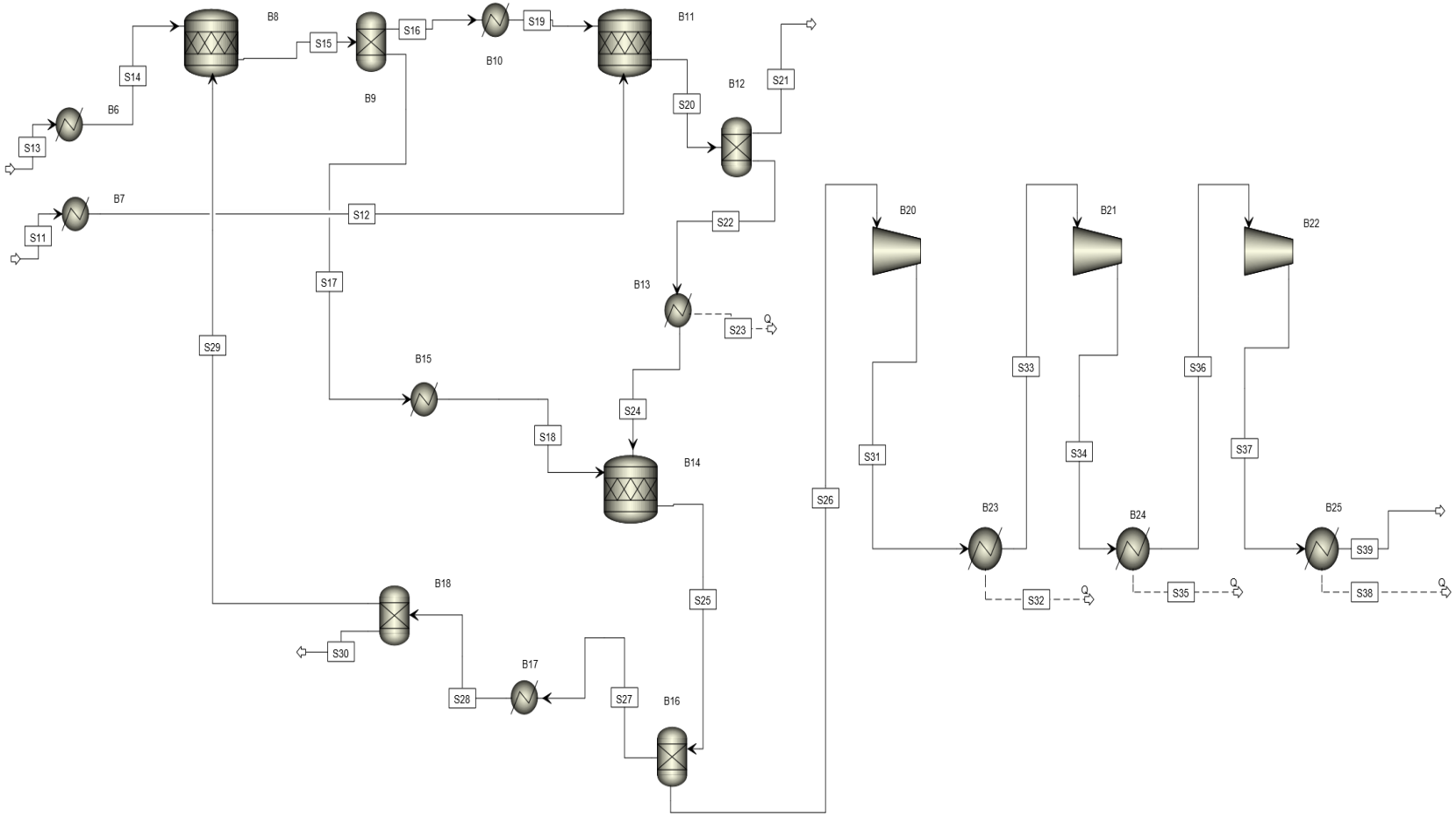

Figure 3.8 The model of third integrated system simulated in Aspen Plus containing hydrogen production Cu-Cl cycle and multistage hydrogen compression.

Hydrogen gas enters into the multistage compression system through stream S26 because compression method is used in this thesis for the storage of hydrogen. Hydrogen first enters into the first compressor B20 which has the compression ratio of 5 [94]. The separate Aspen Plus model of multistage compression system is shown in Figure 3.10. The compressor increases its pressure and temperature as well, and then it moves towards the first intercooler B23 which cools the gas at the same temperature as first compressor input by releasing heat and transfers it to the second turbine B21. The compression ratio of the second turbine is 5, and it increases its pressure to 25 bar and second intercooler B24 cools the gas again at same inlet temperature and shifts it towards third compressor B22. The compression ratio for the third turbine is 30, and it increases the gas pressure to 750 bar, and third intercooler B25 releases high temperature and moves the gas towards storage tank. The heat released from the intercoolers is used to provide the heat in the dryer and comes back to the intercoolers through the cooling tower.

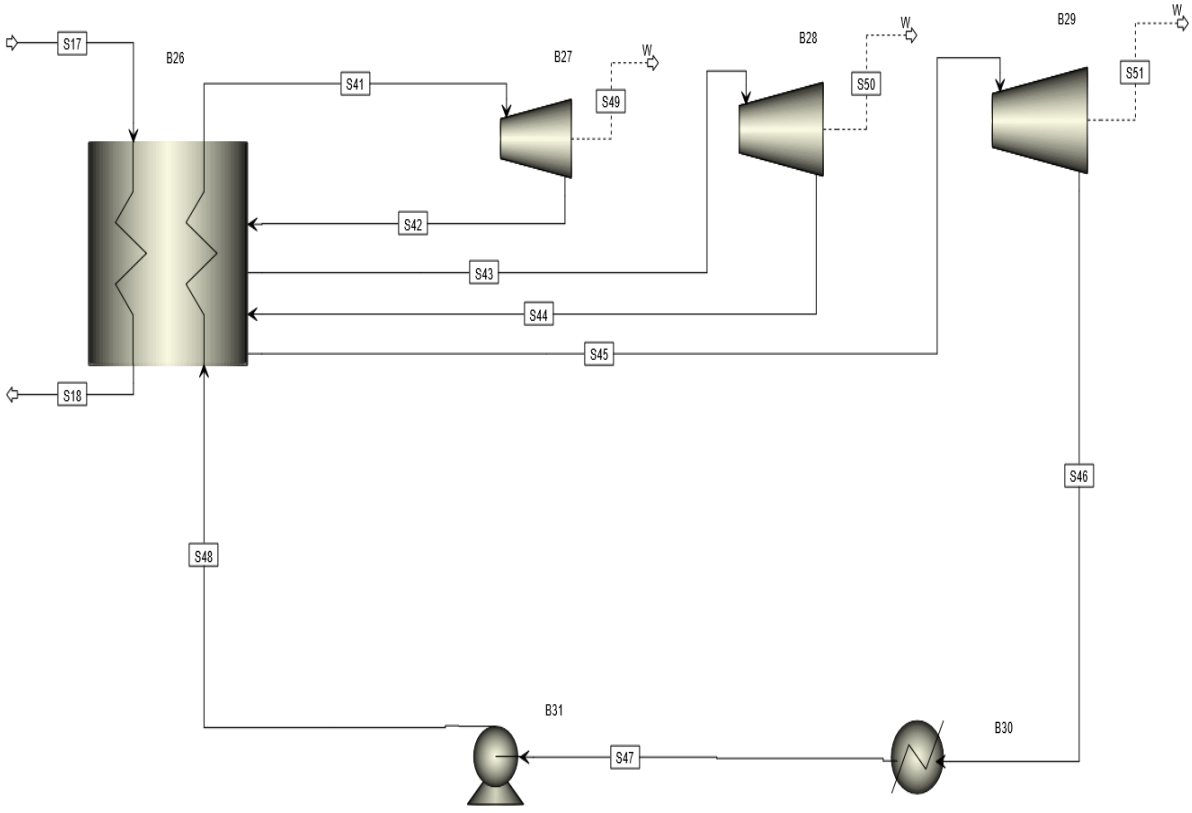

Figure 3.9 Aspen Plus model of the multistage reheat Rankine cycle.

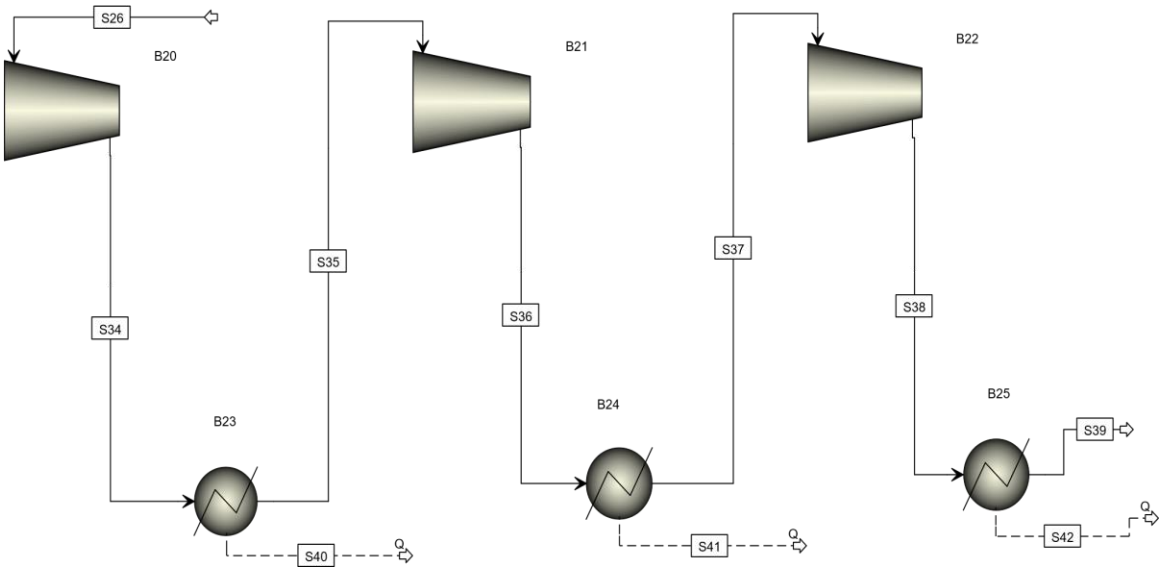

Figure 3.10 Aspen Plus model of multistage hydrogen compression system.

Chapter 4: Thermodynamic Analysis

In this chapter the comprehensive thermodynamic analysis of the three proposed integrated systems and the major assumptions considered during the modeling and simulation of systems thermodynamic parameters calculations.

4.1 Thermodynamic analysis

The comprehensive thermodynamic energy and exergy analyses are conducted for each system individually and its components as well and presented in the upcoming section of this chapter.

4.1.1 Mass balance equation

The general mass balance equation of conservation of mass for a control volume can be written as:

$$\sum_i \dot{m}_i - \sum_e \dot{m}_e = \frac{dm_{CV}}{dt} \tag{4.1}$$

In this equation, m represents mass, $\dot{m}$ represents mass flow rate, subscripts i denotes to the inlet while subscripts e denotes to the exit and CV is representing control volume on which balance is being applied.

4.1.2 Energy balance equation

According to the first law of thermodynamics one can write comprehensive and general energy balance equation for control volume as:

$$\dot{Q} - \dot{W} + \sum_i \dot{m}_\iota \left(h_i + \frac{V_i^2}{2} + gZ_i\right) - \sum_e \dot{m}_e \left(h_e + \frac{V_e^2}{2} + gZ_e\right) = \frac{dE_{CV}}{dt} \tag{4.2}$$

In the described energy equation, $\dot{Q}$ represents heat transfer rate, $\dot{W}$ represents work rate, E represent energy and t represents time while other symbols h represent specific enthalpy, v represents velocity, g represents gravitational acceleration and Z represents the elevation.

4.1.3 Entropy balance equation

The general entropy balance equation for a control volume can be described as follows:

$$\dot{S}_{gen} = \frac{dS_{CV}}{dt} = \sum_e \dot{m}_e s_e - \sum_i \dot{m}_i s_i - \sum_k \left(\frac{\dot{Q}_k}{T_k}\right) \quad (4.3)$$

S_{gen} is representing the entropy generated during the process, $\dot{m}$ represents mass flow rate, $\dot{Q}$ represents the heat transfer rate and T represents the temperature.

4.1.4 Exergy balance equation

Both first and second laws of thermodynamics are included in exergy analysis. The detailed exergy analysis is valuable for providing more effective and efficient approach for the utilization of energy for different thermodynamic processes. Basically the physical and chemical exergy are most widely used forms of exergy. The physical exergy can be defined as work potential obtained when system connects with the environment while chemical exergy is taken into consideration when chemical change occurs. One can write the general exergy balance for control volume according to second law of thermodynamics as:

$$\dot{E}x^Q + \sum_i \dot{m}_i ex_i = \sum_e \dot{m}_e ex_e + \dot{E}x_w + \dot{E}x_d \quad (4.4)$$

In the described equation, subscripts i denotes the inlet while subscripts e denotes the exit and $\dot{E}x_d$ represents the exergy destruction. Some other terms are described below:

$$E\dot{x}^Q = \dot{Q}_i \left(1 - \frac{T_0}{T_s}\right) \quad (4.5)$$

Factor $E\dot{x}^Q$ denotes the exergy rate because of heat transfer, T_0 represents the ambient temperature and T_s denotes the boundary temperature.

$$E\dot{x}_W = W \quad (4.6)$$

In the above equation, $E\dot{x}_W$ represents the exergy rate due to mechanical or electrical work which is equal to work rate.

$$ex = ex_{ph} + ex_{ch} \quad (4.7)$$

The factor ex_{ph} represents the physical energy and ex_{ch} represents the chemical exergy.

$$ex_{ph} = h - h_0 - T_0(s - s_0) \quad (4.8)$$

In the above equation 4.8, h and s represents the specific enthalpy and entropy of flow and h_0 and s_0 denotes the specific enthalpy and entropy of reference state. The chemical exergy can be described as:

$$ex_{ch} = \sum x_j \, ex_{ch}^0 + RT_0 \sum x_j \ln(x_j) \quad (4.9)$$

In above described equation, x_j represents the mole fraction of component j, ex_{cg}^0 denotes standard specific chemical exergy, R is universal gas constant and T_0 represents the reference temperature.

4.2 Assumptions

The major assumptions considered while doing analysis and development of the proposed system for hydrogen and power production and the property methods used during the analysis are described below for each system individually.

The assumptions made for system 1 are listed as follows:

- The system operates under steady-state conditions [90].
- No starting up periods is considered for hydrogen production cycle [94].
- All gases in the chemical exergy equations are considered as real gases.
- The changes in kinetic and potential energies are neglected [96].
- STEAMNBS is the property method used for Aspen Plus modeling of water (H_2O) which ranges from 0 to 1700 ℃ and maximum allowable pressure is 1000 MPa [94].
- The Aspen Plus property method used for the analysis to deal with real components is SOLID and RK-SOAVE property method is selected as second choice [97].
- No heat losses and pressure drops take place in heat exchangers of hydrogen production Cu-Cl cycle [98].
- For all the turbines, the isentropic efficiency of 72% is considered [99].
- The efficiency of electrical generator is considered as 95% [94].
- No heat losses occurs in the steam turbines.
- No heat losses occurs in hydrogen compressors because of the adiabatic consideration.

- For all the compressors, the isentropic efficiency of 72% is considered [99].

The simulation is conducted considering the steady state operating conditions because starting and shut down of the power plants is negligible as compared to their life. Gases included in chemical exergy equation are ideal gases whereas all other gases are considered as real gases because real gases provide more accurate results then the ideal gases. The kinetic and gravitational energies are neglected because they are negligible as compared to the enthalpy values. SOLID property method is used for Aspen Plus modeling because this property method deals with the chemical reactions as well. Aspen Plus takes the isentropic efficiency of turbines and compressors as 72%. The heat losses in heat exchangers and compressors are negligible as compared to the amount of heat and work thus no heat losses are considered.

The assumptions made for system 2 are listed as follows:

- The system operates under steady-state conditions [90].
- No starting up period considered.
- All gases in the chemical exergy equations are considered as real gases.
- The changes in kinetic and potential energies are neglected [96].
- The Aspen Plus property method used for the analysis to deal with real components is SOLID and RK-SOAVE property method is selected as second choice.
- No heat losses and pressure drops take place in heat exchangers of integrated system [94].
- The reference conditions are taken as 25 ℃ temperature and 1 atm pressure.
- The adiabatic conditions are considered for compressors and turbines.
- For all the turbines and compressors, the isentropic efficiency of 72% is considered [99].

The steady state operation is considered because the start up and shut down period of plants is negligible as compared to the life of plant. All the gases are considered as real gases except those which are included in chemical exergy equation. The kinetic and gravitational energies are neglected because they as very small as compared to the enthalpy

properties. SOLID property method is used for Aspen Plus because it deals with the chemical reactions as well.

The assumptions made for system 3 are listed as follows:

- The system operates under steady-state conditions [90].
- All gases in the chemical exergy equations are considered as real gases.
- The changes in kinetic and potential energies are neglected [96].
- The Aspen Plus property method used for the analysis to deal with real components is SOLID and RK-SOAVE property method is selected as second choice [94].
- The reference conditions are taken as 25 ℃ temperature and 1 atm pressure.
- The mechanical efficiency of compressor is considered as 95% [100].
- The adiabatic conditions are considered for compressors and turbines.
- No heat losses and pressure drops take place in heat exchangers of integrated system.
- Salinity of sea water for reverse osmosis unit is considered as 35000 PPM [89].
- The isentropic efficiency of pumps included in desalination is considered as 85% [88].
- Recovery ratio for desalination is considered as 60 % [87].

The steady state operating condition are considered and all the gases are treated as real gases instead of the gases included in chemical exergy equation. The kinetic and gravitational energies are neglected because they are negligible as compared to the enthalpy values. The heat losses in heat exchangers and compressors are negligible as compared to the amount of heat and work thus no heat losses are considered. The salinity of the salt water is close to 35000 PPM and recovery ratio is considered as 60% from the previous study.

4.3 Thermodynamic analysis of system 1

The thermodynamic analysis is conducted on the system and the energy, entropy and exergy balance equations of all components of the integrated system 1 are described in Tables 4.1 for the components depicted in Figure 3.2 and 3.3. Stoichiometric reactor

operates on the provided conversion percentage of reactants including mass and energy balance [95].

The exergy destruction and exergy efficiency of each component [101] are obtained through exergy analysis of integrated system 1 including the Rankine cycle, hydrogen production Cu-Cl cycle, hydrogen compression cycle and multistage Rankine cycle. These are calculated and equations are tabulated in Table 4.2

For the first integrated system producing hydrogen from steel industrial waste heat. The energy and exergy efficiencies of subsystems and for the overall system are described in the coming section. The energy efficiency of the subsystem Rankine cycle (RC) can be described as:

$$\eta_{RC} = \frac{W_{Turb(B2)}}{\dot{m}_{S5}(h_{S5} - h_{S10})} \tag{4.10}$$

In the equation described above, W_{Turb} is the power produced by the turbine B2. The subscripts for the components and streams refers to the Figure 3.2. The energy efficiency of the thermochemical Cu-Cl cycle is as follows:

$$\eta_{Cu-Cl} = \frac{\dot{m}_{H_2} LHV_{H_2}}{\dot{Q}_{in} + \dot{W}_e} \tag{4.11}$$

$$\dot{Q}_{in} = \dot{Q}_{B6} + \dot{Q}_{B7} + \dot{Q}_{B10} + \dot{Q}_{B11} + \dot{Q}_{B17} + \dot{Q}_{B8} + \dot{Q}_{B23} + \dot{Q}_{B24} + \dot{Q}_{B25} \tag{4.12}$$

In the efficiency equation of Cu-Cl cycle, LHV is the lower heating value of hydrogen gas, Q_{in} is the heat total heat input and W_e is the electric power supplied to the electrolyzer. The energy efficiency of the multistage Rankine cycle (MSRC) is as follows:

$$\eta_{MSRC} = \frac{\dot{W}_{Turb(27)} + \dot{W}_{Turb(28)} + \dot{W}_{Turb(29)}}{\dot{m}_{S21}(h_{S40} - h_{S21})} \tag{4.13}$$

The subscripts of the components and streams refers to the Figure 3.3. The factor W_{Turb} is the power produced by the three turbines.

The heat released from the condenser can be formulated as:

$$\dot{Q}_{heating} = \dot{m}_{40}(h_{46} - h_{45}) + \dot{m}_{22}(h_{44} - h_{43}) \tag{4.14}$$

Table 4.1 The energy, entropy and exergy balance equations on all components of integrated system 1 demonstrated in Figures 3.2 and 3.3 and the subscripts of component and stream names also refers to Figures 3.2 and 3.3.

Component	Energy balance equation	Entropy balance equation	Exergy balance equation
B1 (heat exchanger)	$\dot{m}_{s1}h_{s1} + \dot{m}_{s3}h_{s3} + \dot{m}_{s10}h_{s10} = \dot{m}_{s2}h_{s2} + \dot{m}_{s4}h_{s4} + \dot{m}_{s5}h_{s5}$	$\dot{m}_{s1}s_{s1} + \dot{m}_{s3}s_{s3} + \dot{m}_{s10}s_{s10} + \dot{S}_{gen} = \dot{m}_{s2}s_{s2} + \dot{m}_{s4}s_{s4} + \dot{m}_{s5}s_{s5}$	$\dot{m}_{s1}ex_{s1} + \dot{m}_{s3}ex_{s3} + \dot{m}_{s10}ex_{s10} = \dot{m}_{s2}ex_{s2} + \dot{m}_{s4}ex_{s4} + \dot{m}_{s5}ex_{s5} + \dot{E}x_d$
B2 (turbine)	$\dot{m}_{s5}h_{s5} = \dot{m}_{s7}h_{s7} + \dot{W}_{out}$	$\dot{m}_{s5}s_{s5} + \dot{S}_{gen} = \dot{m}_{s7}s_{s7}$	$\dot{m}_{s5}ex_{s5} = \dot{m}_{s7}ex_{s7} + \dot{W}_{out} + \dot{E}x_d$
B3 (heat exchanger)	$\dot{m}_{s7}h_{s7} = \dot{m}_{s9}h_{s9} + \dot{Q}_{out}$	$\dot{m}_{s7}s_{s7} + \dot{S}_{gen} = \dot{m}_{s9}s_{s9} + \frac{\dot{Q}_{out}}{T_0}$	$\dot{m}_{s7}ex_{s7} = \dot{m}_{s9}ex_{s9} + \dot{E}x_{\dot{Q}_{out}} + \dot{E}x_d$
B4 (pump 1)	$\dot{m}_{s9}h_{s9} + \dot{W}_{in} = \dot{m}_{s10}h_{s10}$	$\dot{m}_{s9}s_{s9} + \dot{S}_{gen} = \dot{m}_{s10}s_{s10}$	$\dot{m}_{s9}ex_{s9} + \dot{W}_{in} = \dot{m}_{s10}ex_{s10} + \dot{E}x_d$
B6 (heat exchanger)	$\dot{m}_{s13}h_{s13} + \dot{Q}_{in} = \dot{m}_{s14}h_{s14}$	$\dot{m}_{s13}s_{s13} + \dot{S}_{gen} + \frac{\dot{Q}_{in}}{T_0} = \dot{m}_{s14}s_{s14}$	$\dot{m}_{s13}ex_{s13} + \dot{E}x_{\dot{Q}_{in}} = \dot{m}_{s14}ex_{s14} + \dot{E}x_d$
B7 (heat exchanger)	$\dot{m}_{s11}h_{s11} + \dot{Q}_{in} = \dot{m}_{s12}h_{s12}$	$\dot{m}_{s11}s_{s11} + \dot{S}_{gen} + \frac{\dot{Q}_{in}}{T_0} = \dot{m}_{s12}s_{s12}$	$\dot{m}_{s11}ex_{s11} + \dot{E}x_{\dot{Q}_{in}} = \dot{m}_{s12}ex_{s12} + \dot{E}x_d$
B8 (stoichiometric reactor)	$\dot{m}_{s14}h_{s14} + \dot{m}_{s29}h_{s29} = \dot{m}_{s15}h_{s15}$	$\dot{m}_{s14}s_{s14} + \dot{m}_{s29}s_{s29} + \dot{S}_{gen} = \dot{m}_{s15}s_{s15}$	$\dot{m}_{s14}ex_{14} + \dot{m}_{s29}ex_{29} = \dot{m}_{s15}ex_{s15} + \dot{E}x_d$
B9 (separator)	$\dot{m}_{s15}h_{s15} = \dot{m}_{s16}h_{s16} + \dot{m}_{s17}h_{s17}$	$\dot{m}_{s15}s_{s15} + \dot{S}_{gen} = \dot{m}_{s16}s_{s16} + \dot{m}_{s17}s_{s17}$	$\dot{m}_{s15}ex_{s15} = \dot{m}_{s16}ex_{s16} + \dot{m}_{s17}ex_{s17} + \dot{E}x_d$
B11 (stoichiometric reactor)	$\dot{m}_{s12}h_{s12} + \dot{m}_{s19}h_{s19} + \dot{Q}_{in} = \dot{m}_{s20}h_{s20}$	$\dot{m}_{s12}s_{s12} + \dot{m}_{s19}s_{s19} + \dot{S}_{gen} + \frac{\dot{Q}_{in}}{T_0} = \dot{m}_{s20}s_{s20}$	$\dot{m}_{s12}ex_{s12} + \dot{m}_{s19}ex_{s19} + \dot{E}x_{\dot{Q}_{in}} = \dot{m}_{s20}ex_{s20} + \dot{E}x_d$
B12 (separator)	$\dot{m}_{s20}h_{s20} = \dot{m}_{s21}h_{s21} + \dot{m}_{s22}h_{s22}$	$\dot{m}_{s20}s_{s20} + \dot{S}_{gen} = \dot{m}_{s21}s_{s21} + \dot{m}_{s22}s_{s22}$	$\dot{m}_{s20}ex_{s20} = \dot{m}_{s21}ex_{s21} + \dot{m}_{s22}ex_{s22} + \dot{E}x_d$
B13 (heat exchanger)	$\dot{m}_{s22}h_{s22} = \dot{m}_{s24}h_{s24} + \dot{Q}_{out}$	$\dot{m}_{s22}s_{s22} + \dot{S}_{gen} = \dot{m}_{s24}s_{s24} + \frac{\dot{Q}_{out}}{T_0}$	$\dot{m}_{s22}ex_{s22} = \dot{m}_{s24}ex_{s24} + \dot{E}x_{\dot{Q}_{out}} + \dot{E}x_d$
B14 (stoichiometric reactor)	$\dot{m}_{s18}h_{s18} + \dot{m}_{s24}h_{s24} + \dot{W}_e = \dot{m}_{s25}h_{s25}$	$\dot{m}_{s18}s_{s18} + \dot{m}_{s24}s_{s24} + \dot{S}_{gen} = \dot{m}_{s25}s_{s25}$	$\dot{m}_{s18}ex_{s18} + \dot{m}_{s24}ex_{s24} + \dot{W}_e = \dot{m}_{s25}ex_{s25} + \dot{E}x_d$

B15 (heat exchanger)	$\dot{m}_{s17}h_{s17} = \dot{m}_{s18}h_{s18} + \dot{Q}_{out}$	$\dot{m}_{s17}s_{s17} + \dot{S}_{gen} = \dot{m}_{s18}s_{s18} + \frac{\dot{Q}_{out}}{T_0}$	$\dot{m}_{s17}ex_{s17} = \dot{m}_{s18}ex_{s87} + \dot{E}x_{\dot{Q}_{out}} + \dot{E}x_d$
B16 (separator)	$\dot{m}_{s25}h_{s25} = \dot{m}_{s26}h_{s26} + \dot{m}_{s27}h_{s27}$	$\dot{m}_{s25}s_{s25} + \dot{S}_{gen} = \dot{m}_{s26}s_{s26} + \dot{m}_{s27}s_{s27}$	$\dot{m}_{s25}ex_{s25} = \dot{m}_{s26}ex_{s26} + \dot{m}_{s27}ex_{s27} + \dot{E}x_d$
B17 (heat exchanger)	$\dot{m}_{s27}h_{s27} + \dot{Q}_{in} = \dot{m}_{s28}h_{s28}$	$\dot{m}_{s27}s_{s27} + \dot{S}_{gen} + \frac{\dot{Q}_{in}}{T_0} = \dot{m}_{s28}s_{s28}$	$\dot{m}_{s27}ex_{s27} + \dot{E}x_{\dot{Q}_{in}} = \dot{m}_{s28}ex_{s28} + \dot{E}x_d$
B18 (Dryer)	$\dot{m}_{s28}h_{s28} = \dot{m}_{s29}h_{s29} + \dot{m}_{s30}h_{s30}$	$\dot{m}_{s28}s_{s28} + \dot{S}_{gen} = \dot{m}_{s29}s_{s29} + \dot{m}_{s30}s_{s30}$	$\dot{m}_{s28}ex_{s28} = \dot{m}_{s29}ex_{s29} + \dot{m}_{s30}ex_{s30} + \dot{E}x_d$
B20 (compressor 1)	$\dot{m}_{s26}h_{s26} + \dot{W}_{in} = \dot{m}_{s31}h_{s31}$	$\dot{m}_{s26}s_{s26} + \dot{S}_{gen} = \dot{m}_{s31}s_{s31}$	$\dot{m}_{s26}ex_{s26} + \dot{W}_{in} = \dot{m}_{s31}ex_{s31} + \dot{E}x_d$
B21 (compressor 1)	$\dot{m}_{s33}h_{s33} + \dot{W}_{in} = \dot{m}_{s34}h_{s34}$	$\dot{m}_{s33}s_{s33} + \dot{S}_{gen} = \dot{m}_{s34}s_{s34}$	$\dot{m}_{s33}ex_{s33} + \dot{W}_{in} = \dot{m}_{s34}ex_{s34} + \dot{E}x_d$
B22 (compressor 1)	$\dot{m}_{s36}h_{s36} + \dot{W}_{in} = \dot{m}_{s37}h_{s37}$	$\dot{m}_{s36}s_{s36} + \dot{S}_{gen} = \dot{m}_{s37}s_{s37}$	$\dot{m}_{s36}ex_{s36} + \dot{W}_{in} = \dot{m}_{s37}ex_{s37} + \dot{E}x_d$
B23 (heat exchanger)	$\dot{m}_{s31}h_{s31} = \dot{m}_{s33}h_{s33} + \dot{Q}_{out}$	$\dot{m}_{s31}s_{s31} + \dot{S}_{gen} = \dot{m}_{s33}s_{s33} + \frac{\dot{Q}_{out}}{T_0}$	$\dot{m}_{s31}ex_{s31} = \dot{m}_{s33}ex_{s33} + \dot{E}x_{\dot{Q}_{out}} + \dot{E}x_d$
B24 (heat exchanger)	$\dot{m}_{s34}h_{s34} = \dot{m}_{s36}h_{s36} + \dot{Q}_{out}$	$\dot{m}_{s34}s_{s34} + \dot{S}_{gen} = \dot{m}_{s36}s_{s36} + \frac{\dot{Q}_{out}}{T_0}$	$\dot{m}_{s34}ex_{s34} = \dot{m}_{s36}ex_{s36} + \dot{E}x_{\dot{Q}_{out}} + \dot{E}x_d$
B25 (heat exchanger)	$\dot{m}_{s37}h_{s37} = \dot{m}_{s39}h_{s39} + \dot{Q}_{out}$	$\dot{m}_{s37}s_{s37} + \dot{S}_{gen} = \dot{m}_{s39}s_{s39} + \frac{\dot{Q}_{out}}{T_0}$	$\dot{m}_{s37}ex_{s37} = \dot{m}_{s39}ex_{s39} + \dot{E}x_{\dot{Q}_{out}} + \dot{E}x_d$
B26 (heat exchanger)	$\dot{m}_{s21}h_{s21} + \dot{m}_{s42}h_{s42} + \dot{m}_{s44}h_{s44} + \dot{m}_{s48}h_{s48} = \dot{m}_{s40}h_{s40} + \dot{m}_{s41}h_{s41} + \dot{m}_{s43}h_{s43} + \dot{m}_{s45}h_{s45}$	$\dot{m}_{s21}s_{s21} + \dot{m}_{s42}s_{s42} + \dot{m}_{s44}s_{s44} + \dot{m}_{s48}s_{s48} + \dot{S}_{gen} = \dot{m}_{s40}s_{s40} + \dot{m}_{s41}s_{s41} + \dot{m}_{s43}s_{s43} + \dot{m}_{s45}s_{s45}$	$\dot{m}_{s21}ex_{s21} + \dot{m}_{s42}ex_{s42} + \dot{m}_{s44}ex_{s44} + \dot{m}_{s48}ex_{s48} = \dot{m}_{s40}ex_{s40} + \dot{m}_{s41}ex_{s41} + \dot{m}_{s43}ex_{s43} + \dot{m}_{s45}ex_{s45} + \dot{E}x_d$
B27 (Turbine 1)	$\dot{m}_{s41}h_{s41} = \dot{m}_{s42}h_{s42} + \dot{W}_{out}$	$\dot{m}_{s41}s_{s41} + \dot{S}_{gen} = \dot{m}_{s42}s_{s42}$	$\dot{m}_{s41}ex_{s41} = \dot{m}_{s42}ex_{s42} + \dot{W}_{out} + \dot{E}x_d$
B28 (Turbine 2)	$\dot{m}_{s43}h_{s43} = \dot{m}_{s44}h_{s44} + \dot{W}_{out}$	$\dot{m}_{s43}s_{s43} + \dot{S}_{gen} = \dot{m}_{s44}s_{s44}$	$\dot{m}_{s43}ex_{s43} = \dot{m}_{s44}ex_{s44} + \dot{W}_{out} + \dot{E}x_d$

B29 (Turbine 3)	$\dot{m}_{s45}h_{s45} = \dot{m}_{s46}h_{s46} + \dot{W}_{out}$	$\dot{m}_{s45}s_{s45} + \dot{S}_{gen} = \dot{m}_{s46}s_{s46}$	$\dot{m}_{s45}ex_{s45} = \dot{m}_{s46}ex_{s46} + \dot{W}_{out} + \dot{E}x_d$
B30 (heat exchanger)	$\dot{m}_{s46}h_{s46} = \dot{m}_{s47}h_{s47} + \dot{Q}_{out}$	$\dot{m}_{s46}s_{s46} + \dot{S}_{gen} = \dot{m}_{s47}s_{s47} + \frac{\dot{Q}_{out}}{T_0}$	$\dot{m}_{s46}ex_{s46} = \dot{m}_{s47}ex_{s47} + \dot{E}x_{\dot{Q}_{out}} + \dot{E}x_d$
B31 (pump)	$\dot{m}_{s47}h_{s47} + \dot{W}_{in} = \dot{m}_{s48}h_{s48}$	$\dot{m}_{s47}s_{s47} + \dot{S}_{gen} = \dot{m}_{s48}s_{s48}$	$\dot{m}_{s47}ex_{s47} + \dot{W}_{in} = \dot{m}_{s48}ex_{s48} + \dot{E}x_d$

The overall energy efficiency of the hydrogen production integrated system 1 can be written as:

$$\eta_{ov} = \frac{\dot{m}_{H_2} LHV_{H_2} + \dot{W}_{net} + \dot{Q}_{heating}}{\dot{Q}_{S1}} \quad (4.15)$$

$$\dot{W}_{net} = \dot{W}_{Turb(B2)} + \dot{W}_{Turb(B27)} + \dot{W}_{Turb(28)} + \dot{W}_{Turb(29)} - \dot{W}_e - \dot{W}_{comp1} - \dot{W}_{comp2} - \dot{W}_{comp3} - \dot{W}_{pump\ B4} - \dot{W}_{B31} \quad (4.16)$$

The exergy efficiency of the subsystem Rankine cycle (RC) can be described as:

$$\psi_{RC} = \frac{W_{Turb(B2)}}{\dot{m}_{S5}(ex_{S5} - ex_{S10})} \quad (4.17)$$

The exergy efficiency of the thermochemical Cu-Cl cycle is as follows:

$$\psi_{Cu-Cl} = \frac{\dot{m}_{H_2} ex_{H_2}}{\dot{E}x_{\dot{Q}_{in}} + \dot{W}_e} \quad (4.18)$$

$$\dot{E}x_{\dot{Q}_{in}} = \dot{E}x_{\dot{Q}_{B6}} + +\dot{E}x_{\dot{Q}_{B7}} + \dot{E}x_{\dot{Q}_{B10}} + \dot{E}x_{\dot{Q}_{B11}} + \dot{E}x_{\dot{Q}_{B17}} + \dot{E}x_{\dot{Q}_{B8}} + \dot{E}x_{\dot{Q}_{B23}} + \dot{E}x_{\dot{Q}_{B24}} + \dot{E}x_{\dot{Q}_{B25}} \quad (4.19)$$

The exergy efficiency of the multistage Rankine cycle (MSRC) is as follows:

$$\psi_{MSRC} = \frac{\dot{W}_{Turb(27)} + \dot{W}_{Turb(28)} + \dot{W}_{Turb(29)}}{\dot{m}_{S21}(ex_{S40} - ex_{S21})} \quad (4.20)$$

Table 0.1 The exergy destruction and exergy efficiency of each component included in integrated system 1. The subscripts of components and streams refers to the Figure 3.2 and 3.3.

Component	Exergy efficiency	Exergy destruction rate
B1 (heat exchanger)	$\psi_{B1} = \frac{\dot{m}_{s2}ex_{s2} + \dot{m}_{s4}ex_{s4} + \dot{m}_{s5}ex_{s5}}{\dot{m}_{s1}ex_{s1} + \dot{m}_{s3}ex_{s3} + \dot{m}_{s10}ex_{s10}}$	$\dot{E}x_d = \dot{m}_{s1}ex_{s1} + \dot{m}_{s3}ex_{s3} + \dot{m}_{s10}ex_{s10} - (\dot{m}_{s2}ex_{s2} + \dot{m}_{s4}ex_{s4} + \dot{m}_{s5}ex_{s5})$
B2 (turbine)	$\psi_{B2} = \frac{\dot{m}_{s7}ex_{s7} + \dot{W}_{out}}{\dot{m}_{s7}ex_{s7}}$	$\dot{E}x_d = \dot{m}_{s5}ex_{s5} - (\dot{m}_{s7}ex_{s7} + \dot{W}_{out})$
B3 (heat exchanger)	$\psi_{B3} = \frac{\dot{m}_{s9}ex_{s9} + \dot{E}x_{\dot{Q}_{out}}}{\dot{m}_{s7}ex_{s7}}$	$\dot{E}x_d = \dot{m}_{s7}ex_{s7} - (\dot{m}_{s9}ex_{s9} + \dot{E}x_{\dot{Q}_{out}})$
B4 (pump 1)	$\psi_{B4} = \frac{\dot{m}_{s10}ex_{s10}}{\dot{m}_{s9}ex_{s9} + \dot{W}_{in}}$	$\dot{E}x_d = \dot{m}_{s9}ex_{s9} + \dot{W}_{in} - \dot{m}_{s10}ex_{s10}$
B6 (heat exchanger)	$\psi_{B6} = \frac{\dot{m}_{s14}ex_{s14}}{\dot{m}_{s13}ex_{s13} + \dot{E}x_{\dot{Q}_{in}}}$	$\dot{E}x_d = \dot{m}_{s13}ex_{s13} + \dot{E}x_{\dot{Q}_{in}} - \dot{m}_{s14}ex_{s14}$
B7 (heat exchanger)	$\psi_{B7} = \frac{\dot{m}_{s12}ex_{s12}}{\dot{m}_{s11}ex_{s11} + \dot{E}x_{\dot{Q}_{in}}}$	$\dot{E}x_d = \dot{m}_{s11}ex_{s11} + \dot{E}x_{\dot{Q}_{in}} - \dot{m}_{s12}ex_{s12}$
B8 (stoichiometric reactor)	$\psi_{B8} = \frac{\dot{m}_{s15}ex_{s15}}{\dot{m}_{s14}ex_{14} + \dot{m}_{s29}ex_{29}}$	$\dot{E}x_d = \dot{m}_{s14}ex_{14} + \dot{m}_{s29}ex_{29} - \dot{m}_{s15}ex_{s15}$
B9 (separator)	$\psi_{B9} = \frac{\dot{m}_{s16}ex_{s16} + \dot{m}_{s17}ex_{s17}}{\dot{m}_{s15}ex_{s15}}$	$\dot{E}x_d = \dot{m}_{s15}ex_{s15} - (\dot{m}_{s16}ex_{s16} + \dot{m}_{s17}ex_{s17})$
B11 (stoichiometric reactor)	$\psi_{B11} = \frac{\dot{m}_{s20}ex_{s20}}{\dot{m}_{s12}ex_{s12} + \dot{m}_{s19}ex_{s19} + \dot{E}x_{\dot{Q}_{in}}}$	$\dot{E}x_d = \dot{m}_{s12}ex_{s12} + \dot{m}_{s19}ex_{s19} + \dot{E}x_{\dot{Q}_{in}} - \dot{m}_{s20}ex_{s20}$
B12 (separator)	$\psi_{B12} = \frac{\dot{m}_{s21}ex_{s21} + \dot{m}_{s22}ex_{s22}}{\dot{m}_{s20}ex_{s20}}$	$\dot{E}x_d = \dot{m}_{s20}ex_{s20} - (\dot{m}_{s21}ex_{s21} + \dot{m}_{s22}ex_{s22})$
B13 (heat exchanger)	$\psi_{B13} = \frac{\dot{m}_{s24}ex_{s24} + \dot{E}x_{\dot{Q}_{out}}}{\dot{m}_{s22}ex_{s22}}$	$\dot{E}x_d = \dot{m}_{s22}ex_{s22} - (\dot{m}_{s24}ex_{s24} + \dot{E}x_{\dot{Q}_{out}})$
B14 (stoichiometric reactor)	$\psi_{B14} = \frac{\dot{m}_{s25}ex_{s25}}{\dot{m}_{s18}ex_{s18} + \dot{m}_{s24}ex_{s24} + \dot{W}_e}$	$\dot{E}x_d = \dot{m}_{s18}ex_{s18} + \dot{m}_{s24}ex_{s24} + \dot{W}_e - \dot{m}_{s25}ex_{s25}$
B15 (heat exchanger)	$\psi_{B15} = \frac{\dot{m}_{s18}ex_{s87} + \dot{E}x_{\dot{Q}_{out}}}{\dot{m}_{s17}ex_{s17}}$	$\dot{E}x_d = \dot{m}_{s17}ex_{s17} - (\dot{m}_{s18}ex_{s87} + \dot{E}x_{\dot{Q}_{out}})$
B16 (separator)	$\psi_{B16} = \frac{\dot{m}_{s26}ex_{s26} + \dot{m}_{s27}ex_{s27}}{\dot{m}_{s25}ex_{s25}}$	$\dot{E}x_d = \dot{m}_{s25}ex_{s25} - (\dot{m}_{s26}ex_{s26} + \dot{m}_{s27}ex_{s27})$

B17 (heat exchanger)	$\psi_{B17} = \frac{\dot{m}_{s28} ex_{s28}}{\dot{m}_{s27} ex_{s27} + \dot{E}x_{\dot{Q}_{in}}}$	$\dot{E}x_d = \dot{m}_{s27} ex_{s27} + \dot{E}x_{\dot{Q}_{in}} - \dot{m}_{s28} ex_{s28}$
B18 (Dryer)	$\psi_{B18} = \frac{\dot{m}_{s29} ex_{s29} + \dot{m}_{s30} ex_{s30}}{\dot{m}_{s28} ex_{s28}}$	$\dot{E}x_d = \dot{m}_{s28} ex_{s28} - (\dot{m}_{s29} ex_{s29} + \dot{m}_{s30} ex_{s30})$
B20 (compressor 1)	$\psi_{B20} = \frac{\dot{m}_{s31} ex_{s31}}{\dot{m}_{s26} ex_{s26} + \dot{W}_{in}}$	$\dot{E}x_d = \dot{m}_{s26} ex_{s26} + \dot{W}_{in} - \dot{m}_{s31} ex_{s31}$
B21 (compressor 1)	$\psi_{B21} = \frac{\dot{m}_{s34} ex_{s34}}{\dot{m}_{s33} ex_{s33} + \dot{W}_{in}}$	$\dot{E}x_d = \dot{m}_{s33} ex_{s33} + \dot{W}_{in} - \dot{m}_{s34} ex_{s34}$
B22 (compressor 1)	$\psi_{B22} = \frac{\dot{m}_{s37} ex_{s37}}{\dot{m}_{s36} ex_{s36} + \dot{W}_{in}}$	$\dot{E}x_d = \dot{m}_{s36} ex_{s36} + \dot{W}_{in} - \dot{m}_{s37} ex_{s37}$
B23 (heat exchanger)	$\psi_{B23} = \frac{\dot{m}_{s33} ex_{s33} + \dot{E}x_{\dot{Q}_{out}}}{\dot{m}_{s31} ex_{s31}}$	$\dot{E}x_d = \dot{m}_{s31} ex_{s31} - (\dot{m}_{s33} ex_{s33} + \dot{E}x_{\dot{Q}_{out}})$
B24 (heat exchanger)	$\psi_{B24} = \frac{\dot{m}_{s36} ex_{s36} + \dot{E}x_{\dot{Q}_{out}}}{\dot{m}_{s34} ex_{s34}}$	$\dot{E}x_d = \dot{m}_{s34} ex_{s34} - (\dot{m}_{s36} ex_{s36} + \dot{E}x_{\dot{Q}_{out}})$
B25 (heat exchanger)	$\psi_{B25} = \frac{\dot{m}_{s39} ex_{s39} + \dot{E}x_{\dot{Q}_{out}}}{\dot{m}_{s37} ex_{s37}}$	$\dot{E}x_d = \dot{m}_{s37} ex_{s37} - (\dot{m}_{s39} ex_{s39} + \dot{E}x_{\dot{Q}_{out}})$
B26 (heat exchanger)	$\psi_{B26} = \frac{\dot{m}_{s40} ex_{s40} + \dot{m}_{s41} ex_{s41} + \dot{m}_{s43} ex_{s43} + \dot{m}_{s45} ex}{\dot{m}_{s21} ex_{s21} + \dot{m}_{s42} ex_{s42} + \dot{m}_{s44} ex_{s44} + \dot{m}_{s48} ex}$	$\dot{E}x_d = \dot{m}_{s21} ex_{s21} + \dot{m}_{s42} ex_{s42} + \dot{m}_{s44} ex_{s44} + \dot{m}_{s48} ex_{s48} - (\dot{m}_{s40} ex_{s40} + \dot{m}_{s41} ex_{s41} + \dot{m}_{s43} ex_{s43} + \dot{m}_{s45} ex_{s45})$
B27 (Turbine 1)	$\psi_{B27} = \frac{\dot{m}_{s42} ex_{s42} + \dot{W}_{out}}{\dot{m}_{s41} ex_{s41}}$	$\dot{E}x_d = \dot{m}_{s41} ex_{s41} - (\dot{m}_{s42} ex_{s42} + \dot{W}_{out})$
B28 (Turbine 2)	$\psi_{B28} = \frac{\dot{m}_{s44} ex_{s44} + \dot{W}_{out}}{\dot{m}_{s43} ex_{s43}}$	$\dot{E}x_d = \dot{m}_{s43} ex_{s43} - (\dot{m}_{s44} ex_{s44} + \dot{W}_{out})$
B29 (Turbine 3)	$\psi_{B29} = \frac{\dot{m}_{s46} ex_{s46} + \dot{W}_{out}}{\dot{m}_{s45} ex_{s45}}$	$\dot{E}x_d = \dot{m}_{s45} ex_{s45} - (\dot{m}_{s46} ex_{s46} + \dot{W}_{out})$
B30 (heat exchanger)	$\psi_{B30} = \frac{\dot{m}_{s47} ex_{s47} + \dot{E}x_{\dot{Q}_{out}}}{\dot{m}_{s46} ex_{s46}}$	$\dot{E}x_d = \dot{m}_{s46} ex_{s46} - (\dot{m}_{s47} ex_{s47} + \dot{E}x_{\dot{Q}_{out}})$
B31 (pump)	$\psi_{B31} = \frac{\dot{m}_{s48} ex_{s48}}{\dot{m}_{s47} ex_{s47} + \dot{W}_{in}}$	$\dot{E}x_d = \dot{m}_{s47} ex_{s47} + \dot{W}_{in} - \dot{m}_{s48} ex_{s48}$

The overall exergy efficiency of the hydrogen integrated system 1 can be written as:

$$\psi_{ov} = \frac{\dot{m}_{H_2} ex_{H_2} + \dot{W}_{net} + \dot{E}x_{Q_{heating}}}{\dot{E}x_{\dot{Q}_{S1}}} \quad (4.21)$$

4.4 Thermodynamic analysis of system 2

The thermodynamics analysis is conducted on the integrated hydrogen production system 2 in this section. Table 4.3 describes the energy, entropy and exergy balance equations of all component of the integrated system 2. The subscripts of components and streams refers to the Figure 3.5.

The integrated system 2 contains thermochemical hydrogen production copper chlorine cycle, hydrogen compression cycle and multistage reheat Rankine cycle. The exergy destruction and exergy efficiency of each component of second integrated system is defined and tabulated in Table 4.4. The subscripts of the components and streams are described according to the Figure 3.5.

For the second integrated system producing hydrogen from cement industrial waste heat. The energy and exergy efficiencies of subsystems and the overall system are described in this section. The energy efficiency of the subsystem thermochemical Cu-Cl cycle can be described as:

$$\eta_{Cu-Cl} = \frac{\dot{m}_{H_2} LHV_{H_2}}{\dot{Q}_{in} + \dot{W}_e} \tag{4.22}$$

$$\dot{Q}_{in} = \dot{Q}_{B1} + \dot{Q}_{B6} + \dot{Q}_{B4} + \dot{Q}_{B2} + \dot{Q}_{B5} + \dot{Q}_{B12} + \dot{Q}_{B23} + \dot{Q}_{B24} + \dot{Q}_{B25} \tag{4.23}$$

The exergy efficiency of the thermochemical Cu-Cl cycle is as follows:

$$\psi_{Cu-Cl} = \frac{\dot{m}_{H_2} ex_{H_2}}{\dot{E}x_{\dot{Q}_{in}} + \dot{W}_e} \tag{4.24}$$

$$\dot{E}x_{\dot{Q}_{in}} = \dot{E}x_{\dot{Q}_{B1}} + \dot{E}x_{B6} + \dot{E}x_{\dot{Q}_{B2}} + \dot{E}x_{\dot{Q}_{B4}} + \dot{E}x_{\dot{Q}_{B5}} + \dot{E}x_{\dot{Q}_{B12}} + \dot{E}x_{\dot{Q}_{B23}} + \dot{E}x_{\dot{Q}_{B24}} + \dot{E}x_{\dot{Q}_{B25}} \tag{4.25}$$

The energy efficiency of the multistage Rankine cycle (MSRC) is as follows:

$$\eta_{MSRC} = \frac{\dot{W}_{Turb(14)} + \dot{W}_{Turb(16)} + \dot{W}_{Turb(17)}}{\dot{m}_{S13}(h_{S4} - h_{S13})} \tag{4.26}$$

The subscripts of the components and streams refers to the Figure 3.5.

Table 0.2 The energy, entropy and exergy balance equations on all components of integrated system 2 containing Cu-Cl cycle, hydrogen compression and multistage reheat Rankine cycle demonstrated in Figure 3.5 and the subscripts of component and stream names also refers to Figure 3.5.

Component	Energy balance equation	Entropy balance equation	Exergy balance equation
B1 (heat exchanger)	$\dot{m}_{s1}h_{s1} + \dot{Q}_{in} = \dot{m}_{s2}h_{s2}$	$\dot{m}_{s1}s_{s1} + \dot{S}_{gen} + \frac{\dot{Q}_{in}}{T_0} = \dot{m}_{s2}s_{s2}$	$\dot{m}_{s1}ex_{s1} + \dot{E}x_{\dot{Q}_{in}} = \dot{m}_{s2}ex_{s2} + \dot{E}x_d$
B2 (stoichiometric reactor)	$\dot{m}_{s2}h_{s2} + \dot{m}_{s2}h_{s2} = \dot{m}_{s3}h_{s3}$	$\dot{m}_{s2}s_{s2} + \dot{m}_{s2}s_{s2} + \dot{S}_{gen} = \dot{m}_{s3}s_{s3}$	$\dot{m}_{s2}ex + \dot{m}_{s2}ex = \dot{m}_{s3}ex_{s3} + \dot{E}x_d$
B3 (separator)	$\dot{m}_{s3}h_{s3} = \dot{m}_{s5}h_{s5} + \dot{m}_{s6}h_{s6}$	$\dot{m}_{s3}s_{s3} + \dot{S}_{gen} = \dot{m}_{s5}s_{s5} + \dot{m}_{s6}s_{s6}$	$\dot{m}_{s3}ex_{s3} = \dot{m}_{s5}ex_{s5} + \dot{m}_{s6}ex_{s6} + \dot{E}x_d$
B5 (stoichiometric reactor)	$\dot{m}_{s7}h_{s7} + \dot{m}_{s9}h_{s9} + \dot{Q}_{in} = \dot{m}_{s10}h_{s10}$	$\dot{m}_{s7}s_{s7} + \dot{m}_{s9}s_{s9} + \dot{S}_{gen} + \frac{\dot{Q}_{in}}{T_0} = \dot{m}_{s10}s_{s10}$	$\dot{m}_{s7}ex_{s7} + \dot{m}_{s9}ex_{s9} + \dot{E}x_{\dot{Q}_{in}} = \dot{m}_{s10}ex_{s10} + \dot{E}x_d$
B6 (heat exchanger)	$\dot{m}_{s8}h_{s8} + \dot{Q}_{in} = \dot{m}_{s9}h_{s9}$	$\dot{m}_{s8}s_{s8} + \dot{S}_{gen} + \frac{\dot{Q}_{in}}{T_0} = \dot{m}_{s9}s_{s9}$	$\dot{m}_{s8}ex_{s8} + \dot{E}x_{\dot{Q}_{in}} = \dot{m}_{s9}ex_{s9} + \dot{E}x_d$
B7 (separator)	$\dot{m}_{s10}h_{s10} = \dot{m}_{s11}h_{s11} + \dot{m}_{s12}h_{s12}$	$\dot{m}_{s10}s_{s10} + \dot{S}_{gen} = \dot{m}_{s11}s_{s11} + \dot{m}_{s12}s_{s12}$	$\dot{m}_{s10}ex_{s10} = \dot{m}_{s11}ex_{s11} + \dot{m}_{s12}ex_{s12} + \dot{E}x_d$
B8 (heat exchanger)	$\dot{m}_{s12}h_{s12} = \dot{m}_{s13}h_{s13} + \dot{Q}_{out}$	$\dot{m}_{s12}s_{s12} + \dot{S}_{gen} = \dot{m}_{s13}s_{s13} + \frac{\dot{Q}_{out}}{T_0}$	$\dot{m}_{s12}ex_{s12} = \dot{m}_{s13}ex_{s13} + \dot{E}x_{\dot{Q}_{out}} + \dot{E}x_d$
B9 (stoichiometric reactor)	$\dot{m}_{s13}h_{s13} + \dot{m}_{s17}h_{s17} + \dot{W}_e = \dot{m}_{s16}h_{s16}$	$\dot{m}_{s13}s_{s13} + \dot{m}_{s17}s_{s17} + \dot{S}_{gen} = \dot{m}_{s16}s_{s16}$	$\dot{m}_{s13}ex_{s13} + \dot{m}_{s17}ex_{s17} + \dot{W}_e = \dot{m}_{s16}ex_{s16} + \dot{E}x_d$
B10 (heat exchanger)	$\dot{m}_{s6}h_{s6} = \dot{m}_{s17}h_{s17} + \dot{Q}_{out}$	$\dot{m}_{s6}s_{s6} + \dot{S}_{gen} = \dot{m}_{s17}s_{s17} + \frac{\dot{Q}_{out}}{T_0}$	$\dot{m}_{s6}ex_{s6} = \dot{m}_{s17}ex_{s17} + \dot{E}x_{\dot{Q}_{out}} + \dot{E}x_d$
B11 (separator)	$\dot{m}_{s16}h_{s16} = \dot{m}_{s19}h_{s19} + \dot{m}_{s20}h_{s20}$	$\dot{m}_{s16}s_{s16} + \dot{S}_{gen} = \dot{m}_{s19}s_{s19} + \dot{m}_{s20}s_{s20}$	$\dot{m}_{s16}ex_{s16} = \dot{m}_{s19}ex_{s19} + \dot{m}_{s20}ex_{s20} + \dot{E}x_d$
B12 (heat exchanger)	$\dot{m}_{s20}h_{s20} + \dot{Q}_{in} = \dot{m}_{s21}h_{s21}$	$\dot{m}_{s20}s_{s20} + \dot{S}_{gen} + \frac{\dot{Q}_{in}}{T_0} = \dot{m}_{s21}s_{s21}$	$\dot{m}_{s20}ex_{s20} + \dot{E}x_{\dot{Q}_{in}} = \dot{m}_{s21}ex_{s21} + \dot{E}x_d$

B13 (heat exchanger)	$\dot{m}_{s11}h_{s11} + \dot{m}_{s22}h_{s22} + \dot{m}_{s24}h_{s24} + \dot{m}_{s30}h_{s30} = \dot{m}_{s4}h_{s4} + \dot{m}_{s15}h_{s15} + \dot{m}_{s23}h_{s23} + \dot{m}_{s25}h_{s25}$	$\dot{m}_{s11}s_{s11} + \dot{m}_{s22}s_{s22} + \dot{m}_{s24}s_{s24} + \dot{m}_{s30}s_{s30} + \dot{S}_{gen} = \dot{m}_{s4}s_{s4} + \dot{m}_{s15}s_{s15} + \dot{m}_{s23}s_{s23} + \dot{m}_{s25}s_{s25}$	$\dot{m}_{s11}ex_{s11} + \dot{m}_{s22}ex_{s22} + \dot{m}_{s24}ex_{s24} + \dot{m}_{s30}ex_{s30} = \dot{m}_{s4}ex_{s4} + \dot{m}_{s15}ex_{s15} + \dot{m}_{s23}ex_{s23} + \dot{m}_{s25}ex_{s25} + \dot{E}x_d$
B14 (Turbine 1)	$\dot{m}_{s15}h_{s15} = \dot{m}_{s22}h_{s22} + \dot{W}_{out}$	$\dot{m}_{s15}s_{s15} + \dot{S}_{gen} = \dot{m}_{s22}s_{s22}$	$\dot{m}_{s15}ex_{s15} = \dot{m}_{s22}ex_{s22} + \dot{W}_{out} + \dot{E}x_d$
B15 (Dryer)	$\dot{m}_{s21}h_{s21} = \dot{m}_{s26}h_{s26} + \dot{m}_{s27}h_{s27}$	$\dot{m}_{s21}s_{s21} + \dot{S}_{gen} = \dot{m}_{s26}s_{s26} + \dot{m}_{s27}s_{s27}$	$\dot{m}_{s21}ex_{s21} = \dot{m}_{s26}ex_{s26} + \dot{m}_{s27}ex_{s27} + \dot{E}x_d$
B16 (Turbine 2)	$\dot{m}_{s23}h_{s23} = \dot{m}_{s24}h_{s24} + \dot{W}_{out}$	$\dot{m}_{s23}s_{s23} + \dot{S}_{gen} = \dot{m}_{s24}s_{s24}$	$\dot{m}_{s23}ex_{s23} = \dot{m}_{s24}ex_{s24} + \dot{W}_{out} + \dot{E}x_d$
B17 (Turbine 3)	$\dot{m}_{s25}h_{s25} = \dot{m}_{s28}h_{s28} + \dot{W}_{out}$	$\dot{m}_{s25}s_{s25} + \dot{S}_{gen} = \dot{m}_{s28}s_{s28}$	$\dot{m}_{s25}ex_{s25} = \dot{m}_{s28}ex_{s28} + \dot{W}_{out} + \dot{E}x_d$
B18 (pump)	$\dot{m}_{s29}h_{s29} + \dot{W}_{in} = \dot{m}_{s30}h_{s30}$	$\dot{m}_{s29}s_{s29} + \dot{S}_{gen} = \dot{m}_{s30}s_{s30}$	$\dot{m}_{s29}ex_{s29} + \dot{W}_{in} = \dot{m}_{s30}ex_{s30} + \dot{E}x_d$
B19 (heat exchanger)	$\dot{m}_{s28}h_{s28} = \dot{m}_{s29}h_{s29} + \dot{Q}_{out}$	$\dot{m}_{s28}s_{s28} + \dot{S}_{gen} = \dot{m}_{s29}s_{s29} + \frac{\dot{Q}_{out}}{T_0}$	$\dot{m}_{s28}ex_{s28} = \dot{m}_{s29}ex_{s29} + \dot{E}x_{\dot{Q}_{out}} + \dot{E}x_d$
B20 (compressor 1)	$\dot{m}_{s19}h_{s19} + \dot{W}_{in} = \dot{m}_{s34}h_{s34}$	$\dot{m}_{s19}s_{s19} + \dot{S}_{gen} = \dot{m}_{s34}s_{s34}$	$\dot{m}_{s19}ex_{s19} + \dot{W}_{in} = \dot{m}_{s34}ex_{s34} + \dot{E}x_d$
B21 (compressor 1)	$\dot{m}_{s35}h_{s35} + \dot{W}_{in} = \dot{m}_{s36}h_{s36}$	$\dot{m}_{s35}s_{s35} + \dot{S}_{gen} = \dot{m}_{s36}s_{s36}$	$\dot{m}_{s35}ex_{s35} + \dot{W}_{in} = \dot{m}_{s36}ex_{s36} + \dot{E}x_d$
B22 (compressor 1)	$\dot{m}_{s37}h_{s37} + \dot{W}_{in} = \dot{m}_{s38}h_{s38}$	$\dot{m}_{s37}s_{s37} + \dot{S}_{gen} = \dot{m}_{s38}s_{s38}$	$\dot{m}_{s37}ex_{s37} + \dot{W}_{in} = \dot{m}_{s38}ex_{s38} + \dot{E}x_d$
B23 (heat exchanger)	$\dot{m}_{s34}h_{s34} = \dot{m}_{s35}h_{s35} + \dot{Q}_{out}$	$\dot{m}_{s34}s_{s34} + \dot{S}_{gen} = \dot{m}_{s35}s_{s35} + \frac{\dot{Q}_{out}}{T_0}$	$\dot{m}_{s34}ex_{s34} = \dot{m}_{s35}ex_{s35} + \dot{E}x_{\dot{Q}_{out}} + \dot{E}x_d$
B24 (heat exchanger)	$\dot{m}_{s36}h_{s36} = \dot{m}_{s37}h_{s37} + \dot{Q}_{out}$	$\dot{m}_{s36}s_{s36} + \dot{S}_{gen} = \dot{m}_{s37}s_{s37} + \frac{\dot{Q}_{out}}{T_0}$	$\dot{m}_{s36}ex_{s36} = \dot{m}_{s37}ex_{s37} + \dot{E}x_{\dot{Q}_{out}} + \dot{E}x_d$
B25 (heat exchanger)	$\dot{m}_{s38}h_{s38} = \dot{m}_{s39}h_{s39} + \dot{Q}_{out}$	$\dot{m}_{s38}s_{s38} + \dot{S}_{gen} = \dot{m}_{s39}s_{s39} + \frac{\dot{Q}_{out}}{T_0}$	$\dot{m}_{s38}ex_{s38} = \dot{m}_{s39}ex_{s39} + \dot{E}x_{\dot{Q}_{out}} + \dot{E}x_d$

Table 0.3 The exergy destruction and exergy efficiencies of all the components of hydrogen production Cu-Cl cycle and the subscripts of components and streams are represented from Figure 3.5.

Component	Exergy efficiency	Exergy destruction rate
B1 (heat exchanger)	$\psi_{B1} = \frac{\dot{m}_{s2} ex_{s2}}{\dot{m}_{s1} ex_{s1} + \dot{E}x_{\dot{Q}_{in}}}$	$\dot{E}x_d = \dot{m}_{s1} ex_{s1} + \dot{E}x_{\dot{Q}_{in}} - \dot{m}_{s2} ex_{s2}$
B2 (stoichiometric reactor)	$\psi_{B2} = \frac{\dot{m}_{s3} ex_{s3}}{\dot{m}_{s2} ex + \dot{m}_{s2} ex}$	$\dot{E}x_d = \dot{m}_{s2} ex + \dot{m}_{s2} ex - \dot{m}_{s3} ex_{s3}$
B3 (separator)	$\psi_{B3} = \frac{\dot{m}_{s5} ex_{s5} + \dot{m}_{s6} ex_{s6}}{\dot{m}_{s3} ex_{s3}}$	$\dot{E}x_d = \dot{m}_{s3} ex_{s3} - (\dot{m}_{s5} ex_{s5} + \dot{m}_{s6} ex_{s6})$
B5 (stoichiometric reactor)	$\psi_{B5} = \frac{\dot{m}_{s10} ex_{s10}}{\dot{m}_{s7} ex_{s7} + \dot{m}_{s9} ex_{s9} + \dot{E}x_{\dot{Q}_{in}}}$	$\dot{E}x_d = \dot{m}_{s7} ex_{s7} + \dot{m}_{s9} ex_{s9} + \dot{E}x_{\dot{Q}_{in}} - \dot{m}_{s10} ex_{s10}$
B6 (heat exchanger)	$\psi_{B6} = \frac{\dot{m}_{s9} ex_{s9}}{\dot{m}_{s8} ex_{s8} + \dot{E}x_{\dot{Q}_{in}}}$	$\dot{E}x_d = \dot{m}_{s8} ex_{s8} + \dot{E}x_{\dot{Q}_{in}} - \dot{m}_{s9} ex_{s9}$
B7 (separator)	$\psi_{B7} = \frac{\dot{m}_{s11} ex_{s11} + \dot{m}_{s12} ex_{s12}}{\dot{m}_{s10} ex_{s10}}$	$\dot{E}x_d = \dot{m}_{s10} ex_{s10} - (\dot{m}_{s11} ex_{s11} + \dot{m}_{s12} ex_{s12})$
B8 (heat exchanger)	$\psi_{B8} = \frac{\dot{m}_{s13} ex_{s13} + \dot{E}x_{\dot{Q}_{out}}}{\dot{m}_{s12} ex_{s12}}$	$\dot{E}x_d = \dot{m}_{s12} ex_{s12} - (\dot{m}_{s13} ex_{s13} + \dot{E}x_{\dot{Q}_{out}})$
B9 (stoichiometric reactor)	$\psi_{B9} = \frac{\dot{m}_{s16} ex_{s16}}{\dot{m}_{s13} ex_{s13} + \dot{m}_{s17} ex_{s17} + \dot{W}_e}$	$\dot{E}x_d = \dot{m}_{s13} ex_{s13} + \dot{m}_{s17} ex_{s17} + \dot{W}_e - \dot{m}_{s16} ex_{s16}$
B10 (heat exchanger)	$\psi_{B10} = \frac{\dot{m}_{s17} ex_{s17} + \dot{E}x_{\dot{Q}_{out}}}{\dot{m}_{s6} ex_{s6}}$	$\dot{E}x_d = \dot{m}_{s6} ex_{s6} - (\dot{m}_{s17} ex_{s17} + \dot{E}x_{\dot{Q}_{out}})$

B11 (separator)	$\psi_{B11} = \frac{\dot{m}_{s19} ex_{s19} + \dot{m}_{s20} ex_{s20}}{\dot{m}_{s16} ex_{s16}}$	$\dot{E}x_d = \dot{m}_{s16} ex_{s16} - (\dot{m}_{s19} ex_{s19} + \dot{m}_{s20} ex_{s20})$
B12 (heat exchanger)	$\psi_{B12} = \frac{\dot{m}_{s21} ex_{s21}}{\dot{m}_{s20} ex_{s20} + \dot{E}x_{\dot{Q}_{in}}}$	$\dot{E}x_d = \dot{m}_{s20} ex_{s20} + \dot{E}x_{\dot{Q}_{in}} - \dot{m}_{s21} ex_{s21}$
B13 (heat exchanger)	$\psi_{B13} = \frac{\dot{m}_{s4} ex_{s4} + \dot{m}_{s15} ex_{s15} + \dot{m}_{s23} ex_{s23} + \dot{m}_{s25} ex_{s25}}{\dot{m}_{s11} ex_{s11} + \dot{m}_{s22} ex_{s22} + \dot{m}_{s24} ex_{s24} + \dot{m}_{s30} ex_{s30}}$	$\dot{E}x_d = \dot{m}_{s11} ex_{s11} + \dot{m}_{s22} ex_{s22} + \dot{m}_{s24} ex_{s24} + \dot{m}_{s30} ex_{s30} - (\dot{m}_{s4} ex_{s4} + \dot{m}_{s15} ex_{s15} + \dot{m}_{s23} ex_{s23} + \dot{m}_{s25} ex_{s25})$
B14 (Turbine 1)	$\psi_{B14} = \frac{\dot{m}_{s22} ex_{s22} + \dot{W}_{out}}{\dot{m}_{s15} ex_{s15}}$	$\dot{E}x_d = \dot{m}_{s15} ex_{s15} - (\dot{m}_{s22} ex_{s22} + \dot{W}_{out})$
B15 (Dryer)	$\psi_{B15} = \frac{\dot{m}_{s26} ex_{s26} + \dot{m}_{s27} ex_{s27}}{\dot{m}_{s21} ex_{s21}}$	$\dot{E}x_d = \dot{m}_{s21} ex_{s21} - (\dot{m}_{s26} ex_{s26} + \dot{m}_{s27} ex_{s27})$
B16 (Turbine 2)	$\psi_{B16} = \frac{\dot{m}_{s24} ex_{s24} + \dot{W}_{out}}{\dot{m}_{s23} ex_{s23}}$	$\dot{E}x_d = \dot{m}_{s23} ex_{s23} - (\dot{m}_{s24} ex_{s24} + \dot{W}_{out})$
B17 (Turbine 3)	$\psi_{B17} = \frac{\dot{m}_{s28} ex_{s28} + \dot{W}_{out}}{\dot{m}_{s25} ex_{s25}}$	$\dot{E}x_d = \dot{m}_{s25} ex_{s25} - (\dot{m}_{s28} ex_{s28} + \dot{W}_{out})$
B18 (pump)	$\psi_{B18} = \frac{\dot{m}_{s30} ex_{s30}}{\dot{m}_{s29} ex_{s29} + \dot{W}_{in}}$	$\dot{E}x_d = \dot{m}_{s29} ex_{s29} + \dot{W}_{in} - \dot{m}_{s30} ex_{s30}$
B19 (heat exchanger)	$\psi_{B19} = \frac{\dot{m}_{s29} ex_{s29} + \dot{E}x_{\dot{Q}_{out}}}{\dot{m}_{s28} ex_{s28}}$	$\dot{E}x_d = \dot{m}_{s28} ex_{s28} - (\dot{m}_{s29} ex_{s29} + \dot{E}x_{\dot{Q}_{out}})$

B20 (compressor 1)	$\psi_{B20} = \frac{\dot{m}_{s34} ex_{s34}}{\dot{m}_{s19} ex_{s19} + \dot{W}_{in}}$	$\dot{E}x_d = \dot{m}_{s19} ex_{s19} + \dot{W}_{in} - \dot{m}_{s34} ex_{s34}$
B21 (compressor 1)	$\psi_{B21} = \frac{\dot{m}_{s36} ex_{s36}}{\dot{m}_{s35} ex_{s35} + \dot{W}_{in}}$	$\dot{E}x_d = \dot{m}_{s35} ex_{s35} + \dot{W}_{in} - \dot{m}_{s36} ex_{s36}$
B22 (compressor 1)	$\psi_{B22} = \frac{\dot{m}_{s38} ex_{s38}}{\dot{m}_{s37} ex_{s37} + \dot{W}_{in}}$	$\dot{E}x_d = \dot{m}_{s37} ex_{s37} + \dot{W}_{in} - \dot{m}_{s38} ex_{s38}$
B23 (heat exchanger)	$\psi_{B23} = \frac{\dot{m}_{s35} ex_{s35} + \dot{E}x_{\dot{Q}_{out}}}{\dot{m}_{s34} ex_{s34}}$	$\dot{E}x_d = \dot{m}_{s34} ex_{s34} - (\dot{m}_{s35} ex_{s35} + \dot{E}x_{\dot{Q}_{out}})$
B24 (heat exchanger)	$\psi_{B24} = \frac{\dot{m}_{s37} ex_{s37} + \dot{E}x_{\dot{Q}_{out}}}{\dot{m}_{s36} ex_{s36}}$	$\dot{E}x_d = \dot{m}_{s36} ex_{s36} - (\dot{m}_{s37} ex_{s37} + \dot{E}x_{\dot{Q}_{out}})$
B25 (heat exchanger)	$\psi_{B25} = \frac{\dot{m}_{s39} ex_{s39} + \dot{E}x_{\dot{Q}_{out}}}{\dot{m}_{s38} ex_{s38}}$	$\dot{E}x_d = \dot{m}_{s38} ex_{s38} - (\dot{m}_{s39} ex_{s39} + \dot{E}x_{\dot{Q}_{out}})$

The exergy efficiency of the multistage Rankine cycle (MSRC) is as follows:

$$\psi_{MSRC} = \frac{\dot{W}_{Turb(14)} + \dot{W}_{Turb(16)} + \dot{W}_{Turb(17)}}{\dot{m}_{S13}(ex_{S4} - ex_{S13})} \quad (4.27)$$

The heat released from the condenser can be formulated as:

$$\dot{Q}_{heating} = \dot{m}_{17}(h_{37} - h_{36}) \quad (4.28)$$

The overall energy efficiency of the hydrogen integrated system 2 can be written as:

$$\eta_{ov} = \frac{\dot{m}_{H_2} LHV_{H_2} + \dot{Q}_{heating} + \dot{W}_{out}}{\dot{Q}_{in} + \dot{W}_{in}} \quad (4.29)$$

$$\dot{W}_{out} = \dot{W}_{Turb(14)} + \dot{W}_{Turb(16)} + \dot{W}_{Turb(17)} \quad (4.30)$$

$$\dot{W}_{in} = \dot{W}_e + \dot{W}_{comp1} + \dot{W}_{comp2} + \dot{W}_{comp3} + \dot{W}_{B18} \quad (4.31)$$

The overall exergy efficiency of the hydrogen integrated system 1 can be written as:

$$\psi_{ov} = \frac{\dot{m}_{H_2} ex_{H_2} + \dot{E}x_{Q_{heating}} + \dot{W}_{out}}{\dot{E}x_{\dot{Q}_{S1}} + \dot{W}_{in}} \tag{4.32}$$

4.5 Thermodynamic analysis of system 3

The thermodynamic analysis is conducted on the integrated hydrogen production system 3 in this section in order to obtain the efficiency and performance information. Table 4.5 describes the energy, entropy and exergy balance equations of all components of the integrated system 3. The subscripts of components and streams refers to the Figures 3.7, 3.8 and 3.9.

The integrated system 3 contains Rankine cycle, thermochemical hydrogen production copper chlorine cycle, hydrogen compression cycle, multistage reheat Rankine cycle and Reverse Osmosis (RO) desalination unit. The exergy destruction and exergy efficiency of each component of third integrated system is defined and tabulated in Table 4.6. The subscripts of the components and streams are described according to Figures 3.7, 3.8 and 3.9.

The third integrated system consists of Rankine cycle, thermochemical Cu-Cl cycle, hydrogen compression system, multistage Rankine cycle and reverse osmosis desalination system. The thermodynamic analysis is conducted on the subsystems and the overall system in order to investigate the performance and efficiencies.

The energy and exergy efficiency of the Rankine cycle (RC) can be described as follows:

$$\eta_{RC} = \frac{W_{Turb(B2)}}{\dot{m}_{S5}(h_{S5} - h_{S10})} \tag{4.33}$$

The exergy efficiency of the subsystem Rankine cycle (RC) can be described as:

$$\psi_{RC} = \frac{W_{Turb(B2)}}{\dot{m}_{S5}(ex_{S5} - ex_{S10})} \tag{4.34}$$

The energy efficiency of the thermochemical Cu-Cl cycle is as follows:

$$\eta_{Cu-Cl} = \frac{\dot{m}_{H_2} LHV_{H_2}}{\dot{Q}_{in} + \dot{W}_e} \tag{4.35}$$

Table 0.4 The energy, entropy and exergy balance equations of third integrated hydrogen production system. The subscripts of components and streams refers to the Figures 3.7, 3.8 and 3.9 and the subscripts for RO desalination unit refers to Figure 3.6.

Component	Energy balance equation	Entropy balance equation	Exergy balance equation
B1 (heat exchanger)	$\dot{m}_{s1}h_{s1} + \dot{m}_{s3}h_{s3} + \dot{m}_{s10}h_{s10} = \dot{m}_{s2}h_{s2} + \dot{m}_{s4}h_{s4} + \dot{m}_{s5}h_{s5}$	$\dot{m}_{s1}s_{s1} + \dot{m}_{s3}s_{s3} + \dot{m}_{s10}s_{s10} + \dot{S}_{gen} = \dot{m}_{s2}s_{s2} + \dot{m}_{s4}s_{s4} + \dot{m}_{s5}s_{s5}$	$\dot{m}_{s1}ex_{s1} + \dot{m}_{s3}ex_{s3} + \dot{m}_{s10}ex_{s10} = \dot{m}_{s2}ex_{s2} + \dot{m}_{s4}ex_{s4} + \dot{m}_{s5}ex_{s5} + \dot{E}x_d$
B2 (turbine)	$\dot{m}_{s5}h_{s5} = \dot{m}_{s7}h_{s7} + \dot{W}_{out}$	$\dot{m}_{s5}s_{s5} + \dot{S}_{gen} = \dot{m}_{s7}s_{s7}$	$\dot{m}_{s5}ex_{s5} = \dot{m}_{s7}ex_{s7} + \dot{W}_{out} + \dot{E}x_d$
B3 (heat exchanger)	$\dot{m}_{s7}h_{s7} = \dot{m}_{s9}h_{s9} + \dot{Q}_{out}$	$\dot{m}_{s7}s_{s7} + \dot{S}_{gen} = \dot{m}_{s9}s_{s9} + \frac{\dot{Q}_{out}}{T_0}$	$\dot{m}_{s7}ex_{s7} = \dot{m}_{s9}ex_{s9} + \dot{E}x_{\dot{Q}_{out}} + \dot{E}x_d$
B4 (pump 1)	$\dot{m}_{s9}h_{s9} + \dot{W}_{in} = \dot{m}_{s10}h_{s10}$	$\dot{m}_{s9}s_{s9} + \dot{S}_{gen} = \dot{m}_{s10}s_{s10}$	$\dot{m}_{s9}ex_{s9} + \dot{W}_{in} = \dot{m}_{s10}ex_{s10} + \dot{E}x_d$
B6 (heat exchanger)	$\dot{m}_{s13}h_{s13} + \dot{Q}_{in} = \dot{m}_{s14}h_{s14}$	$\dot{m}_{s13}s_{s13} + \dot{S}_{gen} + \frac{\dot{Q}_{in}}{T_0} = \dot{m}_{s14}s_{s14}$	$\dot{m}_{s13}ex_{s13} + \dot{E}x_{\dot{Q}_{in}} = \dot{m}_{s14}ex_{s14} + \dot{E}x_d$
B7 (heat exchanger)	$\dot{m}_{s11}h_{s11} + \dot{Q}_{in} = \dot{m}_{s12}h_{s12}$	$\dot{m}_{s11}s_{s11} + \dot{S}_{gen} + \frac{\dot{Q}_{in}}{T_0} = \dot{m}_{s12}s_{s12}$	$\dot{m}_{s11}ex_{s11} + \dot{E}x_{\dot{Q}_{in}} = \dot{m}_{s12}ex_{s12} + \dot{E}x_d$
B8 (stoichiometric reactor)	$\dot{m}_{s14}h_{s14} + \dot{m}_{s29}h_{s29} = \dot{m}_{s15}h_{s15}$	$\dot{m}_{s14}s_{s14} + \dot{m}_{s29}s_{s29} + \dot{S}_{gen} = \dot{m}_{s15}s_{s15}$	$\dot{m}_{s14}ex_{14} + \dot{m}_{s29}ex_{29} = \dot{m}_{s15}ex_{s15} + \dot{E}x_d$
B9 (separator)	$\dot{m}_{s15}h_{s15} = \dot{m}_{s16}h_{s16} + \dot{m}_{s17}h_{s17}$	$\dot{m}_{s15}s_{s15} + \dot{S}_{gen} = \dot{m}_{s16}s_{s16} + \dot{m}_{s17}s_{s17}$	$\dot{m}_{s15}ex_{s15} = \dot{m}_{s16}ex_{s16} + \dot{m}_{s17}ex_{s17} + \dot{E}x_d$
B11 (stoichiometric reactor)	$\dot{m}_{s12}h_{s12} + \dot{m}_{s19}h_{s19} + \dot{Q}_{in} = \dot{m}_{s20}h_{s20}$	$\dot{m}_{s12}s_{s12} + \dot{m}_{s19}s_{s19} + \dot{S}_{gen} + \frac{\dot{Q}_{in}}{T_0} = \dot{m}_{s20}s_{s20}$	$\dot{m}_{s12}ex_{s12} + \dot{m}_{s19}ex_{s19} + \dot{E}x_{\dot{Q}_{in}} = \dot{m}_{s20}ex_{s20} + \dot{E}x_d$
B12 (separator)	$\dot{m}_{s20}h_{s20} = \dot{m}_{s21}h_{s21} + \dot{m}_{s22}h_{s22}$	$\dot{m}_{s20}s_{s20} + \dot{S}_{gen} = \dot{m}_{s21}s_{s21} + \dot{m}_{s22}s_{s22}$	$\dot{m}_{s20}ex_{s20} = \dot{m}_{s21}ex_{s21} + \dot{m}_{s22}ex_{s22} + \dot{E}x_d$
B13 (heat exchanger)	$\dot{m}_{s22}h_{s22} = \dot{m}_{s24}h_{s24} + \dot{Q}_{out}$	$\dot{m}_{s22}s_{s22} + \dot{S}_{gen} = \dot{m}_{s24}s_{s24} + \frac{\dot{Q}_{out}}{T_0}$	$\dot{m}_{s22}ex_{s22} = \dot{m}_{s24}ex_{s24} + \dot{E}x_{\dot{Q}_{out}} + \dot{E}x_d$

B14 (stoichiometric reactor)	$\dot{m}_{s18}h_{s18} + \dot{m}_{s24}h_{s24} + \dot{W}_e = \dot{m}_{s25}h_{s25}$	$\dot{m}_{s18}s_{s18} + \dot{m}_{s24}s_{s24} + \dot{S}_{gen} = \dot{m}_{s25}s_{s25}$	$\dot{m}_{s18}ex_{s18} + \dot{m}_{s24}ex_{s24} + \dot{W}_e = \dot{m}_{s25}ex_{s25} + \dot{E}x_d$
B15 (heat exchanger)	$\dot{m}_{s17}h_{s17} = \dot{m}_{s18}h_{s18} + \dot{Q}_{out}$	$\dot{m}_{s17}s_{s17} + \dot{S}_{gen} = \dot{m}_{s18}s_{s18} + \frac{\dot{Q}_{out}}{T_0}$	$\dot{m}_{s17}ex_{s17} = \dot{m}_{s18}ex_{s87} + \dot{E}x_{\dot{Q}_{out}} + \dot{E}x_d$
B16 (separator)	$\dot{m}_{s25}h_{s25} = \dot{m}_{s26}h_{s26} + \dot{m}_{s27}h_{s27}$	$\dot{m}_{s25}s_{s25} + \dot{S}_{gen} = \dot{m}_{s26}s_{s26} + \dot{m}_{s27}s_{s27}$	$\dot{m}_{s25}ex_{s25} = \dot{m}_{s26}ex_{s26} + \dot{m}_{s27}ex_{s27} + \dot{E}x_d$
B17 (heat exchanger)	$\dot{m}_{s27}h_{s27} + \dot{Q}_{in} = \dot{m}_{s28}h_{s28}$	$\dot{m}_{s27}s_{s27} + \dot{S}_{gen} + \frac{\dot{Q}_{in}}{T_0} = \dot{m}_{s28}s_{s28}$	$\dot{m}_{s27}ex_{s27} + \dot{E}x_{\dot{Q}_{in}} = \dot{m}_{s28}ex_{s28} + \dot{E}x_d$
B18 (Dryer)	$\dot{m}_{s28}h_{s28} = \dot{m}_{s29}h_{s29} + \dot{m}_{s30}h_{s30}$	$\dot{m}_{s28}s_{s28} + \dot{S}_{gen} = \dot{m}_{s29}s_{s29} + \dot{m}_{s30}s_{s30}$	$\dot{m}_{s28}ex_{s28} = \dot{m}_{s29}ex_{s29} + \dot{m}_{s30}ex_{s30} + \dot{E}x_d$
B20 (compressor 1)	$\dot{m}_{s26}h_{s26} + \dot{W}_{in} = \dot{m}_{s31}h_{s31}$	$\dot{m}_{s26}s_{s26} + \dot{S}_{gen} = \dot{m}_{s31}s_{s31}$	$\dot{m}_{s26}ex_{s26} + \dot{W}_{in} = \dot{m}_{s31}ex_{s31} + \dot{E}x_d$
B21 (compressor 1)	$\dot{m}_{s33}h_{s33} + \dot{W}_{in} = \dot{m}_{s34}h_{s34}$	$\dot{m}_{s33}s_{s33} + \dot{S}_{gen} = \dot{m}_{s34}s_{s34}$	$\dot{m}_{s33}ex_{s33} + \dot{W}_{in} = \dot{m}_{s34}ex_{s34} + \dot{E}x_d$
B22 (compressor 1)	$\dot{m}_{s36}h_{s36} + \dot{W}_{in} = \dot{m}_{s37}h_{s37}$	$\dot{m}_{s36}s_{s36} + \dot{S}_{gen} = \dot{m}_{s37}s_{s37}$	$\dot{m}_{s36}ex_{s36} + \dot{W}_{in} = \dot{m}_{s37}ex_{s37} + \dot{E}x_d$
B23 (heat exchanger)	$\dot{m}_{s31}h_{s31} = \dot{m}_{s33}h_{s33} + \dot{Q}_{out}$	$\dot{m}_{s31}s_{s31} + \dot{S}_{gen} = \dot{m}_{s33}s_{s33} + \frac{\dot{Q}_{out}}{T_0}$	$\dot{m}_{s31}ex_{s31} = \dot{m}_{s33}ex_{s33} + \dot{E}x_{\dot{Q}_{out}} + \dot{E}x_d$
B24 (heat exchanger)	$\dot{m}_{s34}h_{s34} = \dot{m}_{s36}h_{s36} + \dot{Q}_{out}$	$\dot{m}_{s34}s_{s34} + \dot{S}_{gen} = \dot{m}_{s36}s_{s36} + \frac{\dot{Q}_{out}}{T_0}$	$\dot{m}_{s34}ex_{s34} = \dot{m}_{s36}ex_{s36} + \dot{E}x_{\dot{Q}_{out}} + \dot{E}x_d$
B25 (heat exchanger)	$\dot{m}_{s37}h_{s37} = \dot{m}_{s39}h_{s39} + \dot{Q}_{out}$	$\dot{m}_{s37}s_{s37} + \dot{S}_{gen} = \dot{m}_{s39}s_{s39} + \frac{\dot{Q}_{out}}{T_0}$	$\dot{m}_{s37}ex_{s37} = \dot{m}_{s39}ex_{s39} + \dot{E}x_{\dot{Q}_{out}} + \dot{E}x_d$
B26 (heat exchanger)	$\dot{m}_{s17}h_{s17} + \dot{m}_{s42}h_{s42} + \dot{m}_{s44}h_{s44} + \dot{m}_{s48}h_{s48} = \dot{m}_{s18}h_{s18} + \dot{m}_{s41}h_{s41} + \dot{m}_{s43}h_{s43} + \dot{m}_{s45}h_{s45}$	$\dot{m}_{s17}s_{s17} + \dot{m}_{s42}s_{s42} + \dot{m}_{s44}s_{s44} + \dot{m}_{s48}s_{s48} + \dot{S}_{gen} = \dot{m}_{s18}s_{s18} + \dot{m}_{s41}s_{s41} + \dot{m}_{s43}s_{s43} + \dot{m}_{s45}s_{s45}$	$\dot{m}_{s17}ex_{s17} + \dot{m}_{s42}ex_{s42} + \dot{m}_{s44}ex_{s44} + \dot{m}_{s48}ex_{s48} = \dot{m}_{s18}ex_{s18} + \dot{m}_{s41}ex_{s41} + \dot{m}_{s43}ex_{s43} + \dot{m}_{s45}ex_{s45} + \dot{E}x_d$

B27 (Turbine 1)	$\dot{m}_{s41}h_{s41} = \dot{m}_{s42}h_{s42} + \dot{W}_{out}$	$\dot{m}_{s41}s_{s41} + \dot{S}_{gen} = \dot{m}_{s42}s_{s42}$	$\dot{m}_{s41}ex_{s41} = \dot{m}_{s42}ex_{s42} + \dot{W}_{out} + \dot{E}x_d$
B28 (Turbine 2)	$\dot{m}_{s43}h_{s43} = \dot{m}_{s44}h_{s44} + \dot{W}_{out}$	$\dot{m}_{s43}s_{s43} + \dot{S}_{gen} = \dot{m}_{s44}s_{s44}$	$\dot{m}_{s43}ex_{s43} = \dot{m}_{s44}ex_{s44} + \dot{W}_{out} + \dot{E}x_d$
B29 (Turbine 3)	$\dot{m}_{s45}h_{s45} = \dot{m}_{s46}h_{s46} + \dot{W}_{out}$	$\dot{m}_{s45}s_{s45} + \dot{S}_{gen} = \dot{m}_{s46}s_{s46}$	$\dot{m}_{s45}ex_{s45} = \dot{m}_{s46}ex_{s46} + \dot{W}_{out} + \dot{E}x_d$
B30 (heat exchanger)	$\dot{m}_{s46}h_{s46} = \dot{m}_{s47}h_{s47} + \dot{Q}_{out}$	$\dot{m}_{s46}s_{s46} + \dot{S}_{gen} = \dot{m}_{s47}s_{s47} + \frac{\dot{Q}_{out}}{T_0}$	$\dot{m}_{s46}ex_{s46} = \dot{m}_{s47}ex_{s47} + \dot{E}x_{\dot{Q}_{out}} + \dot{E}x_d$
B31 (pump)	$\dot{m}_{s47}h_{s47} + \dot{W}_{in} = \dot{m}_{s48}h_{s48}$	$\dot{m}_{s47}s_{s47} + \dot{S}_{gen} = \dot{m}_{s48}s_{s48}$	$\dot{m}_{s47}ex_{s47} + \dot{W}_{in} = \dot{m}_{s48}ex_{s48} + \dot{E}x_d$
Pump 2	$\dot{m}_{44}h_{44} + \dot{W}_{in} = \dot{m}_{45}h_{45}$	$\dot{m}_{44}s_{44} + \dot{S}_{gen} = \dot{m}_{45}s_{45}$	$\dot{m}_{44}ex_{44} + \dot{W}_{in} = \dot{m}_{45}ex_{45} + \dot{E}x_d$
Filter	$\dot{m}_{45}h_{45} = \dot{m}_{46}h_{46}$	$\dot{m}_{45}s_{45} + \dot{S}_{gen} = \dot{m}_{46}s_{46}$	$\dot{m}_{45}ex_{45} = \dot{m}_{46}ex_{46} + \dot{E}x_d$
3-way valve	$\dot{m}_{46}h_{46} = \dot{m}_{47}h_{47} + \dot{m}_{51}h_{51}$	$\dot{m}_{46}s_{46} + \dot{S}_{gen} = \dot{m}_{47}s_{47} + \dot{m}_{51}s_{51}$	$\dot{m}_{46}ex_{46} = \dot{m}_{47}ex_{47} + \dot{m}_{51}ex_{51} + \dot{E}x_d$
Throttle valve 1	$\dot{m}_{51}h_{51} = \dot{m}_{52}h_{52}$	$\dot{m}_{51}s_{51} + \dot{S}_{gen} = \dot{m}_{52}s_{52}$	$\dot{m}_{51}ex_{51} = \dot{m}_{52}ex_{52} + \dot{E}x_d$
Chemical treatment	$\dot{m}_{47}h_{47} = \dot{m}_{48}h_{48}$	$\dot{m}_{47}s_{47} + \dot{S}_{gen} = \dot{m}_{48}s_{48}$	$\dot{m}_{47}ex_{47} = \dot{m}_{48}ex_{48} + \dot{E}x_d$
Pump 3	$\dot{m}_{48}h_{48} + \dot{W}_{in} = \dot{m}_{49}h_{49}$	$\dot{m}_{48}s_{48} + \dot{S}_{gen} = \dot{m}_{49}s_{49}$	$\dot{m}_{48}ex_{48} + \dot{W}_{in} = \dot{m}_{49}ex_{49} + \dot{E}x_d$
RO module	$\dot{m}_{49}h_{49} = \dot{m}_{50}h_{50}$	$\dot{m}_{49}s_{49} + \dot{S}_{gen} = \dot{m}_{50}s_{50}$	$\dot{m}_{49}ex_{49} = \dot{m}_{50}ex_{50} + \dot{E}x_d$
Mixing chamber	$\dot{m}_{50}h_{50} + \dot{m}_{52}h_{52} = \dot{m}_{53}h_{53}$	$\dot{m}_{50}s_{50} + \dot{m}_{52}s_{52} + \dot{S}_{gen} = \dot{m}_{53}s_{53}$	$\dot{m}_{50}ex_{50} + \dot{m}_{52}ex_{52} = \dot{m}_{53}ex_{53} + \dot{E}x_d$
Throttle valve 2	$\dot{m}_{53}h_{53} = \dot{m}_{54}h_{54}$	$\dot{m}_{53}s_{53} + \dot{S}_{gen} = \dot{m}_{54}s_{54}$	$\dot{m}_{53}ex_{53} = \dot{m}_{54}ex_{54} + \dot{E}x_d$

$$\dot{Q}_{in} = \dot{Q}_{B6} + \dot{Q}_{B7} + \dot{Q}_{B10} + \dot{Q}_{B11} + \dot{Q}_{B17} + \dot{Q}_{B8} + \dot{Q}_{B23} + \dot{Q}_{B24} + \dot{Q}_{B25} \quad (4.36)$$

The exergy efficiency of the thermochemical Cu-Cl cycle is as follows:

$$\psi_{Cu-Cl} = \frac{\dot{m}_{H_2}ex_{H_2}}{\dot{E}x_{\dot{Q}_{in}} + \dot{W}_e} \quad (4.37)$$

Table 0.5 The exergy destruction and the exergy efficiency of each component of third integrated system. The subscripts of components and streams refers to Figures 3.7, 3.8 and 3.9 and the subscripts for RO desalination unit refers to Figure 3.6.

Component	Exergy efficiency	Exergy destruction rate
B1 (heat exchanger)	$\psi_{B1} = \frac{\dot{m}_{s2}ex_{s2} + \dot{m}_{s4}ex_{s4} + \dot{m}_{s5}ex_{s5}}{\dot{m}_{s1}ex_{s1} + \dot{m}_{s3}ex_{s3} + \dot{m}_{s10}ex_{s10}}$	$\dot{E}x_d = \dot{m}_{s1}ex_{s1} + \dot{m}_{s3}ex_{s3} + \dot{m}_{s10}ex_{s10} - (\dot{m}_{s2}ex_{s2} + \dot{m}_{s4}ex_{s4} + \dot{m}_{s5}ex_{s5})$
B2 (turbine)	$\psi_{B2} = \frac{\dot{m}_{s7}ex_{s7} + \dot{W}_{out}}{\dot{m}_{s5}ex_{s5}}$	$\dot{E}x_d = \dot{m}_{s5}ex_{s5} - (\dot{m}_{s7}ex_{s7} + \dot{W}_{out})$
B3 (heat exchanger)	$\psi_{B3} = \frac{\dot{m}_{s9}ex_{s9} + \dot{E}x_{\dot{Q}_{out}}}{\dot{m}_{s7}ex_{s7}}$	$\dot{E}x_d = \dot{m}_{s7}ex_{s7} - (\dot{m}_{s9}ex_{s9} + \dot{E}x_{\dot{Q}_{out}})$
B4 (pump 1)	$\psi_{B4} = \frac{\dot{m}_{s10}ex_{s10}}{\dot{m}_{s9}ex_{s9} + \dot{W}_{in}}$	$\dot{E}x_d = \dot{m}_{s9}ex_{s9} + \dot{W}_{in} - \dot{m}_{s10}ex_{s10}$
B6 (heat exchanger)	$\psi_{B6} = \frac{\dot{m}_{s14}ex_{s14}}{\dot{m}_{s13}ex_{s13} + \dot{E}x_{\dot{Q}_{in}}}$	$\dot{E}x_d = \dot{m}_{s13}ex_{s13} + \dot{E}x_{\dot{Q}_{in}} - \dot{m}_{s14}ex_{s14}$
B7 (heat exchanger)	$\psi_{B7} = \frac{\dot{m}_{s12}ex_{s12}}{\dot{m}_{s11}ex_{s11} + \dot{E}x_{\dot{Q}_{in}}}$	$\dot{E}x_d = \dot{m}_{s11}ex_{s11} + \dot{E}x_{\dot{Q}_{in}} - \dot{m}_{s12}ex_{s12}$
B8 (stoichiometric reactor)	$\psi_{B8} = \frac{\dot{m}_{s15}ex_{s15}}{\dot{m}_{s14}ex_{14} + \dot{m}_{s29}ex_{29}}$	$\dot{E}x_d = \dot{m}_{s14}ex_{14} + \dot{m}_{s29}ex_{29} - \dot{m}_{s15}ex_{s15}$
B9 (separator)	$\psi_{B9} = \frac{\dot{m}_{s16}ex_{s16} + \dot{m}_{s17}ex_{s17}}{\dot{m}_{s15}ex_{s15}}$	$\dot{E}x_d = \dot{m}_{s15}ex_{s15} - (\dot{m}_{s16}ex_{s16} + \dot{m}_{s17}ex_{s17})$
B11 (stoichiometric reactor)	$\psi_{B11} = \frac{\dot{m}_{s20}ex_{s20}}{\dot{m}_{s12}ex_{s12} + \dot{m}_{s19}ex_{s19} + \dot{E}x_{\dot{Q}_{in}}}$	$\dot{E}x_d = \dot{m}_{s12}ex_{s12} + \dot{m}_{s19}ex_{s19} + \dot{E}x_{\dot{Q}_{in}} - \dot{m}_{s20}ex_{s20}$
B12 (separator)	$\psi_{B12} = \frac{\dot{m}_{s21}ex_{s21} + \dot{m}_{s22}ex_{s22}}{\dot{m}_{s20}ex_{s20}}$	$\dot{E}x_d = \dot{m}_{s20}ex_{s20} - (\dot{m}_{s21}ex_{s21} + \dot{m}_{s22}ex_{s22})$
B13 (heat exchanger)	$\psi_{B13} = \frac{\dot{m}_{s24}ex_{s24} + \dot{E}x_{\dot{Q}_{out}}}{\dot{m}_{s22}ex_{s22}}$	$\dot{E}x_d = \dot{m}_{s22}ex_{s22} - (\dot{m}_{s24}ex_{s24} + \dot{E}x_{\dot{Q}_{out}})$
B14 (stoichiometric reactor)	$\psi_{B14} = \frac{\dot{m}_{s25}ex_{s25}}{\dot{m}_{s18}ex_{s18} + \dot{m}_{s24}ex_{s24} + \dot{W}_e}$	$\dot{E}x_d = \dot{m}_{s18}ex_{s18} + \dot{m}_{s24}ex_{s24} + \dot{W}_e - \dot{m}_{s25}ex_{s25}$
B15 (heat exchanger)	$\psi_{B15} = \frac{\dot{m}_{s18}ex_{s87} + \dot{E}x_{\dot{Q}_{out}}}{\dot{m}_{s17}ex_{s17}}$	$\dot{E}x_d = \dot{m}_{s17}ex_{s17} - (\dot{m}_{s18}ex_{s87} + \dot{E}x_{\dot{Q}_{out}})$

B16 (separator)	$\psi_{B16} = \frac{\dot{m}_{s26}ex_{s26} + \dot{m}_{s27}ex_{s27}}{\dot{m}_{s25}ex_{s25}}$	$\dot{E}x_d = \dot{m}_{s25}ex_{s25} - (\dot{m}_{s26}ex_{s26} + \dot{m}_{s27}ex_{s27})$
B17 (heat exchanger)	$\psi_{B17} = \frac{\dot{m}_{s28}ex_{s28}}{\dot{m}_{s27}ex_{s27} + \dot{E}x_{\dot{Q}_{in}}}$	$\dot{E}x_d = \dot{m}_{s27}ex_{s27} + \dot{E}x_{\dot{Q}_{in}} - \dot{m}_{s28}ex_{s28}$
B18 (Dryer)	$\psi_{B18} = \frac{\dot{m}_{s29}ex_{s29} + \dot{m}_{s30}ex_{s30}}{\dot{m}_{s28}ex_{s28}}$	$\dot{E}x_d = \dot{m}_{s28}ex_{s28} - (\dot{m}_{s29}ex_{s29} + \dot{m}_{s30}ex_{s30})$
B20 (compressor 1)	$\psi_{B20} = \frac{\dot{m}_{s31}ex_{s31}}{\dot{m}_{s26}ex_{s26} + \dot{W}_{in}}$	$\dot{E}x_d = \dot{m}_{s26}ex_{s26} + \dot{W}_{in} - \dot{m}_{s31}ex_{s31}$
B21 (compressor 1)	$\psi_{B21} = \frac{\dot{m}_{s34}ex_{s34}}{\dot{m}_{s33}ex_{s33} + \dot{W}_{in}}$	$\dot{E}x_d = \dot{m}_{s33}ex_{s33} + \dot{W}_{in} - \dot{m}_{s34}ex_{s34}$
B22 (compressor 1)	$\psi_{B22} = \frac{\dot{m}_{s37}ex_{s37}}{\dot{m}_{s36}ex_{s36} + \dot{W}_{in}}$	$\dot{E}x_d = \dot{m}_{s36}ex_{s36} + \dot{W}_{in} - \dot{m}_{s37}ex_{s37}$
B23 (heat exchanger)	$\psi_{B23} = \frac{\dot{m}_{s33}ex_{s33} + \dot{E}x_{\dot{Q}_{out}}}{\dot{m}_{s31}ex_{s31}}$	$\dot{E}x_d = \dot{m}_{s31}ex_{s31} - (\dot{m}_{s33}ex_{s33} + \dot{E}x_{\dot{Q}_{out}})$
B24 (heat exchanger)	$\psi_{B24} = \frac{\dot{m}_{s36}ex_{s36} + \dot{E}x_{\dot{Q}_{out}}}{\dot{m}_{s34}ex_{s34}}$	$\dot{E}x_d = \dot{m}_{s34}ex_{s34} - (\dot{m}_{s36}ex_{s36} + \dot{E}x_{\dot{Q}_{out}})$
B25 (heat exchanger)	$\psi_{B25} = \frac{\dot{m}_{s39}ex_{s39} + \dot{E}x_{\dot{Q}_{out}}}{\dot{m}_{s37}ex_{s37}}$	$\dot{E}x_d = \dot{m}_{s37}ex_{s37} - (\dot{m}_{s39}ex_{s39} + \dot{E}x_{\dot{Q}_{out}})$
B26 (heat exchanger)	$\psi_{B26} = \frac{\dot{m}_{s18}ex_{s18} + \dot{m}_{s41}ex_{s41} + \dot{m}_{s43}ex_{s43} + \dot{m}_{s45}ex_{s}}{\dot{m}_{s17}ex_{s17} + \dot{m}_{s42}ex_{s42} + \dot{m}_{s44}ex_{s44} + \dot{m}_{s48}ex_{s}}$	$\dot{E}x_d = \dot{m}_{s17}ex_{s17} + \dot{m}_{s42}ex_{s42} + \dot{m}_{s44}ex_{s44} + \dot{m}_{s48}ex_{s48} - (\dot{m}_{s18}ex_{s18} + \dot{m}_{s41}ex_{s41} + \dot{m}_{s43}ex_{s43} + \dot{m}_{s45}ex_{s45})$
B27 (Turbine 1)	$\psi_{B27} = \frac{\dot{m}_{s42}ex_{s42} + \dot{W}_{out}}{\dot{m}_{s41}ex_{s41}}$	$\dot{E}x_d = \dot{m}_{s41}ex_{s41} - (\dot{m}_{s42}ex_{s42} + \dot{W}_{out})$
B28 (Turbine 2)	$\psi_{B28} = \frac{\dot{m}_{s44}ex_{s44} + \dot{W}_{out}}{\dot{m}_{s43}ex_{s43}}$	$\dot{E}x_d = \dot{m}_{s43}ex_{s43} - (\dot{m}_{s44}ex_{s44} + \dot{W}_{out})$
B29 (Turbine 3)	$\psi_{B29} = \frac{\dot{m}_{s46}ex_{s46} + \dot{W}_{out}}{\dot{m}_{s45}ex_{s45}}$	$\dot{E}x_d = \dot{m}_{s45}ex_{s45} - (\dot{m}_{s46}ex_{s46} + \dot{W}_{out})$
B30 (heat exchanger)	$\psi_{B30} = \frac{\dot{m}_{s47}ex_{s47} + \dot{E}x_{\dot{Q}_{out}}}{\dot{m}_{s46}ex_{s46}}$	$\dot{E}x_d = \dot{m}_{s46}ex_{s46} - (\dot{m}_{s47}ex_{s47} + \dot{E}x_{\dot{Q}_{out}})$
B31 (pump)	$\psi_{B31} = \frac{\dot{m}_{s48}ex_{s48}}{\dot{m}_{s47}ex_{s47} + \dot{W}_{in}}$	$\dot{E}x_d = \dot{m}_{s47}ex_{s47} + \dot{W}_{in} - \dot{m}_{s48}ex_{s48}$
Pump 2	$\psi_{Pump\,2} = \frac{\dot{m}_{45}ex_{45}}{\dot{m}_{44}ex_{44} + \dot{W}_{in}}$	$\dot{E}x_d = \dot{m}_{44}ex_{44} + \dot{W}_{in} - \dot{m}_{45}ex_{45}$

Filter	$\psi_{Filter} = \frac{\dot{m}_{46} ex_{46}}{\dot{m}_{45} ex_{45}}$	$\dot{E}x_d = \dot{m}_{45} ex_{45} - \dot{m}_{46} ex_{46}$
3-way valve	$\psi_{3-way\ valve} = \frac{\dot{m}_{47} ex_{47} + \dot{m}_{51} ex_{51}}{\dot{m}_{46} ex_{46}}$	$\dot{E}x_d = \dot{m}_{46} ex_{46} - (\dot{m}_{47} ex_{47} + \dot{m}_{51} ex_{51})$
Throttle valve 1	$\psi_{Th\ valve\ 1} = \frac{\dot{m}_{52} ex_{52}}{\dot{m}_{51} ex_{51}}$	$\dot{E}x_d = \dot{m}_{51} ex_{51} - \dot{m}_{52} ex_{52}$
Chemical treatment	$\psi_{Chem\ treatment} = \frac{\dot{m}_{48} ex_{48}}{\dot{m}_{47} ex_{47}}$	$\dot{E}x_d = \dot{m}_{47} ex_{47} - \dot{m}_{48} ex_{48}$
Pump 3	$\psi_{Pump\ 3} = \frac{\dot{m}_{s49} ex_{s49}}{\dot{m}_{s48} ex_{s48} + \dot{W}_{in}}$	$\dot{E}x_d = \dot{m}_{48} ex_{48} + \dot{W}_{in} - \dot{m}_{49} ex_{49}$
RO module	$\psi_{RO\ module} = \frac{\dot{m}_{50} ex_{50}}{\dot{m}_{49} ex_{49}}$	$\dot{E}x_d = \dot{m}_{49} ex_{49} - \dot{m}_{50} ex_{50}$
Mixing chamber	$\psi_{Mixing\ chamber} = \frac{\dot{m}_{53} ex_{53}}{\dot{m}_{50} ex_{50} + \dot{m}_{52} ex_{52}}$	$\dot{E}x_d = \dot{m}_{50} ex_{50} + \dot{m}_{52} ex_{52} - \dot{m}_{53} ex_{53}$
Throttle valve 2	$\psi_{Th\ valve\ 2} = \frac{\dot{m}_{54} ex_{54}}{\dot{m}_{53} ex_{53}}$	$\dot{E}x_d = \dot{m}_{53} ex_{53} - \dot{m}_{54} ex_{54}$

$$\dot{E}x_{\dot{Q}_{in}} = \dot{E}x_{\dot{Q}_{B6}} + +\dot{E}x_{\dot{Q}_{B7}} + \dot{E}x_{\dot{Q}_{B10}} + \dot{E}x_{\dot{Q}_{B11}} + \dot{E}x_{\dot{Q}_{B17}} + \dot{E}x_{\dot{Q}_{B8}} + \dot{E}x_{\dot{Q}_{B23}} + \dot{E}x_{\dot{Q}_{B24}} + \dot{E}x_{\dot{Q}_{B25}} \quad (4.38)$$

The energy efficiency of the multistage Rankine cycle (MSRC) is as follows:

$$\eta_{MSRC} = \frac{\dot{W}_{Turb(27)} + \dot{W}_{Turb(28)} + \dot{W}_{Turb(29)}}{\dot{m}_{S17}(h_{S18} - h_{S17})} \quad (4.39)$$

The exergy efficiency of the multistage Rankine cycle (MSRC) is as follows:

$$\psi_{MSRC} = \frac{\dot{W}_{Turb(27)} + \dot{W}_{Turb(28)} + \dot{W}_{Turb(29)}}{\dot{m}_{S17}(ex_{S18} - ex_{S17})} \quad (4.40)$$

The additional heat flow from the condenser is used for the heat output which can be expressed by the relation:

$$\dot{Q}_{heating} = \dot{m}_{38}(h_{58} - h_{57}) \quad (4.41)$$

The subscripts of components and stream names for reverse osmosis desalination system refers to the Figure 3.6. The energy and exergy efficiencies of reverse osmosis desalination unit included in integrated system 3 can be written as [87]

$$\eta_{RO} = \frac{\dot{m}_{fw} h_{fw}}{\dot{W}_{in,RO} + \dot{m}_{sw} h_{sw}} \quad (4.42)$$

$$\dot{W}_{in,RO} = \dot{W}_{pump2} + \dot{W}_{pump3} \quad (4.43)$$

$$\psi_{RO} = \frac{\dot{m}_{fw} ex_{fw}}{\dot{W}_{in,RO} + \dot{m}_{sw} ex_{sw}} \quad (4.44)$$

In the equations mentioned above, fw represents fresh water, sw represents sea water and $W_{in,RO}$ represents the total work of two pumps.

The overall energy efficiency of the hydrogen integrated system 3 can be written as:

$$\eta_{ov} = \frac{\dot{m}_{H_2} LHV_{H_2} + \dot{W}_{net} + \dot{m}_{fw} h_{fw} + \dot{Q}_{heating}}{\dot{Q}_{S1} + \dot{m}_{sw} h_{sw}} \quad (4.45)$$

The overall exergy efficiency of the third system is given as follows:

$$\psi_{ov} = \frac{\dot{m}_{H_2} ex_{H_2} + \dot{W}_{net} + \dot{m}_{fw} ex_{fw} + \dot{E}x_{Q_{heating}}}{\dot{Q}_{S1} + \dot{m}_{sw} ex_{sw}} \quad (4.46)$$

$$\dot{W}_{net} = \dot{W}_{Turb(B2)} + \dot{W}_{Turb(B27)} + \dot{W}_{Turb(28)} + \dot{W}_{Turb(29)} - \dot{W}_e - \dot{W}_{comp1} - \dot{W}_{comp2} - \dot{W}_{comp3} - \dot{W}_{pump\ B4} - \dot{W}_{B31} - \dot{W}_{pump2} - \dot{W}_{pump3} \quad (4.47)$$

Chapter 5: Results and Discussion

The results of the simulation, thermodynamic analysis and the design of the three proposed integrated hydrogen production system utilizing industrial waste heat are presented in this chapter. In this chapter, each hydrogen production system consists of separate section including specific results.

5.1 System 1 results

The energy and exergy analysis is conducted on the proposed hydrogen production system 1 and results of thermodynamic analysis and simulation are described in this chapter. Aspen Plus software is used to calculate all stream properties and excel calculations are conducted for other performance parameters like energy and exergy efficiencies, chemical exergies and exergy destruction rates. The major results containing energy and exergy efficiencies, operational requirements of system and exergy destruction rates are presented in this section. Hydrogen production specifications like production rate, production temperature and production pressure and the overall efficiencies of system 1 are tabulated in Table 5.1.

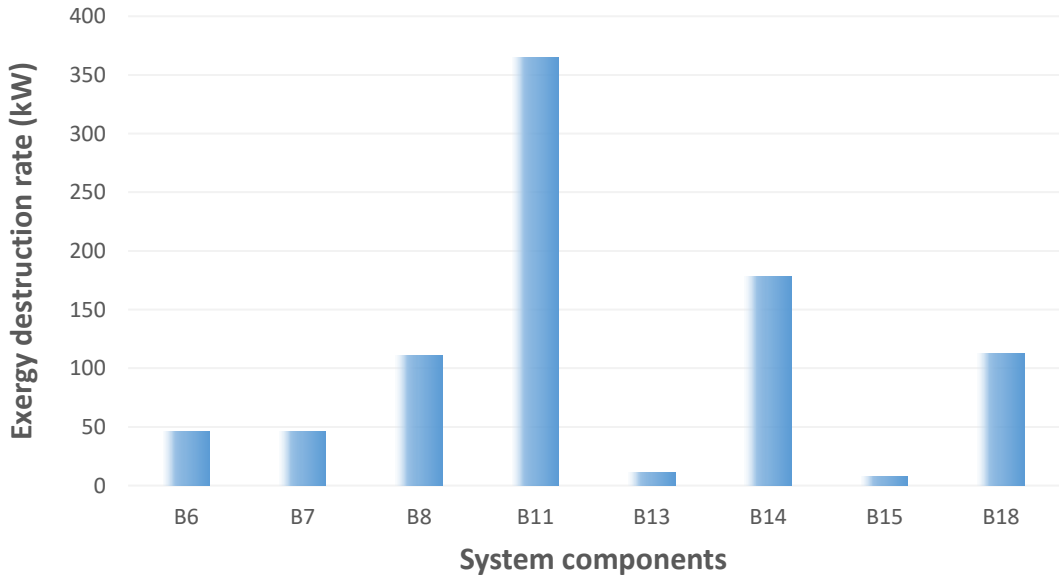

Figure 5.1 Exergy destruction of the components in the Cu-Cl hydrogen production cycle in system 1 (component names referenced in Figures 3.2 and 3.3).

Table 5.1 describes the major parameters like energy and exergy efficiency, exergy destruction rate, produced work rate and produced hydrogen specification. The overall energy efficiency of the second system is 39.8% and the exergy efficiency is calculated as 40.5%.

Table 5.1 Results of hydrogen production system 1

Parameter	**Value**	**Unit**
Flue gas flow rate	9.21	kg/s
Work rate	1.326	MW
Hydrogen production rate	64.8	kg/h
Hydrogen production pressure	750	Bar
Hydrogen production temperature	25	℃
Energy efficiency	39.8	%
Exergy efficiency	40.5	%

The exergy destruction rates of the hydrogen production Cu-Cl cycle included in system 1 are presented in Figure 5.1. The maximum destruction rate take place in decomposition reactor B11 and the second highest destruction rate occurs in electrolyzer B14 and exergy destruction of other components are also presented.

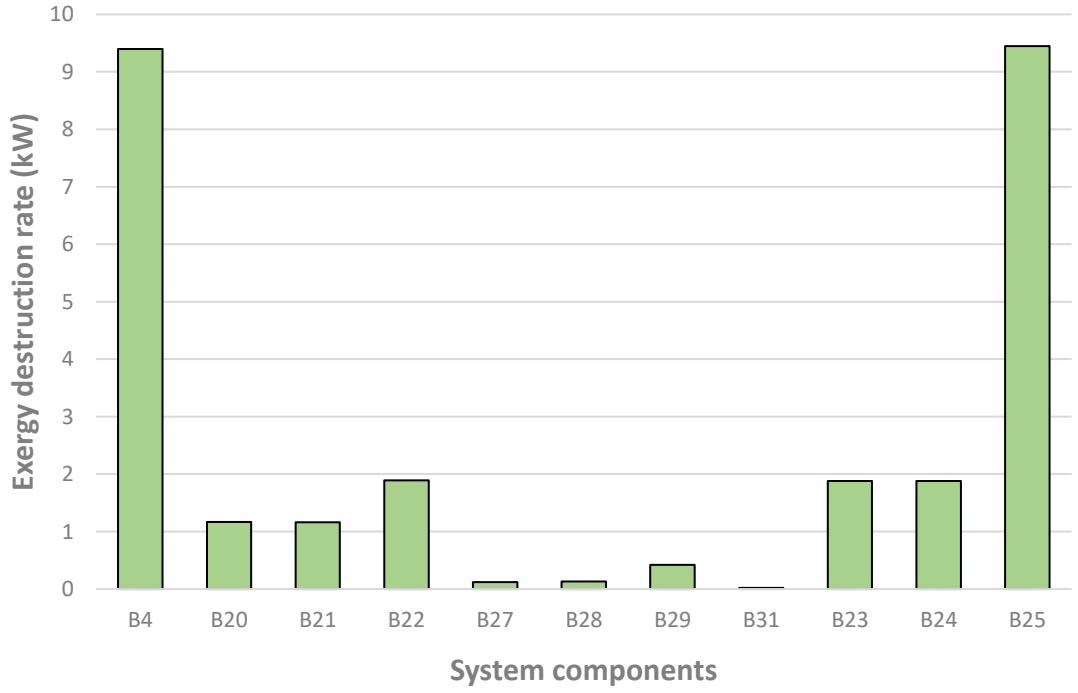

Figure 5.2 Exergy destruction of components other than the Cu-Cl cycle.

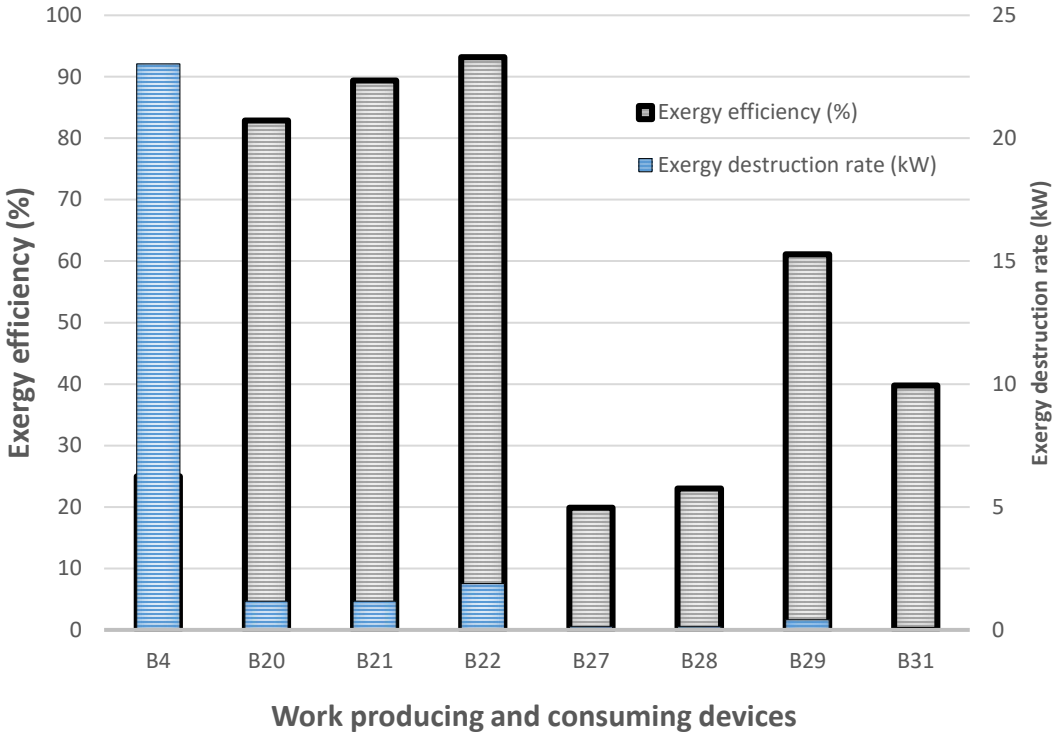

Figure 5.3 Exergy efficiency and exergy destruction rates of work producing and consuming devices.

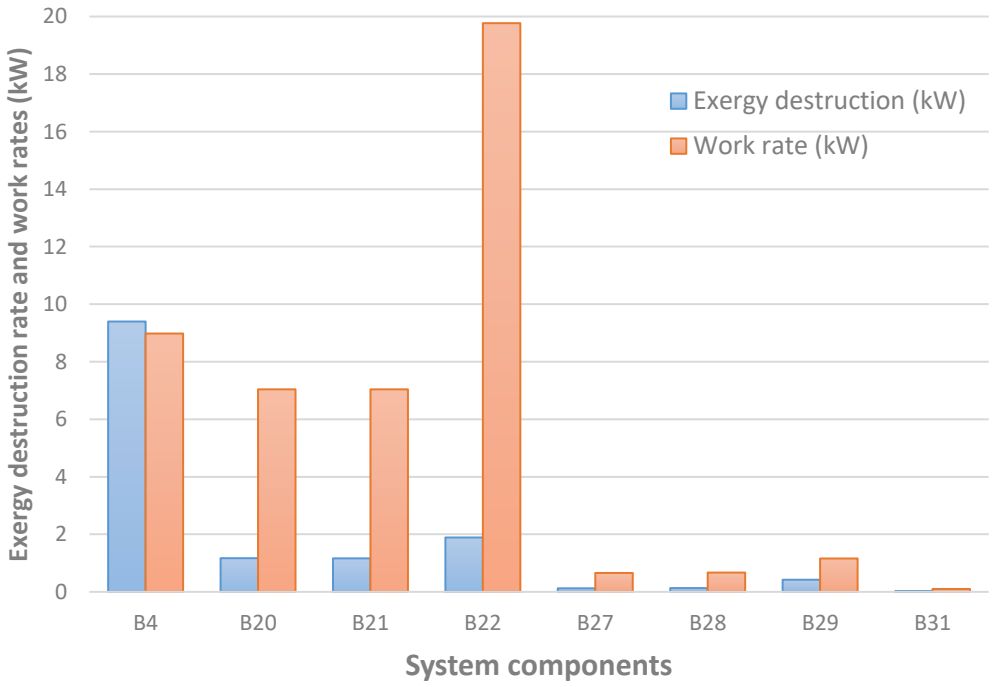

Figure 5.4 Exergy destruction rates and work rate of work producing and consuming devices.

The exergy destructions of the components other then copper chlorine cycle are presented in Figure 5.2. The maximum exergy destruction rate takes place in the third intercooler B25 and the second highest exergy destruction rate occurs in pump B4 because of the high flow rate. Exergy destruction rates of other components are also presented in the Figure.

Figure 5.3 describes the exergy efficiencies and exergy destruction rates of the work producing or consuming devices included in hydrogen production system 1. The maximum exergy efficiency belongs to the third compressor B22 which is 93% and maximum exergy destruction takes place in pump B4 due to the high flow rate of water. Exergy efficiencies and exergy destruction rates of other components are also drawn in the Figure 5.3.

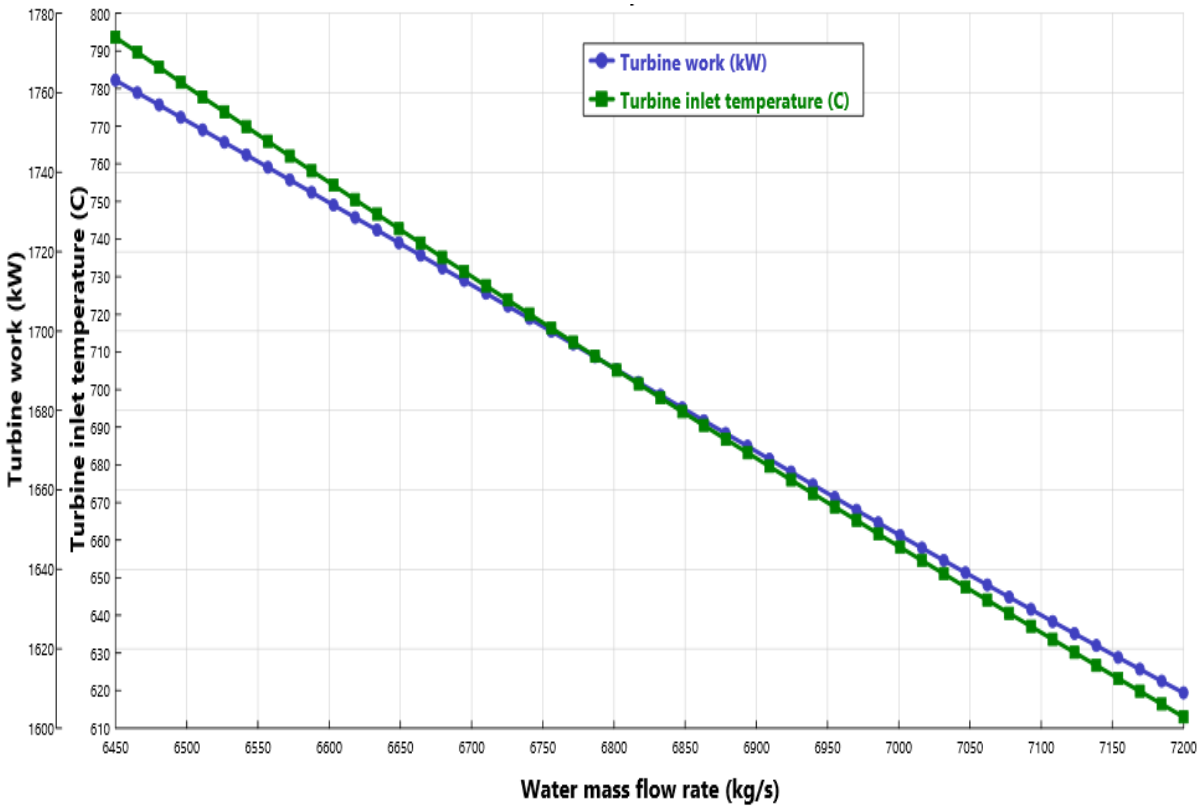

Figure 5.5 Effect of water mass flow rate on turbine inlet stream temperature and work produced by the turbine.

The work rate and the exergy destruction rates of the work producing or consuming devices in hydrogen production system 1 are compared in Figure 5.4. The maximum work rate is consumed by the third compressor B20 because of its high compression ratio and maximum

exergy destruction take place in B4 pump. All the work producing and consuming devices belonging to the system 1 are compared with respect to work rates and exergy destructions.

Different parametric studies are conducted on the system by varying different factors. The Figure 5.5 represents the effect of water flow rate on turbine work and turbine inlet temperature. With the increase in water mass flow rate, pump will be required to deal with higher flow rate and due to higher flow rate, the turbine inlet temperature will decrease. This decrease in the turbine inlet temperature will result in the reduction of turbine power as well.

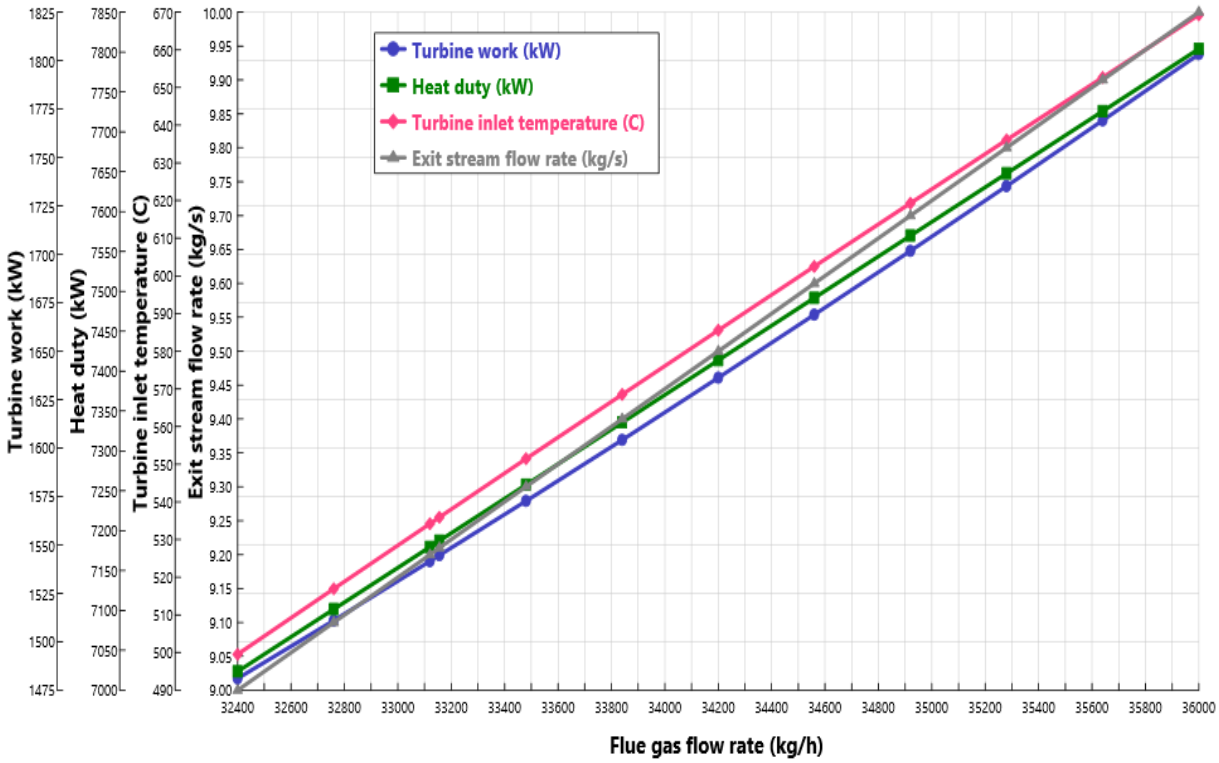

Figure 5.6 Effect of flow rate of flue gas on different parameters like turbine work, heat duty, turbine inlet temperature and exit stream flow rate.

Figure 5.6 represents the effect of flue gas flow rate on various parameters of the system like turbine work, heat duty, turbine inlet temperature and exit stream flow rate. By increasing the mass flow rate of flue gas coming from steel furnace, the flow rate of outlet stream S2 also increases simultaneously. The increase in flow rate of flue gas will impact on the heat duty associated with this stream and it will increase the heat duty. By increasing the mass flow rate, the inlet temperature of the turbine increase which results in increase

turbine power. So as a result, with the increase in flue gas flow rate, all four parameters turbine work, heat duty, turbine inlet temperature and exit stream flow rate will increase and it can be seen from the Figure 5.6.

The effect of water flow rate which in being circulated in the Rankine cycle as working fluid is plotted against the turbine power and pump work in Figure 5.7. As the mass flow rate of water will increase, the pump will be required to deal with higher flow rate. This higher flow rate will enhance the work associated with it. And with the increase in mass flow rate, turbine inlet temperature will decrease and this reduction in turbine inlet temperature will result in reduced turbine power. In the Figure 5.7, we can clearly see that with the increase in the flow rate of water which is circulating in the Rankine cycle, the work associated with the pump B4 increase while on the contrary, the power associated with the turbine decreases.

The Figure 5.8 represents the effect of variation in flue gas temperature on other parameters like turbine work, heat duty and turbine inlet temperature. As the temperature of the flue gas increases, the heat duty associated with that stream also increases and graph represents this increase. As the flue gas temperature will increased, heat transferred to the Rankine cycle from heat exchanger B1 also increase. The increased heat transfer results in increasing the temperature of turbine inlet stream S5 and this increased temperature results in increasing the turbine power. Thus the Figure 5.8 is representing the impact of flue gas temperature on heat duty associated with the same stream, the temperature of stream S5 which is entering into the turbine B2 and the power associated with the turbine. So with the increase in flue gas temperature, all these three factors increases.

The parametric study conducted in Figure 5.9 the effect of number of moles of H_2O entering into the heat exchange B1 associated with the Cu-Cl cycle on the heat duty of the same stream and the turbine power. Two mole of H_2O produces one mole of hydrogen so it is studied that how heat is increasing by increasing the moles of H_2O which increases the hydrogen production. As the number of moles of H_2O increases, the heat duty associated with that stream starts increasing and the increased heat duty of this stream will reduce the heat duty associated with the Rankine cycle stream and it results in decreasing the turbine power.

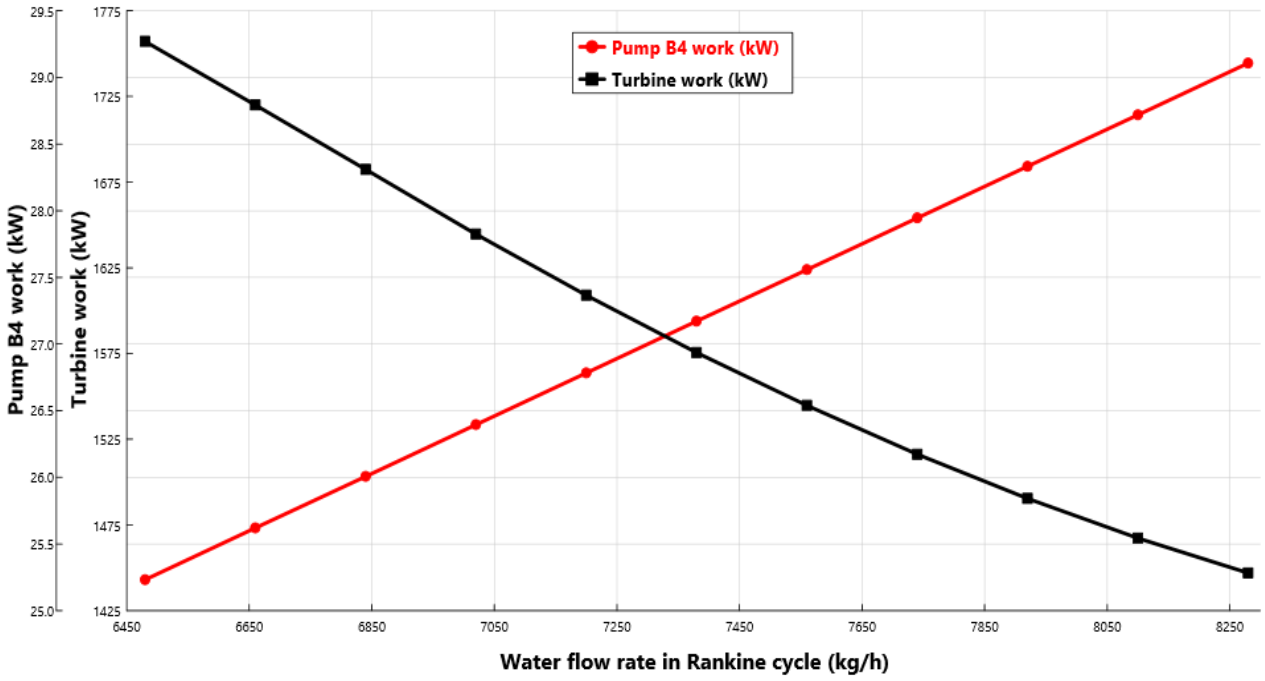

Figure 5.7 Water flow rate of Rankine cycle plotted against the pump work and turbine power.

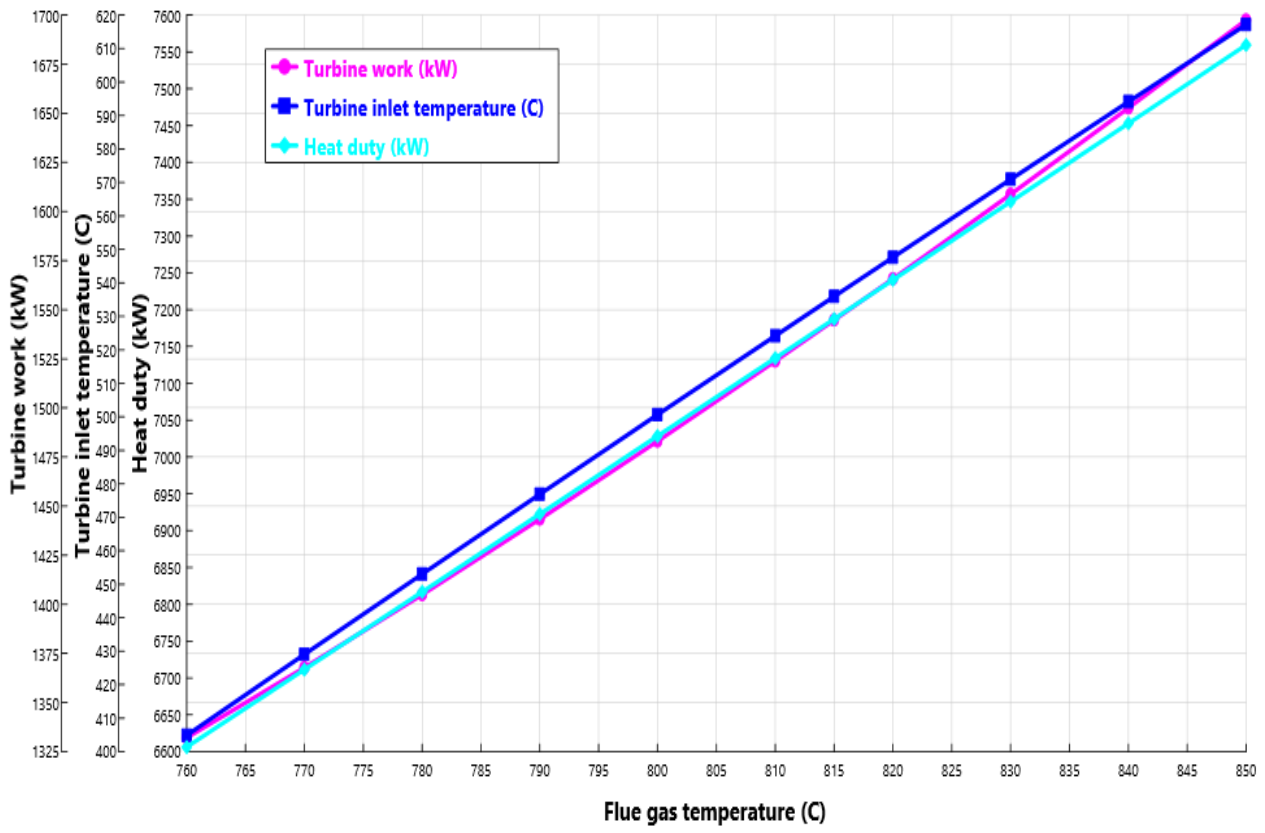

Figure 5.8 Effect of flue gas temperature on turbine inlet temperature, turbine work and heat duty.

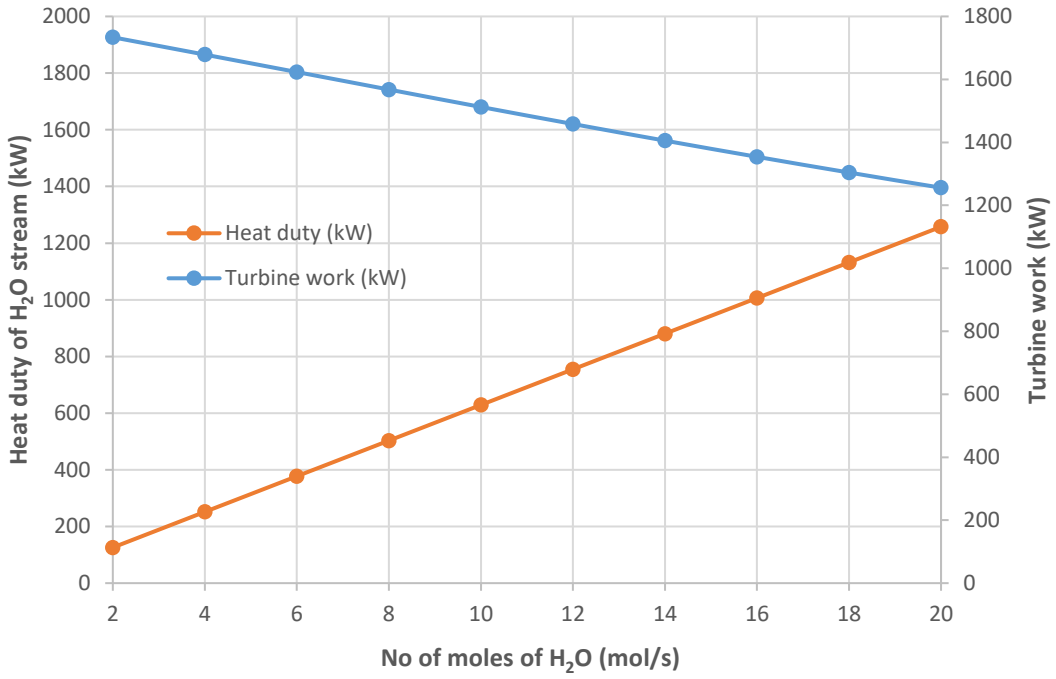

Figure 5.9 Number of moles of water plotted against the heat duty of water steam and turbine work.

Figure 5.10 represents the effect of number of moles on the heat duty of the same stream and turbine inlet temperature. By increasing the number of moles of H_2O, the heat duty associated with the same stream increases. This increased heat duty results in decreasing the heat duty of the stream associated with the Rankine cycle and reduced heat duty of the stream associated with the Rankine cycle results in decreasing the turbine inlet temperature which further reduces turbine power as well.

The increase in number of moles of H_2O results in increased hydrogen production because two moles of H_2O produces one mole of hydrogen. The Figure 5.11 represents the effects of increased water flow rate for increasing hydrogen production on turbine inlet temperature, heat duty associated with the same stream leading towards Cu-Cl cycle and turbine power.

The energy and exergy efficiencies of the subsystems of the proposed system 1 are presented in Figure 5.12. The energy efficiency of the Rankine cycle in system 1 is 20.4% and exergy efficiency is 23.1%. The energy efficiency of Cu-Cl cycle is 40.4% and the

exergy efficiency is 41.4 %. The energy efficiency of the multistage reheat Rankine cycle is 34.5% and exergy efficiency is 38.1%.

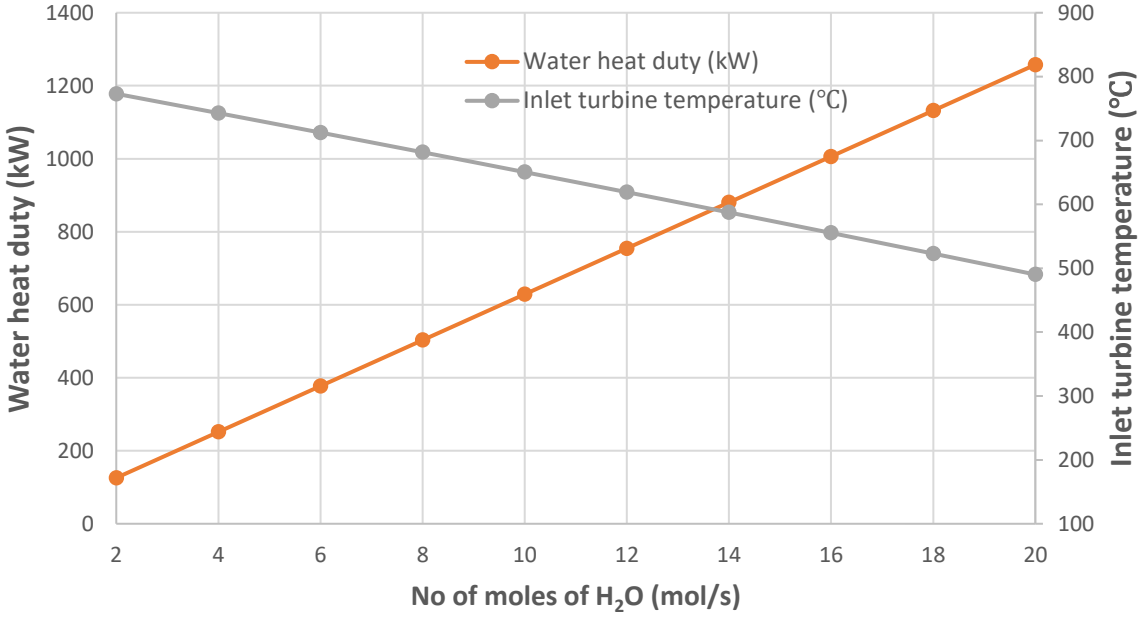

Figure 5.10 Number of moles of H_2O plotted against the heat duty and inlet turbine temperature.

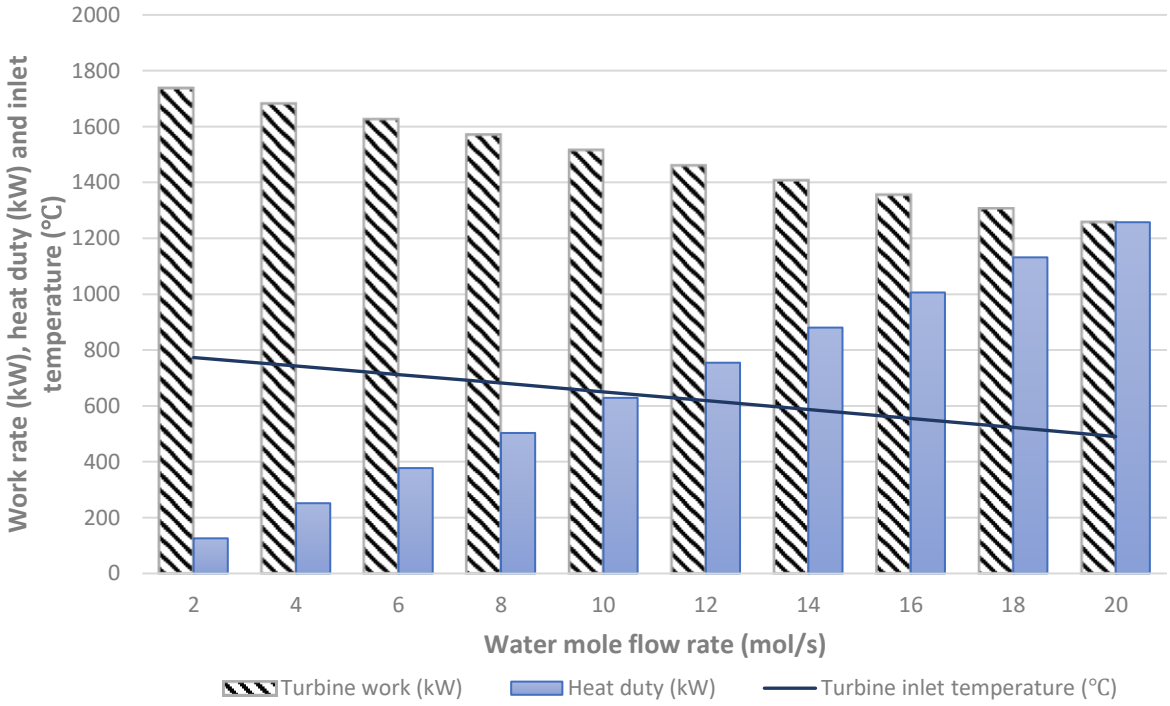

Figure 5.11 Effect of water flow rate associated with the Cu-Cl cycle on the heat duty of the same stream, turbine inlet temperature and turbine work.

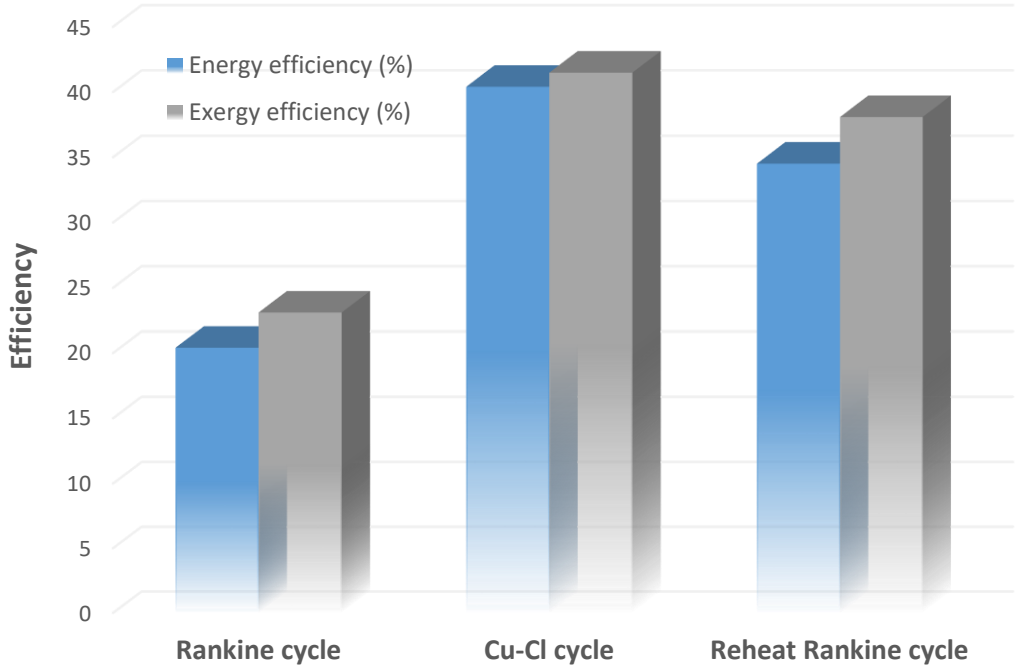

Figure 5.12 Energy and exergy efficiencies of the main subsystems of proposed system 1.

5.2 System 2 results

In this section, the energy and exergy analysis is performed on the proposed hydrogen production system 2 and results of thermodynamic analysis and simulation are described. The reference conditions are taken as 25 ℃ temperature and 1 atm pressure. Aspen Plus software is used to calculate all stream properties and excel calculations are conducted for other performance parameters like energy and exergy efficiencies, chemical exergies and exergy destruction rates. The major results containing energy and exergy efficiencies, operational requirements of system and exergy destruction rates are presented in this section. Hydrogen production specifications like production rate, production temperature and production pressure and the overall efficiencies of system 2 are tabulated in Table 5.2.

Table 5.2 describes the major parameters like energy and exergy efficiency, exergy destruction rate, produced work rate and produced hydrogen specification. The overall energy efficiency of the second system is 32.7% and the exergy efficiency is calculated as 32%.

Table 5.2 Major results of the hydrogen production system 2 from cement industrial waste heat.

Parameter	**Value**	**Unit**
Hydrogen production pressure	750	Bar
Hydrogen production temperature	25	℃
Flue gas flow rate	31.71	kg/s
Hydrogen production rate	140.8	kg/h
Energy efficiency	32.7	%
Exergy efficiency	32	%

Various parametric studies are conducted on integrated system 2 in order to see the effect of different variables on the system. Figure 5.13 represents the exergy destruction rates associated with the Cu-Cl cycle components existing in the second proposed hydrogen production system. The maximum exergy destruction rate takes place in decomposition reactor B5. The second highest exergy destruction rate occurs in electrolyzer B9 and exergy destruction rates of other components are also presented in the Figure 5.13.

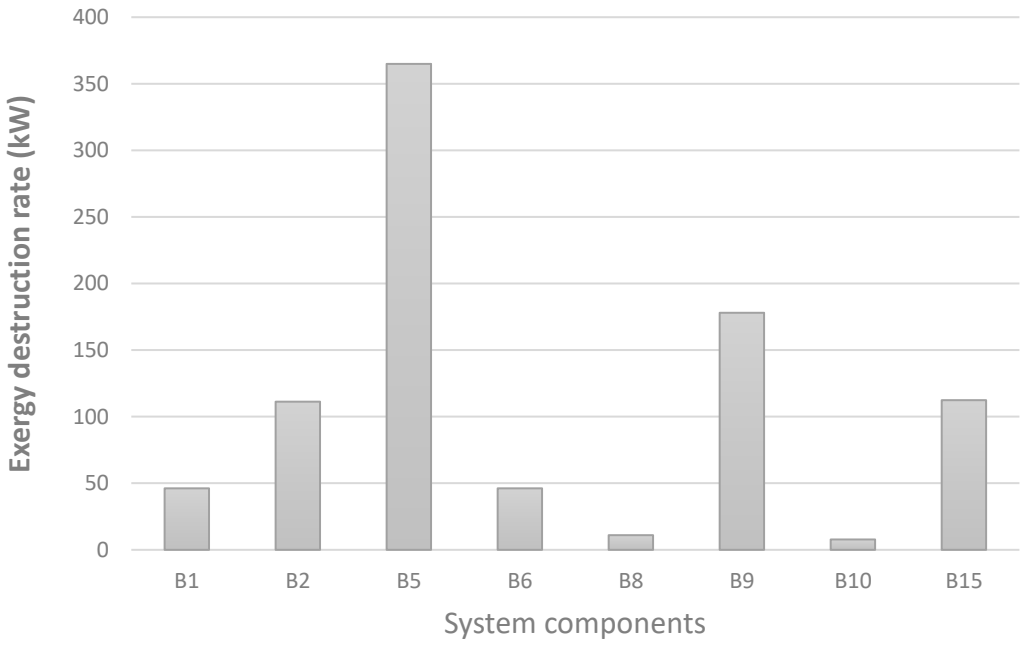

Figure 5.13 Exergy destruction rates of the components including the Cu-Cl cycle (component names referenced in Figure 3.5).

The exergy destruction rates of the components other then the hydrogen production Cu-Cl cycle are presented in Figure 5.14. The maximum exergy destruction rate takes place

in the third intercooler B25 and the second highest exergy destruction rate occurs in the third compressor B22. The exergy destruction rates of the other components are also presented in Figure 5.14.

The exergy efficiency and the work rates of the work producing and consuming devices including in system 2 are plotted in Figure 5.15. All the components which are either producing or consuming the work, are included in this bar chart. The third compressor B22 has the maximum exergy efficiency and the maximum work rate is also produced by the same compressor B22 because of high compression ratio. The second compressor B21 carries the second highest exergy efficiency and also the second highest work rate is presented by the same component.

Figure 5.16 shows the plot of exergy destruction rate, work rate and exergy efficiency of all the work producing and consuming devices in system 2. The maximum exergy destruction rate, work rate and exergy efficiency occurs in third compressor B22.

The second top exergy destruction rate, work rate and exergy efficiency take place in the second compressor B21. The exergy efficiency, work rates and exergy destruction rates are also included in Figure 5.16.

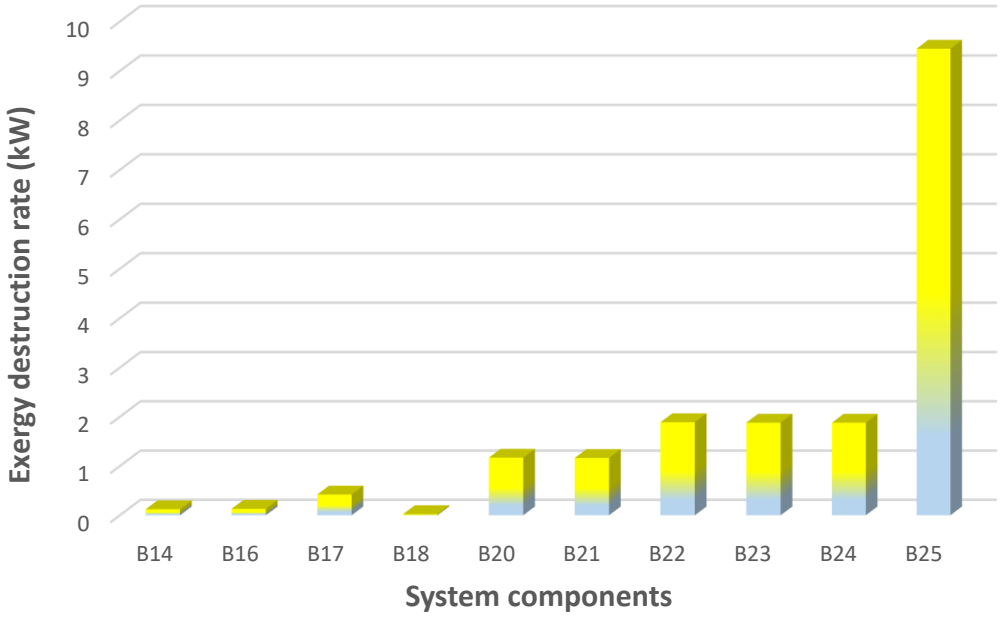

Figure 5.14 Exergy destruction rates of the components other than the Cu-Cl cycle.

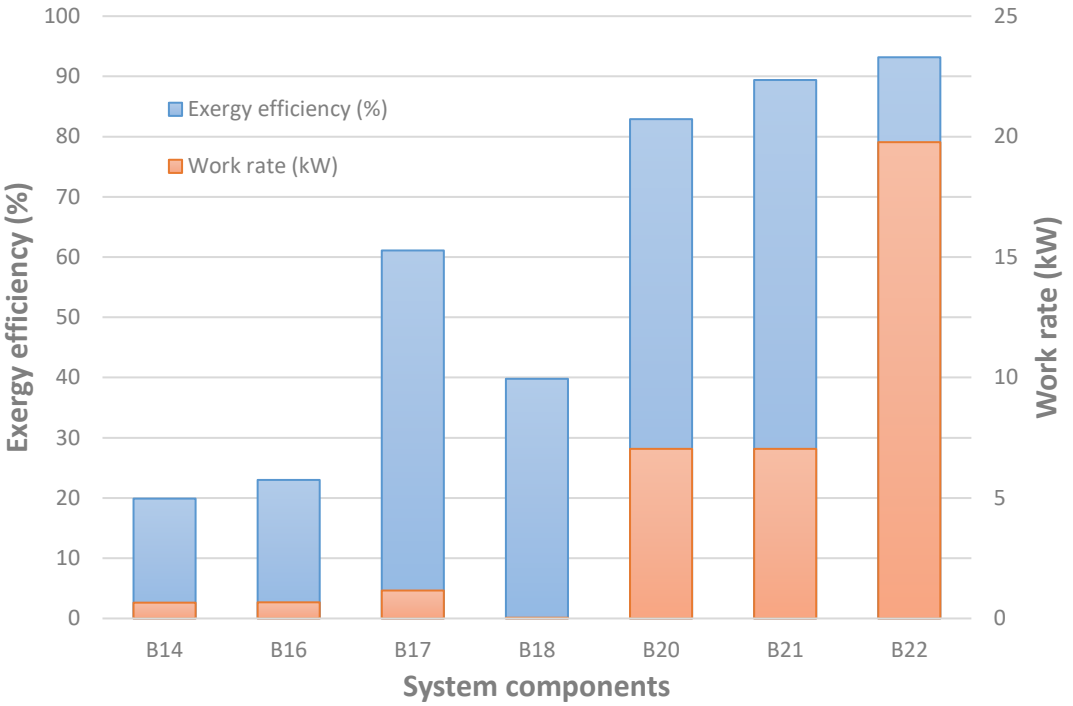

Figure 5.15 Exergy efficiency and work rates of work producing and work consuming devices in system 2.

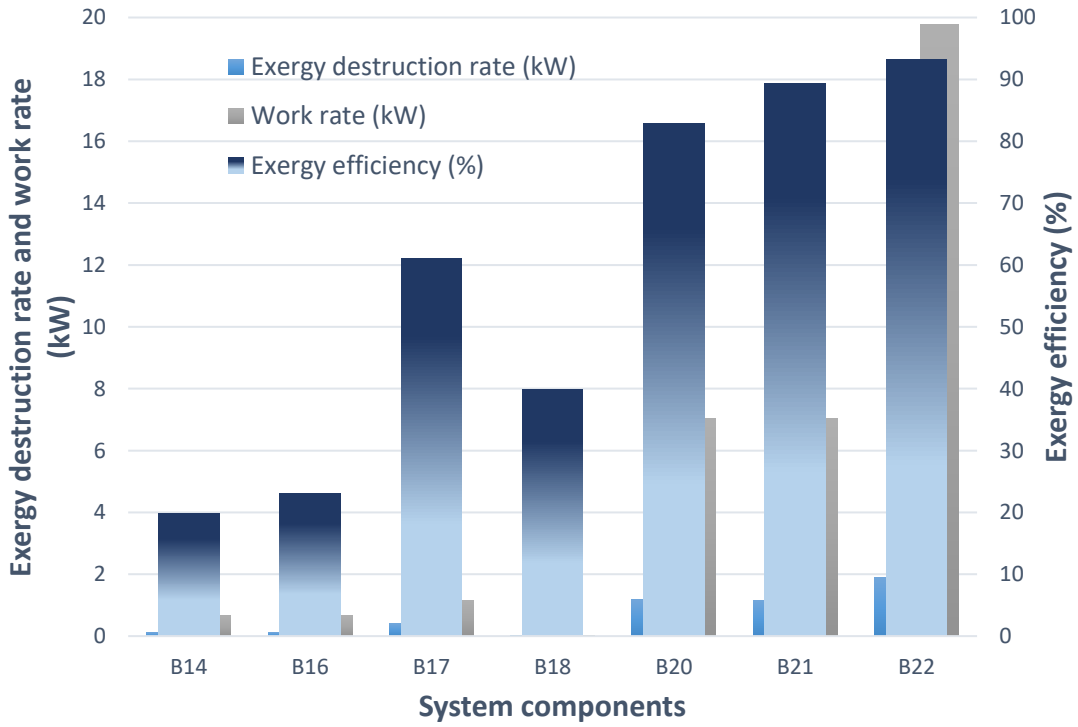

Figure 5.16 Exergy destruction rates, work rates and exergy efficiencies of work producing or consuming devices in system 2.

The stream S3 contains the water which is used in hydrogen production Cu-Cl cycle and stream S26 contains $CuCl_2$ which reacts with water in hydrolysis reactor B2. According to the hydrogen production Cu-Cl cycle, two mole of water are required to produce one mole of hydrogen. So production of hydrogen and oxygen is plotted against the flow rate of water and cupric chloride which is provided in Cu-Cl cycle in Figure 5.17. The energy efficiency of the hydrogen production Cu-Cl cycle is 40.396% and the exergy efficiency is calculated as 41.48%.

The turbine work and pump work of the Rankine cycle are plotted against the water flow rate of the Rankine cycle. Figure 18 shows the effect of the water flow rate on the turbine work and pump work. As the water flow rate increases, the turbine work starts decreasing, and at the same time, the pump work increases because the pump must deal with a high flow rate with a required high work input. So with an increase in the water flow rate, the power produced by the turbine decreases, while the work consumed by the pump continues to increases.

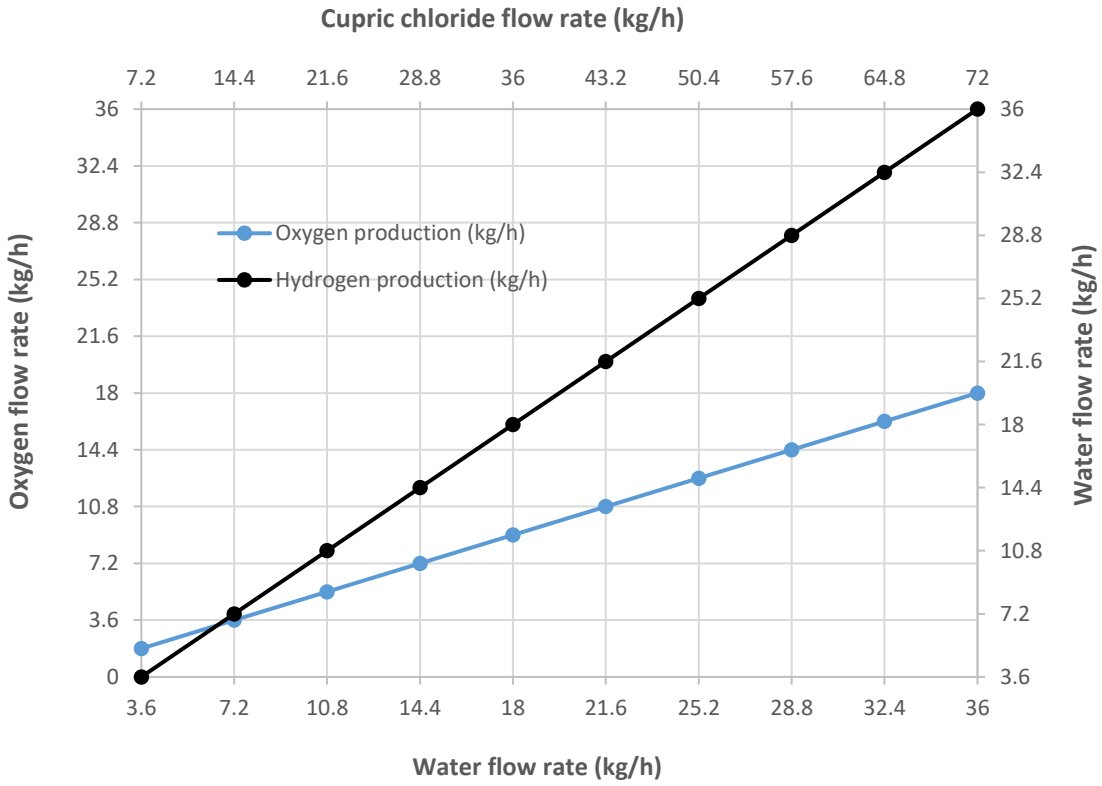

Figure 5.17 Production of hydrogen and oxygen with respect to the water and $CuCl_2$ flow rates.

The water flow rate is plotted against the heat duty of water stream and number of moles of hydrogen produced in Figure 5.19. The water flow rate is chosen from 2 to 40 moles per second. The hydrogen production of proposed system 2 is 19.547 mol/s and for this much hydrogen production, double moles of water is required to be supplied to the hydrogen production Cu-Cl cycle. So the number of moles of hydrogen produced is half of the water supplied to the Cu-Cl cycle according to the balanced reaction equation. Figure 5.19 shows that with the increase in the flow rate of water, heat duty associated with the same stream increases and number of moles of hydrogen produced is also increased at the same time.

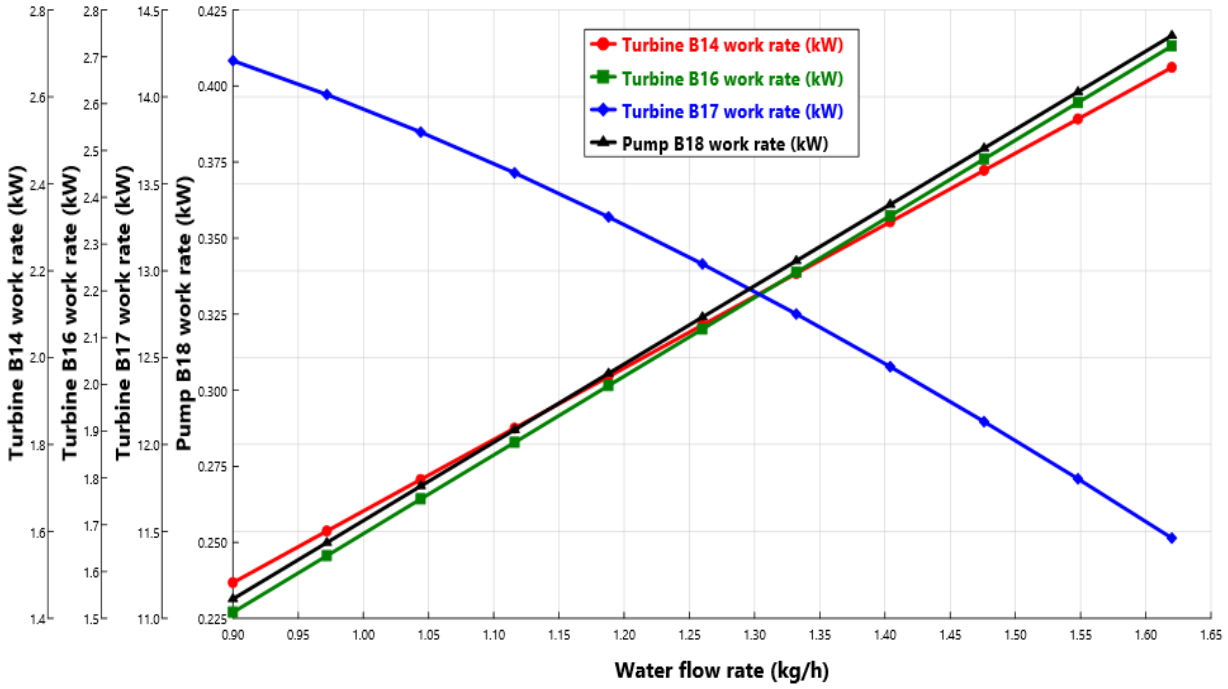

Figure 5.18 Effects of water flow rate on turbine and pump power.

The turbine work and the pump work of Rankine cycle is plotted against the water flow rate of the Rankine cycle. Figure 5.20 represents the effect of water flow rate on the turbine work and pump work. As the water flow rate starts increasing, the turbine work starts decreasing and at the same time, pump work start increasing because pump has to deal with high flow rate which required high work input. So with the increase in water flow rate, the power produced by the turbine keep on decreasing while on the opposite side, the work consumed by the pump keep on increasing.

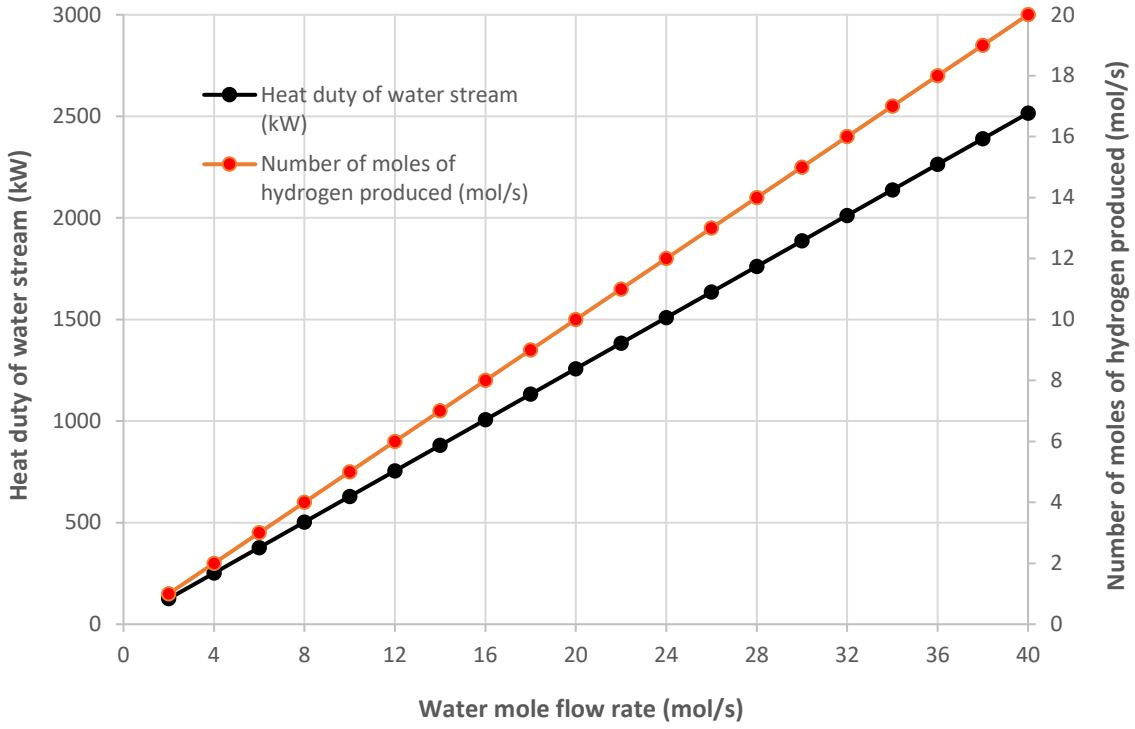

Figure 5.19 Water flow rate plotted against the heat duty of water stream and number of moles of hydrogen produced.

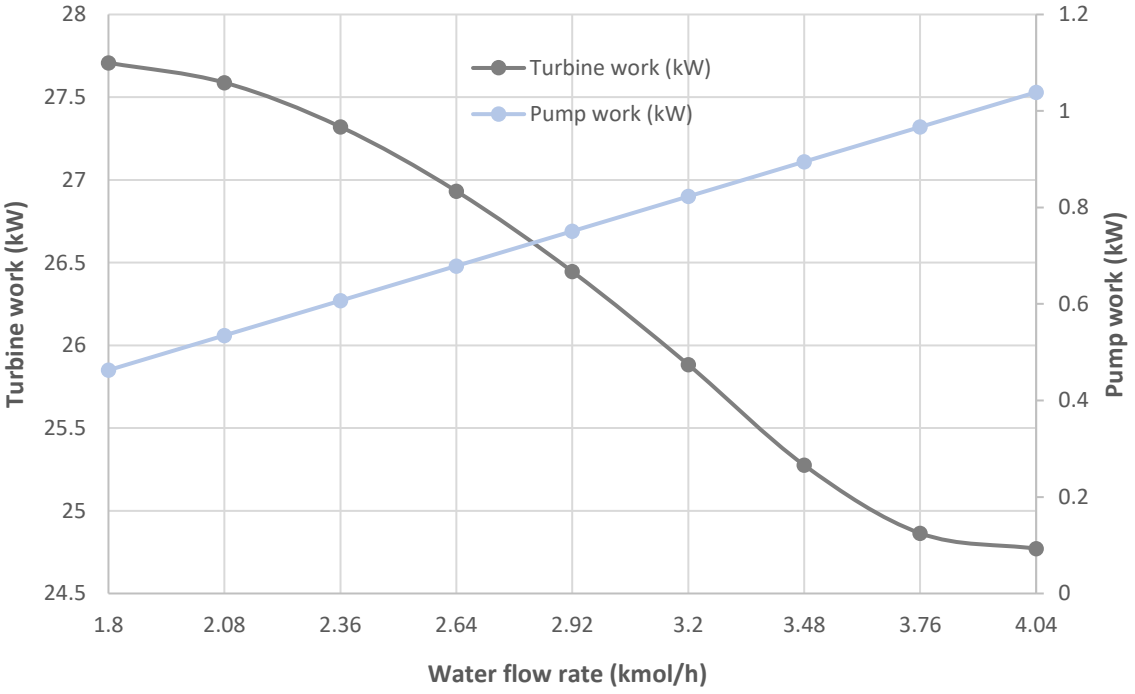

Figure 5.20 Plot of turbine work and pump work of Rankine cycle against the water flow rate.

The energy and exergy efficiencies of the major subsystems of proposed system 2 are shown in Figure 5.21. The energy efficiency of Cu-Cl cycle is 40.4% and the exergy efficiency is 41.46%. The energy efficiency of multistage reheat Rankine cycle is 34.78% and exergy efficiency is 38.19%.

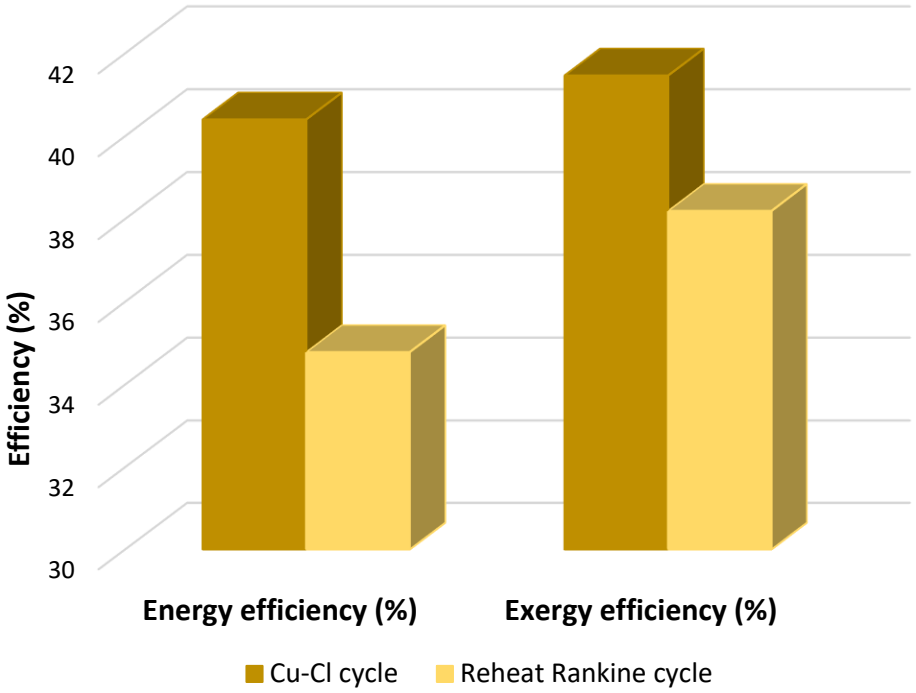

Figure 5.21 Energy and exergy efficiencies of the main subsystems of proposed system 2.

5.3 System 3 results

The energy and exergy analyses is performed on the proposed hydrogen production system 3 and results of thermodynamic analysis and simulation are described in this section. The ambient conditions are taken as 25 °C temperature and 1 atm pressure. Some excel calculations are conducted for measuring performance parameters like energy and exergy efficiencies, chemical exergies and exergy destruction rates. The major results containing energy and exergy efficiencies, operational requirements of system and exergy destruction rates are presented in this section. Hydrogen production specifications like production rate, production temperature and production pressure and the overall efficiencies of system 3 are tabulated in Table 5.3. The overall energy efficiency of the second system is 48.6% and exergy efficiency is calculated as 40.5%.

Table 5.3 describes the major parameters like energy and exergy efficiency, exergy destruction rate, produced work rate and produced hydrogen specification.

The exergy destruction rates of hydrogen production Cu-Cl cycle included in proposed system 3 are plotted in Figure 5.22. The maximum exergy destruction rate exists in decomposition reactor B11. The second highest exergy destruction rate occurs in the electrolyzer B14. The exergy destruction rates of other components included in Cu-Cl cycle are also plotted in Figure 5.22.

Table 5.3 The performance parameters of proposed hydrogen production system 3.

Parameter	**Value**	**Unit**
Exhaust gas flow rate	6.366	kg/s
Work rate	1.811	MW
Hydrogen production pressure	750	Bar
Hydrogen production temperature	25	℃
Hydrogen production rate	43.2	kg/h
Energy efficiency	48.6	%
Exergy efficiency	40.2	%

The exergy destruction rates of the components other then hydrogen production Cu-Cl cycle are plotted separately. In Figure 5.23, the exergy destruction rates of the components except Cu-Cl cycle are described. The highest exergy destruction rate takes place in pump B4 because of the high flow rate of water. The second highest exergy destruction rate occurs in third intercooler B25. The third highest exergy destruction rates takes place in the third compressor B22. The exergy destruction rates of the other components are also described in Figure 5.23.

The work producing or consuming devices are investigated separately on the basis of their work rates and exergy destruction rates. In Figure 5.24, the work rates and the exergy destruction rates of work producing or consuming devices are compared. The maximum work rate is consumed in the pump B4 and the maximum exergy destruction rate also occurs in the same components. The second highest work rate consumed by the third compressor B22 and the reason behind high work rate is its high compression ratio. The maximum exergy destruction rate also belongs to the same component B22. The

exergy destruction rates and work rates of other work producing or consuming devices are also plotted in Figure 5.24.

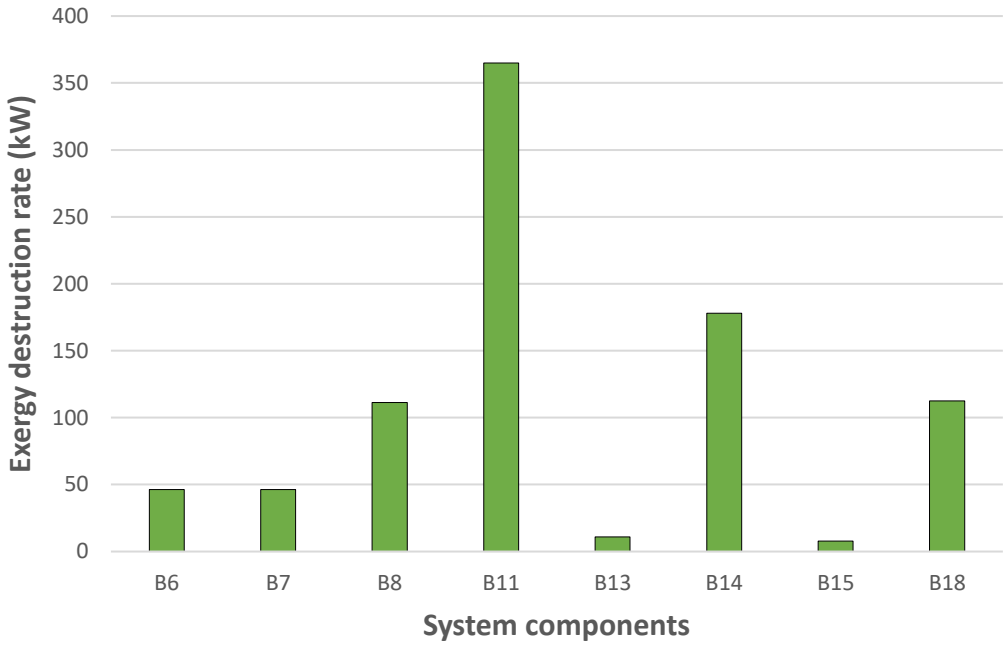

Figure 5.22 Exergy destruction rates of components included in hydrogen production Cu-Cl cycle (component names referenced in Figures 3.7. 3.8 and 3.9).

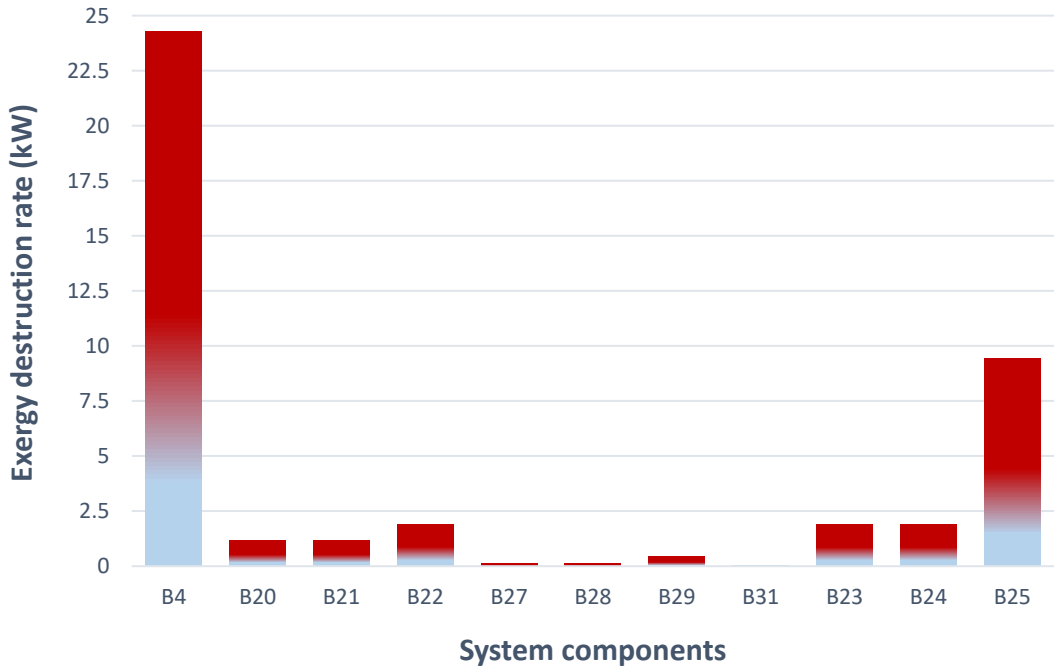

Figure 5.23 Exergy destruction rates of components excluding the Cu-Cl cycle.

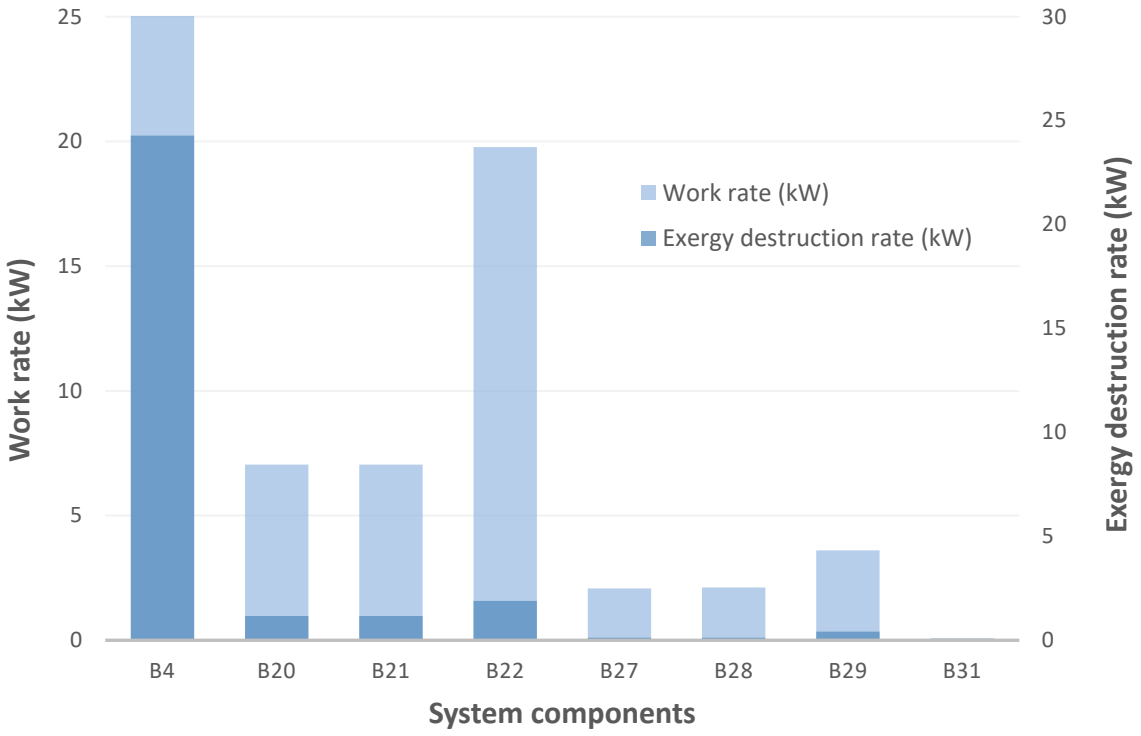

Figure 5.24 Eork rates and exergy destruction rates comparison of work producing and consuming devices in system 3.

The effect of changing water flow rate in stream S3 which is leading towards the hydrogen production Cu-Cl cycle is discussed on the heat duty of the same stream and the turbine power. As the heat duty of the stream S3 will increase, the heat duty of the stream associated with Rankine cycle will decrease simultaneously. Figure 5.25 shows that with the increase in inlet water flow rate, the heat duty associated with the same stream starts on increasing. While the turbine power starts on decreasing with the increase in the inlet water flow rate.

In Figure 5.26, the effect of input water flow rate which enters into the Cu-Cl cycle is discussed on the turbine inlet temperature and turbine work. With the increase in input water flow rate, the heat duty associated with this stream starts increasing and as a result, the heat duty associated with the Rankine cycle stream starts decreasing. This reduction in the heat duty leads to the decrease in turbine inlet temperature and reduced turbine inlet temperature causes the decrease in turbine work.

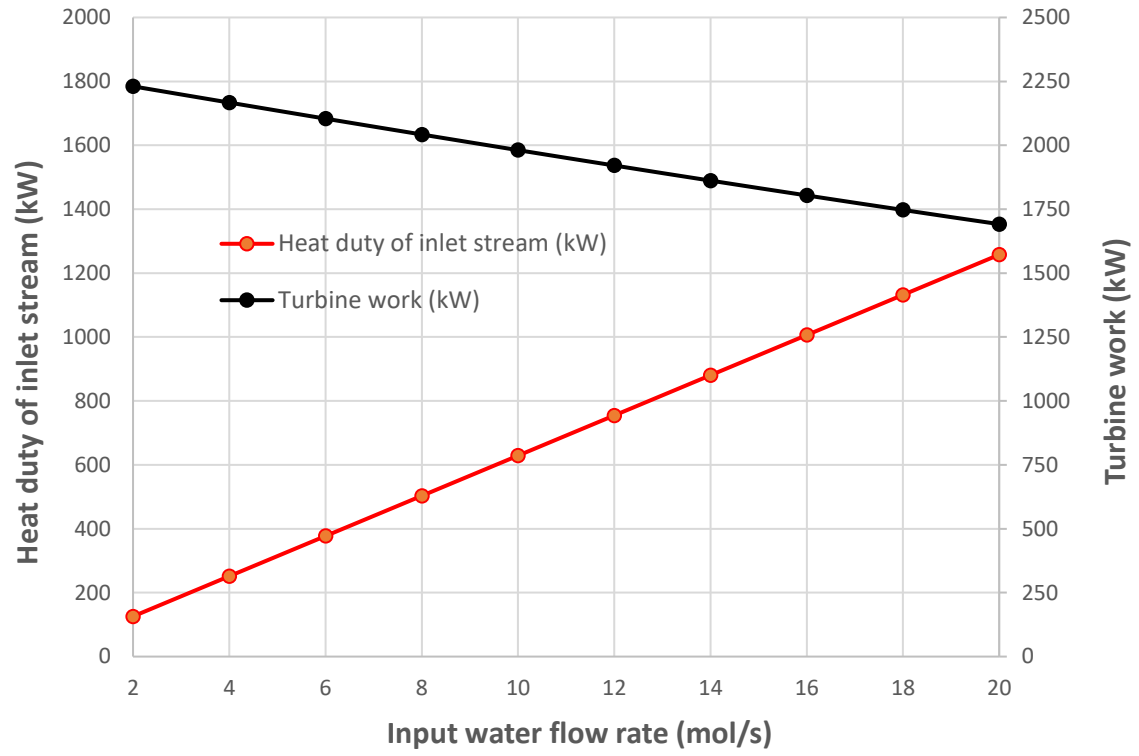

Figure 5.25 Heat duty and the turbine power plotted against the input water flow rate.

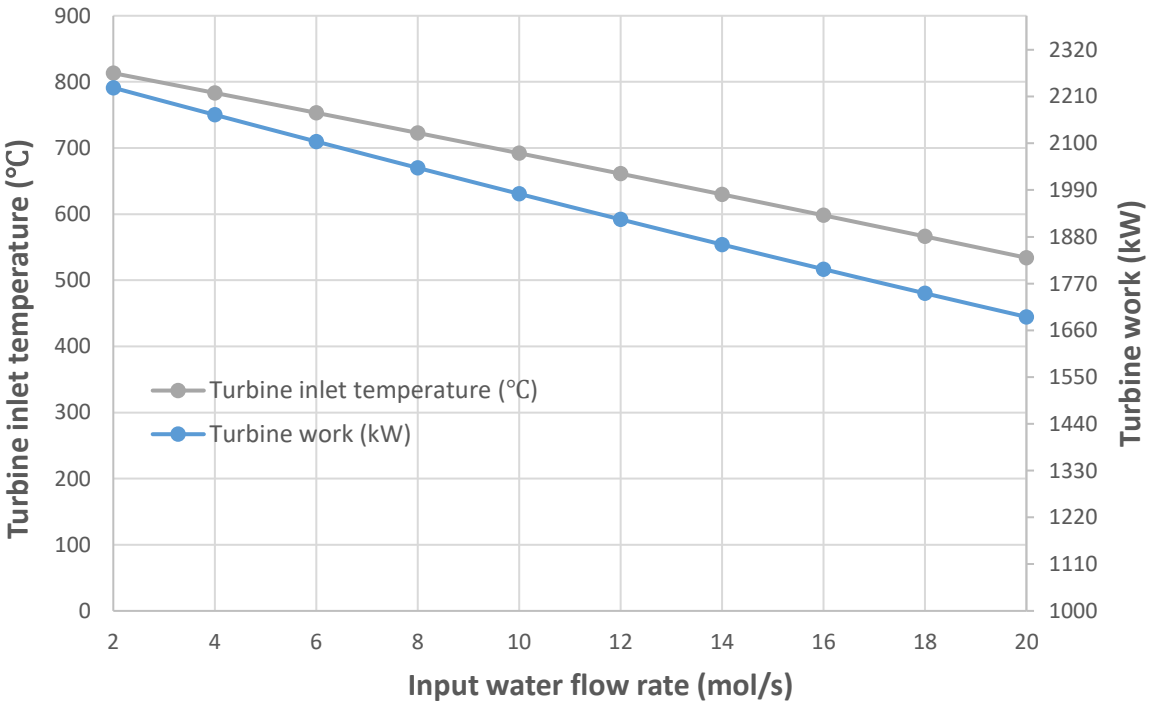

Figure 5.26 Turbine inlet temperature and turbine work plotted against the input water flow rate.

The effect of change in water flow rate in Rankine cycle on some other parameters is studied. The variation in turbine work, turbine inlet temperature and turbine inlet mass flow is plotted against the water flow rate in Figure 5.27. The graph presents that with the increase in water flow rate, the inlet temperature of turbine decreases in a proper sequence and turbine inlet mass flow increases simultaneously with increase in water flow rate. As the turbine inlet temperature increases, it results in the increased turbine power. So Figure 5.27 presents the impact of water flow rate on three different parameters and it can be seen clearly that with the increase in water flow rate, the turbine inlet temperature and turbine power decrease while turbine inlet mass flow increases.

Figure 5.28 shows a parametric study by varying the flue gas flow rate and to see its effect on the heat duty and outlet stream temperature. As the flue gas flow rate will increase, the heat duty will increase simultaneously in a proper sequence. The increase heat duty results in increasing the outlet stream temperature as well. This outlet stream is the same which enters into the turbine.

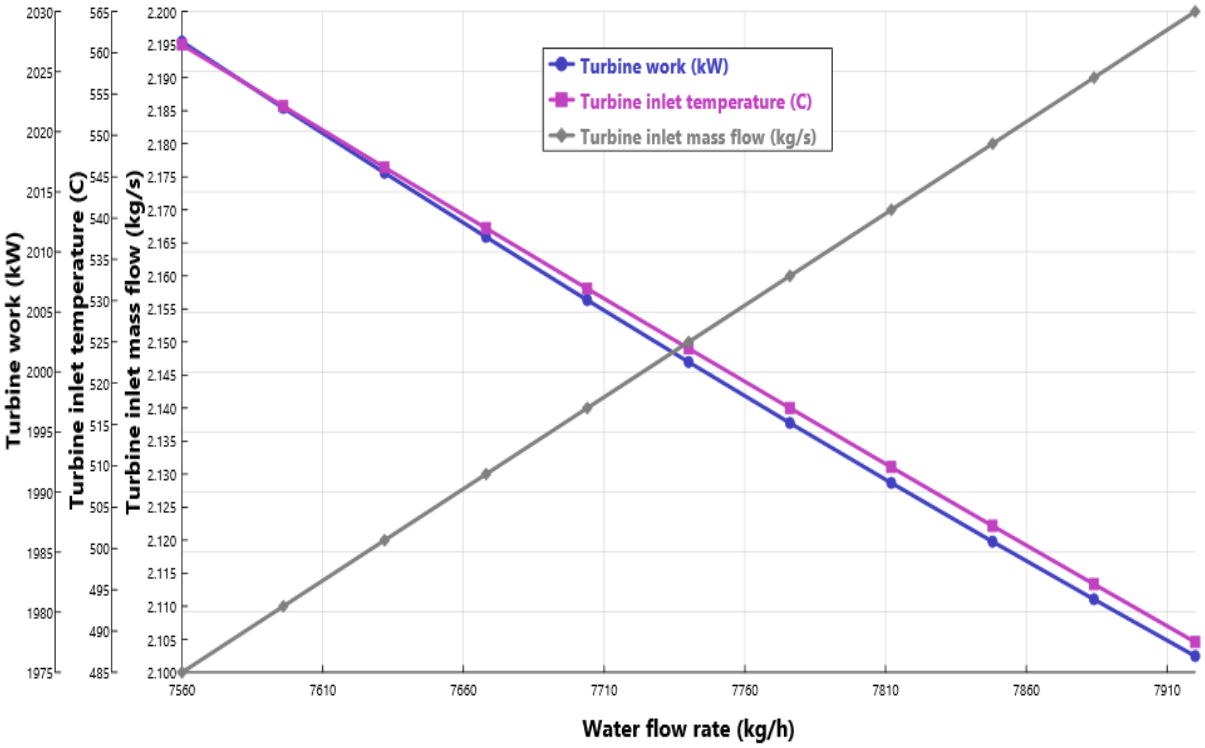

Figure 5.27 Effect of water mass flow rate on turbine work, turbine inlet temperature and turbine inlet mass flow rate.

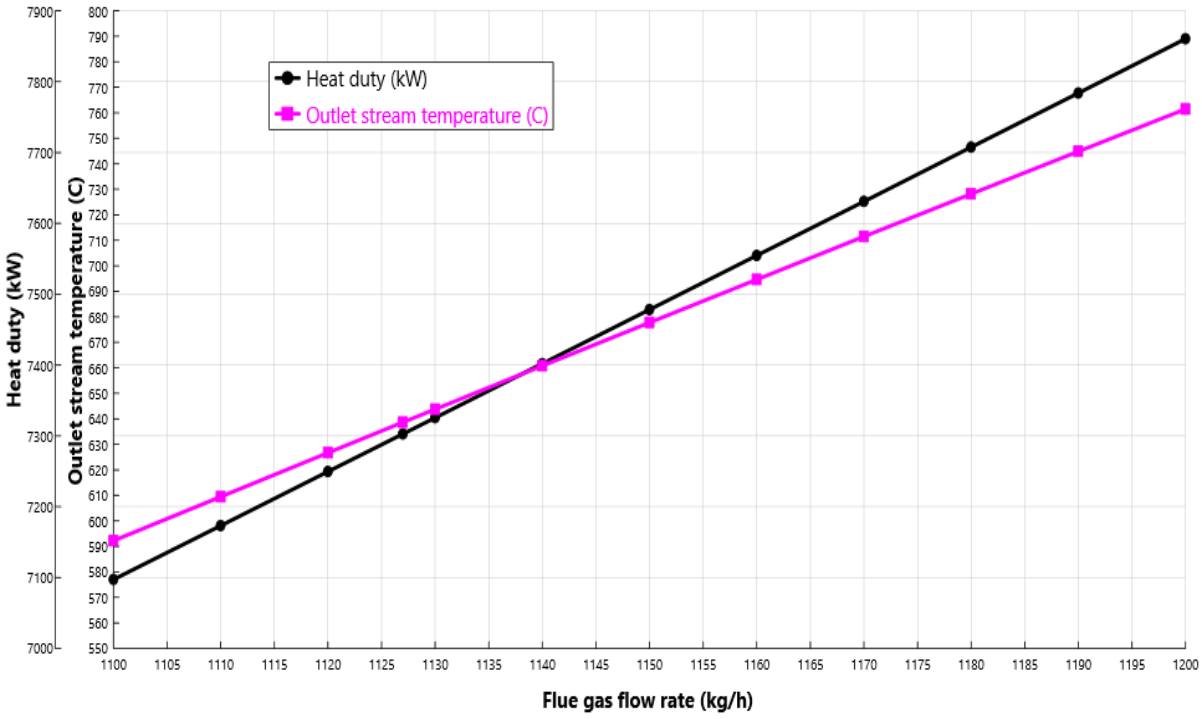

Figure 5.28 Effect of flue gas flow rate on heat duty and outlet stream temperature.

In Figure 5.29, the flue gas flow rate is plotted against the turbine work and heat duty. With the increase in flue gas flow rate, the heat duty of the stream increases simultaneously. And as the heat duty associated with the turbine inlet stream increases, this increased heat duty result in the increased turbine power. So as a result, when heat duty increases with the increase in flue gas flow rate, the turbine work also increases and it can be seen clearly from the Figure 5.29.

The turbine work rate, heat duty of water inlet stream and turbine inlet temperature are studied by varying the ambient water temperature. Figure 5.30 represents the effects of ambient temperature on the turbine work rate, heat duty and turbine inlet temperature. With the increase in ambient temperature, the heat duty associated with the stream leading towards the Cu-Cl cycle decreases and the reason behind it is when water will be introduced at high temperature, it will absorb less amount of heat. This decrease in heat duty results in the increase in the heat duty of the stream associated with the Rankine cycle. So the turbine inlet temperature increases with the increase in ambient temperature which causes the turbine work to increase which can be seen from the Figure.

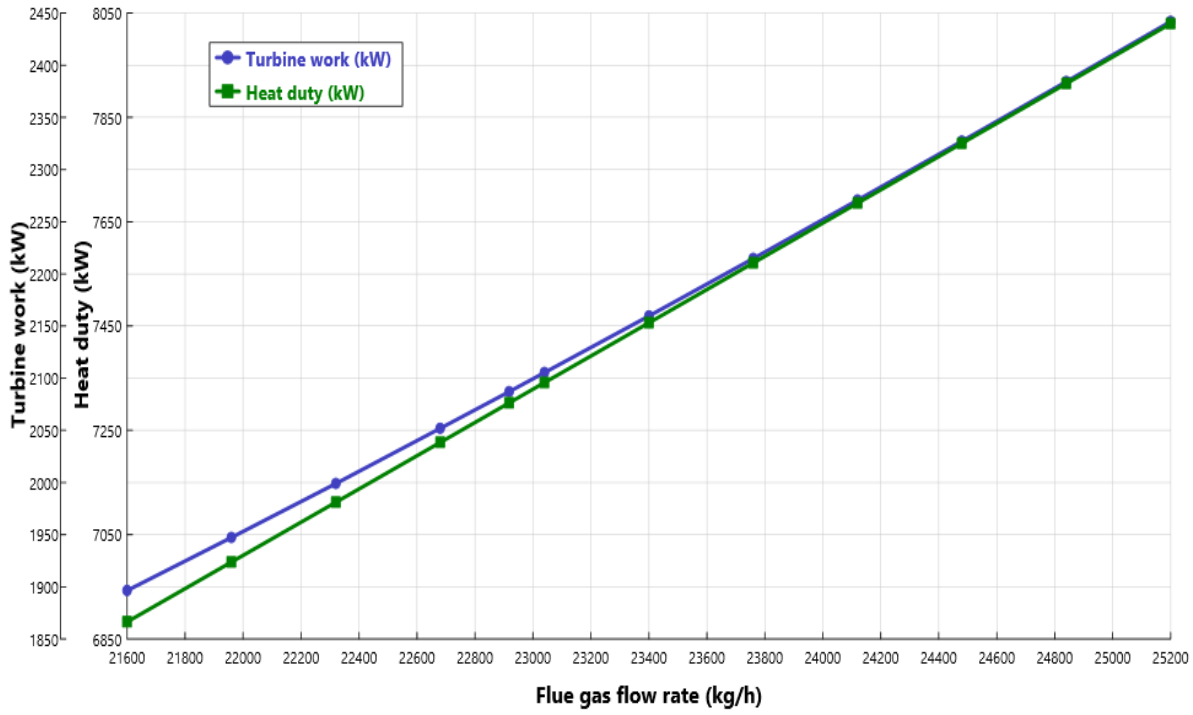

Figure 5.29 Flue gas flow rate plotted again the heat duty and turbine work rate.

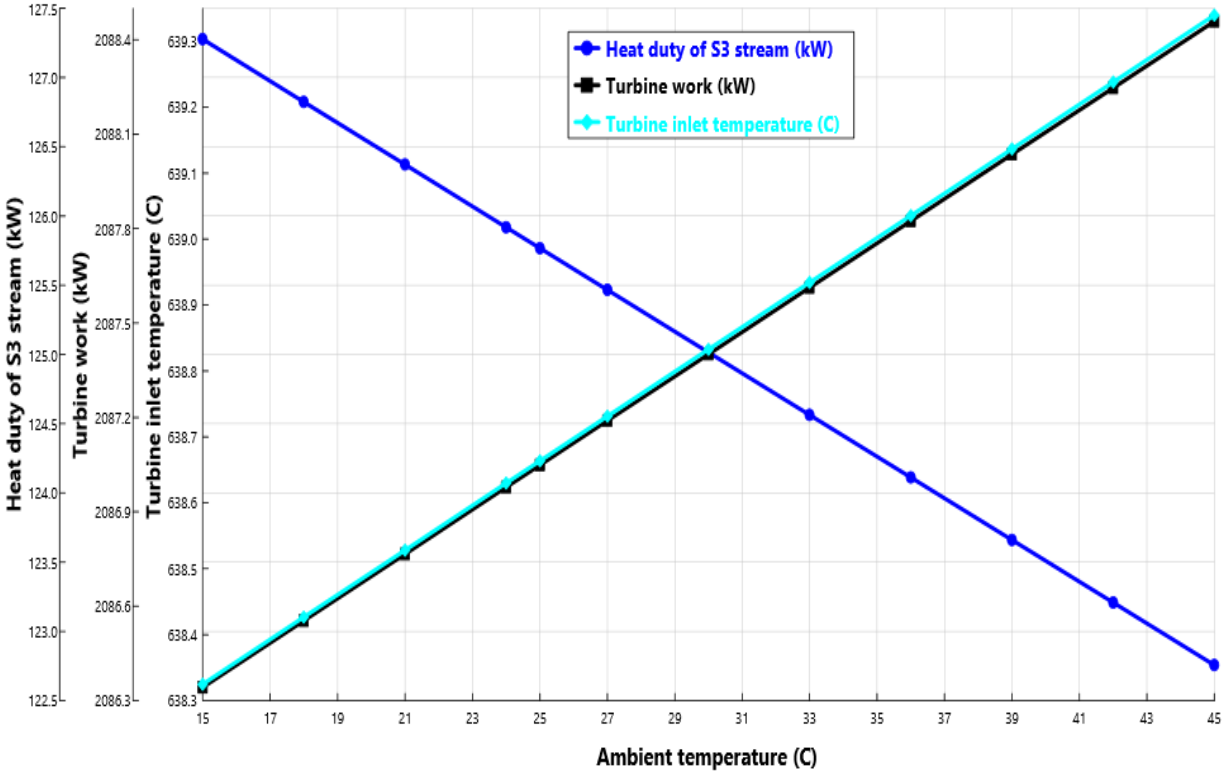

Figure 5.30 Effect of ambient water temperature on turbine work, heat duty and turbine inlet temperature.

For multistage reheat Rankine cycle, several parametric studies are conducted in order to consider the effect of different variables on the system. In Figure 5.31, the total turbine work rate and heat duty of the inlet stream from block B26 is plotted against the inlet temperature of hydrogen chloride gas. Figure 5.32 shows that with the increase in inlet temperature, total turbine work and heat duty both increases continuously. The total turbine work is the summation of all three turbines B27, B28 and B29 included in multistage reheat Rankine cycle.

The effect of input flow rate of hydrogen chloride gas is also studied. Figure 5.30 shows the effect of input flow rate of HCl gas on the heat duty and total work rates of the turbines. With increase in the mass flow rate of HCl gas, the heat duty of respective stream in block B26 increases and total work rate from turbines also increases continuously. The total work rate is representing the sum of the work rates of all three turbine of multistage reheat Rankine cycle.

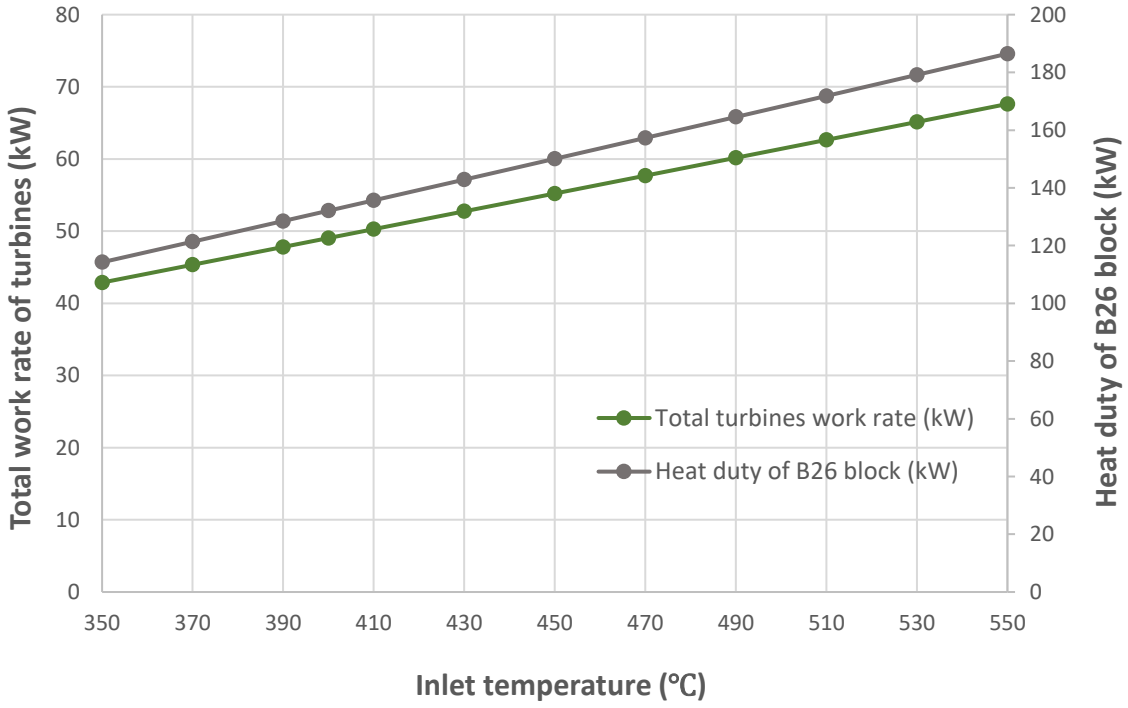

Figure 5.31 Effect on inlet temperature of HCl on total work rate of turbines and heat duty.

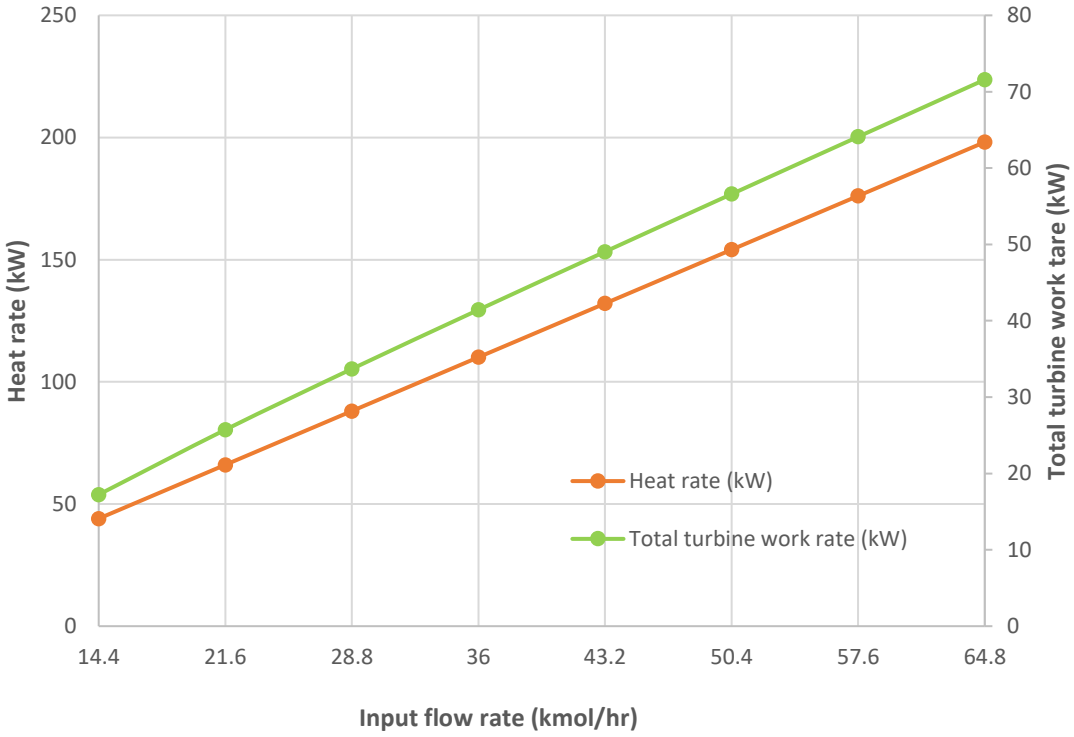

Figure 5.32 Effect of input flow rate on the heat duty and turbine work rate.

The specific work of low pressure pump (pump 2) and high pressure pump (pump 3) included in reverse osmosis desalination unit is compared with the previous study. Figure 5.33 displays the comparison of the current result and previous study in terms of the specific work of both pumps. The specific work is considered because both systems are dealing with different mass flow rates of water.

The results of the efficiencies of reverse osmosis desalination unit are compared with the previous study conducted on the same type of desalination unit. The energy and exergy efficiencies concluded in that previous study were 60.3% and 30% respectively. While the efficiencies found is this thesis are much closer and comparable to this study. The energy and exergy efficiencies of reverse osmosis desalination unit are found to be 62.86% and 29.69% respectively [87]. The comparison of the energy and exergy efficiencies of current results and previous study is plotted in Figure 3.34.

Figure 5.35 exhibits the effect of water flow rate circulating as a working fluid on the turbines work rates and the pump work rate consumed. It shows that with the increase

in water flow rate, the work rates of first and second turbine keeps on increasing in a proper sequence and work rate of the third turbine reduces a bit in the proper sequence. The work rate consumed by the pump keep on increasing continuously because when pump will be required to operate with high flow rate, it consumes more amount of work.

Stream S3 contains water and this stream leads towards hydrogen production Cu-Cl cycle. The number of moles of water entering from this stream will be effecting the hydrogen production because cycle shows that two moles of water are required to produce one mole of hydrogen. So the effect of water flow rate is studied on different parameters like work rate, heat duty and turbine inlet temperature and presented in Figure 5.36. By increasing the water flow rate, turbine inlet temperature decreases and this decreased temperature then results in decreasing the turbine work rate. While heat duty increases with the increase in the water flow rate because more water will absorb more heat and Cu-Cl cycle will also require more heat for higher hydrogen production.

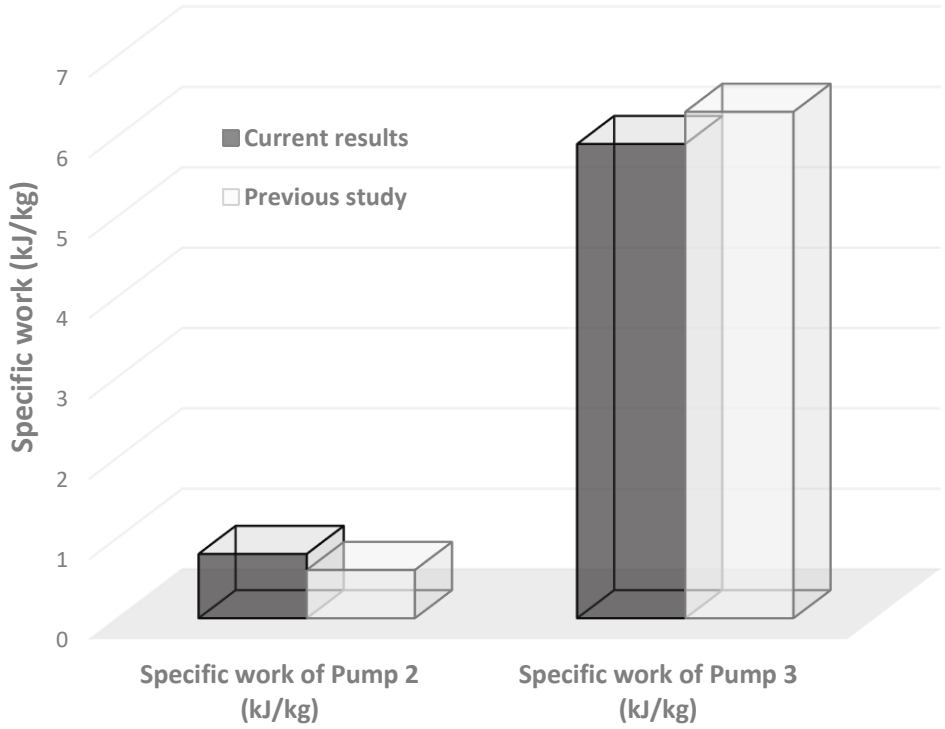

Figure 5.33 Comparison of specific work rates of desalination pumps with a previous study [87].

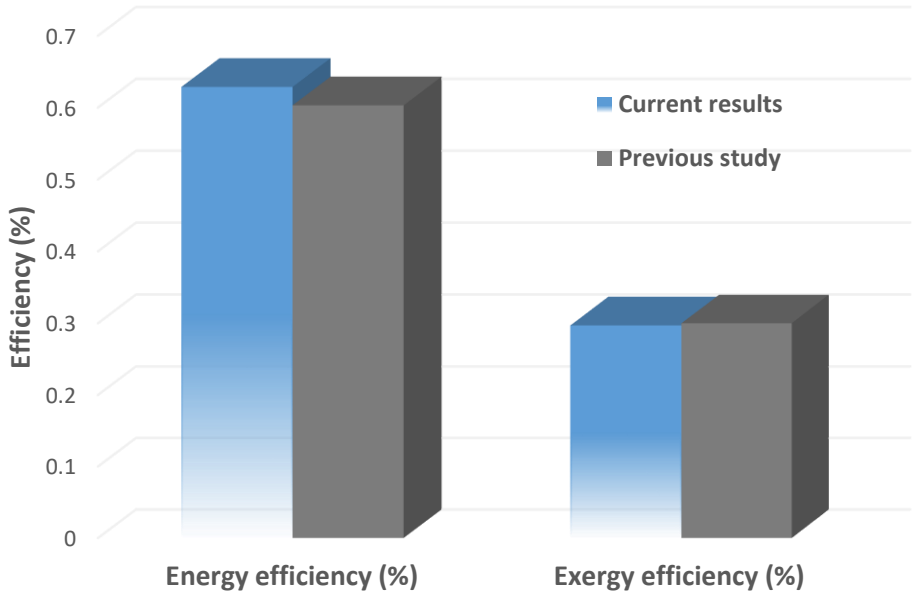

Figure 5.34 Comparison of energy and exergy efficiencies of reverse osmosis desalination unit with previous study.

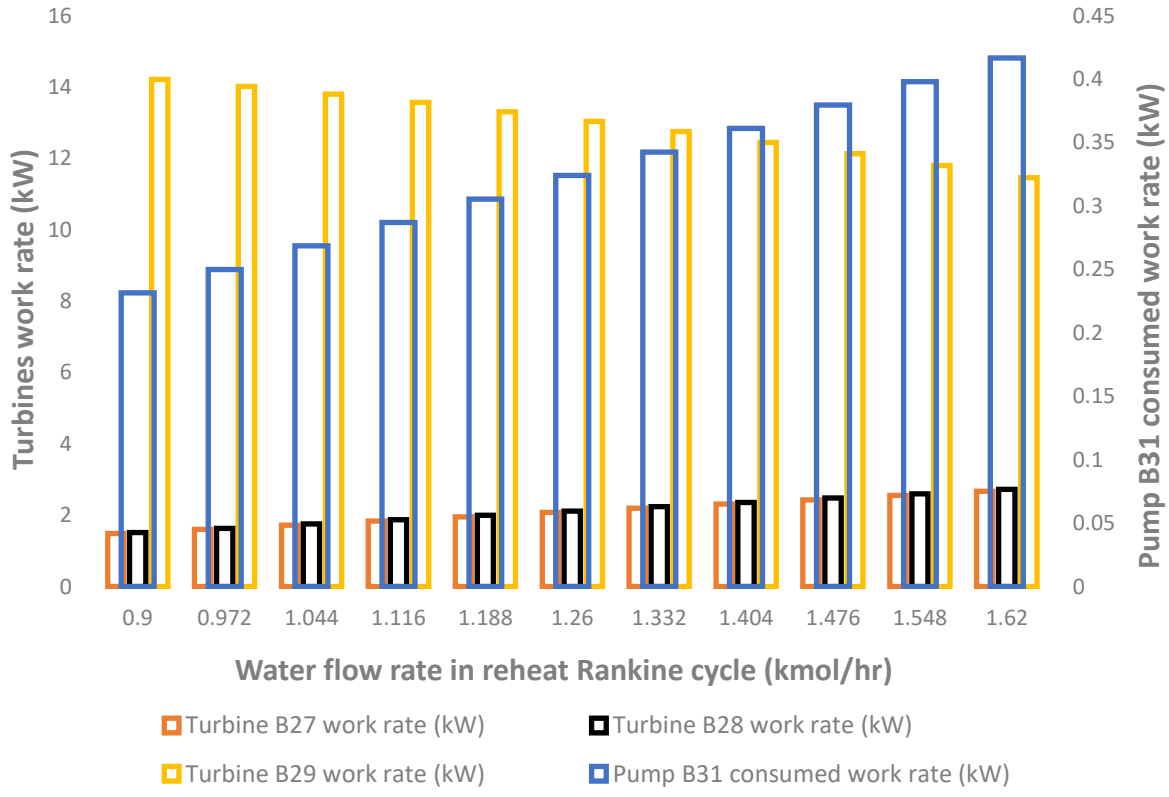

Figure 5.35 Effect of water flow rate on the turbine work rate and consumed work rate of pump.

The reverse osmosis unit integrated with the proposed system 3 is designed to produce 17.4 kg/s of fresh water having the salinity of 450 PPM and the salinity of sea water is 35000 PPM [88] and to achieve 17.4 kg/s of fresh water, 29 kg/s of sea water is supplied through the condenser. With this mass flow rate, fresh water can be supplied to a community of 1500 houses. The pressure of low pressure pump (pump 2) is set as 650 kPa and pressure of high pressure pump (pump 3) is provided as 6000 kPa [89]. The membrane recovery ratio is taken as 60% and to operate this mass flow rate, low pressure turbine consumes 18.42 kW of work and high pressure turbine absorbs 181 kW of work. Some parametric studies are conducted on the reverse osmosis desalination unit to see the variations with changing some parameters.

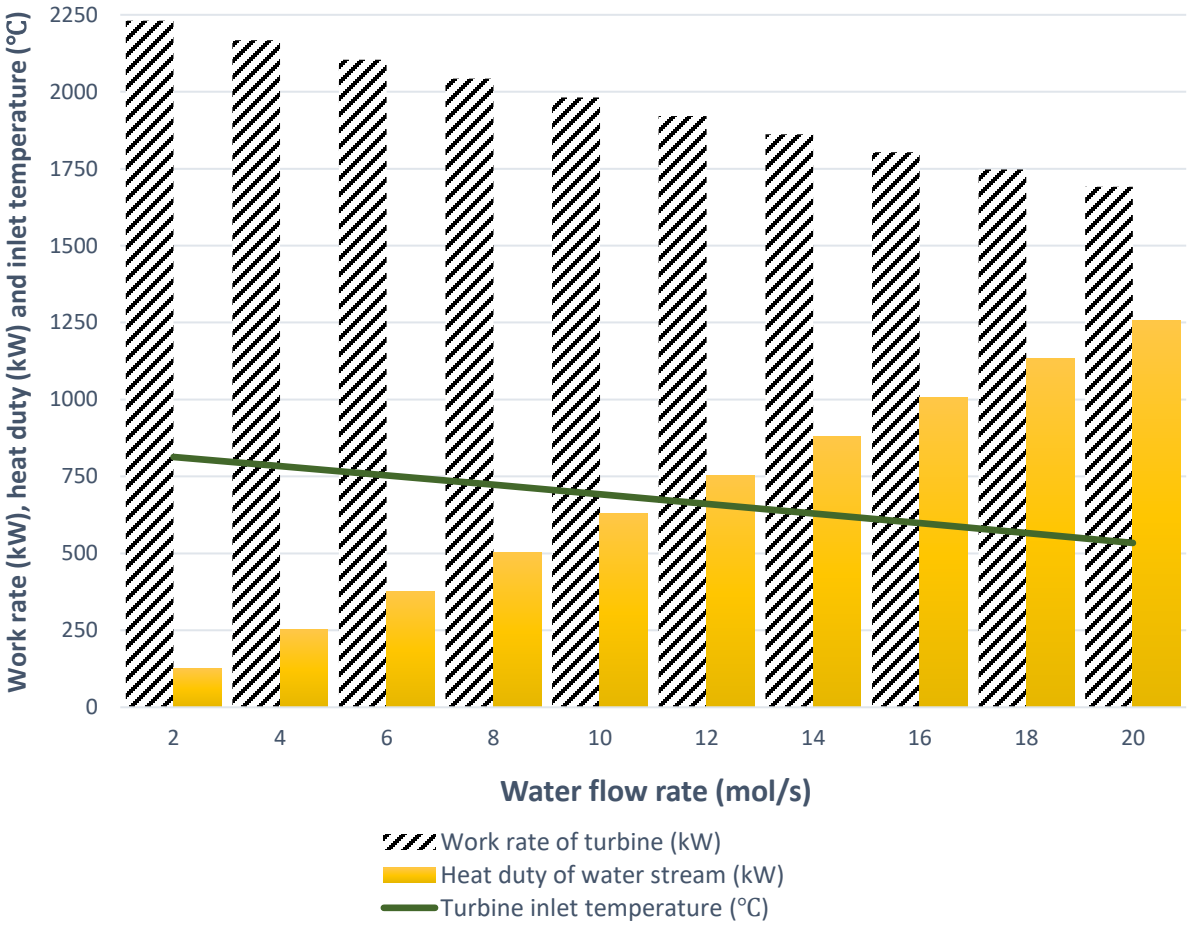

Figure 5.36 Variation in work rate, heat duty and turbine inlet temperature with respect to the water flow rate.

Figure 5.37 shows the effect of sea water temperature on low pressure and high pressure work rates. With the increase in sea water temperature, work rate of low pressure pump as well as work rate of high pressure pump increase continuously. The effect of pumps efficiency also effect the pump work rate. The Figure 5.38 represents the effect of pump efficiency on low pressure and high pressure pump work rates. Graph shows that with increase in the pump efficiency, the work rate consumption of both low pressure and high pressure pump decreases.

The work of the low pressure and high pressure pump included in reverse osmosis desalination unit highly depends upon the flow rate they deal with. In Figure 5.39, the work rates of low pressure and high pressure pump are plotted against the fresh water flow rate. The red line plotted in the graphs represents to the low pressure work with respect to the left side axis while blue line represents the work rate of high pressure pump with respect to the right axis. The work rates of both low pressure and high pressure pump increase continuously with increase in fresh water flow rate.

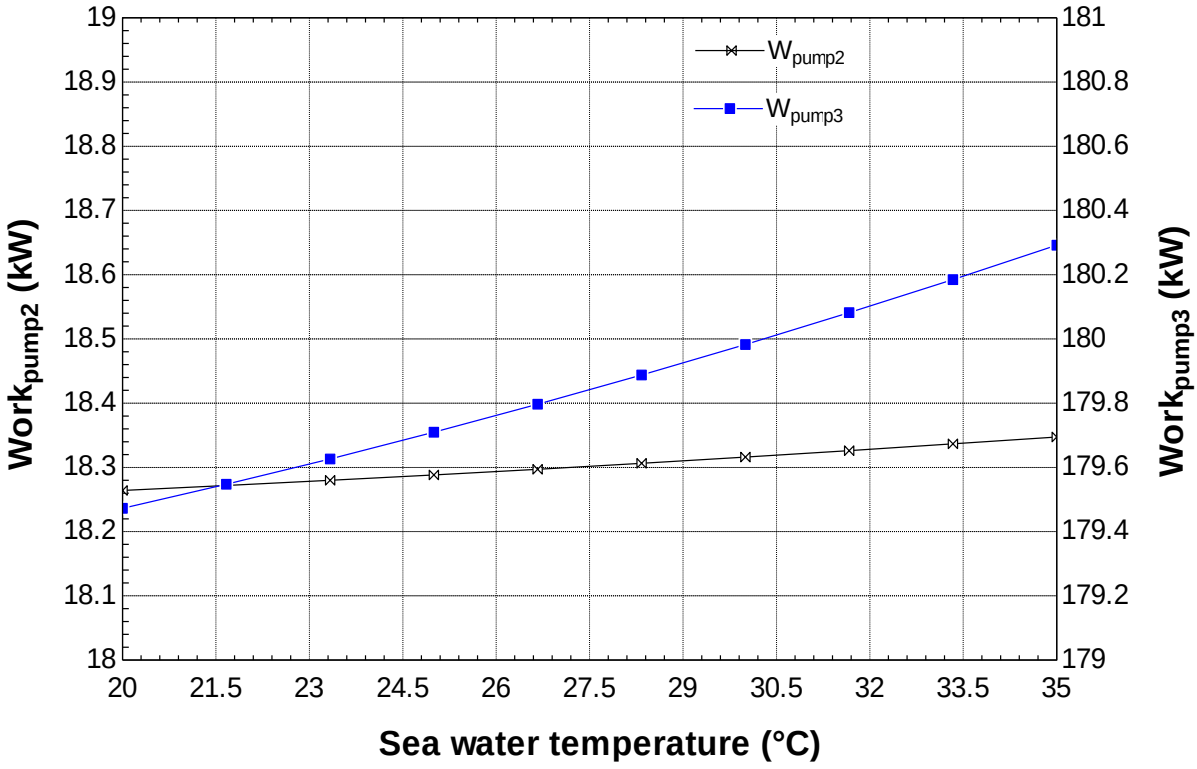

Figure 5.37 Effect of sea water temperature on low pressure and high pressure work rates.

The work rates of low pressure and high pressure pump depends upon the pump pressure as well. One study is conducted in order to see the effect of pump pressure on work rates of desalination unit pumps. The Figure 5.40 represents the effect of pressure of desalination unit pumps on their work rates. On one side of the graph, the work rate of low pressure pump is plotted against the different pressure ranges. While on the other side of the graph, the work rate of high pressure pump is plotted against the different pressure ranges to see its effect on work rate. So the work rate of both pumps keep on increasing with the increase in pressure.

Figure 5.41 shows the effect of sea water flow rate on the energy and exergy efficiency of reverse osmosis desalination unit. Energy efficiency of the desalination unit is plotted on one side while exergy efficiency is plotted on the other side of the graph. The flow rate of fresh water directly depends upon the supply of sea water. So the graph shows that with the increase in mass flow rate of the sea water, both energy and exergy efficiencies of reverse osmosis desalination unit decreases.

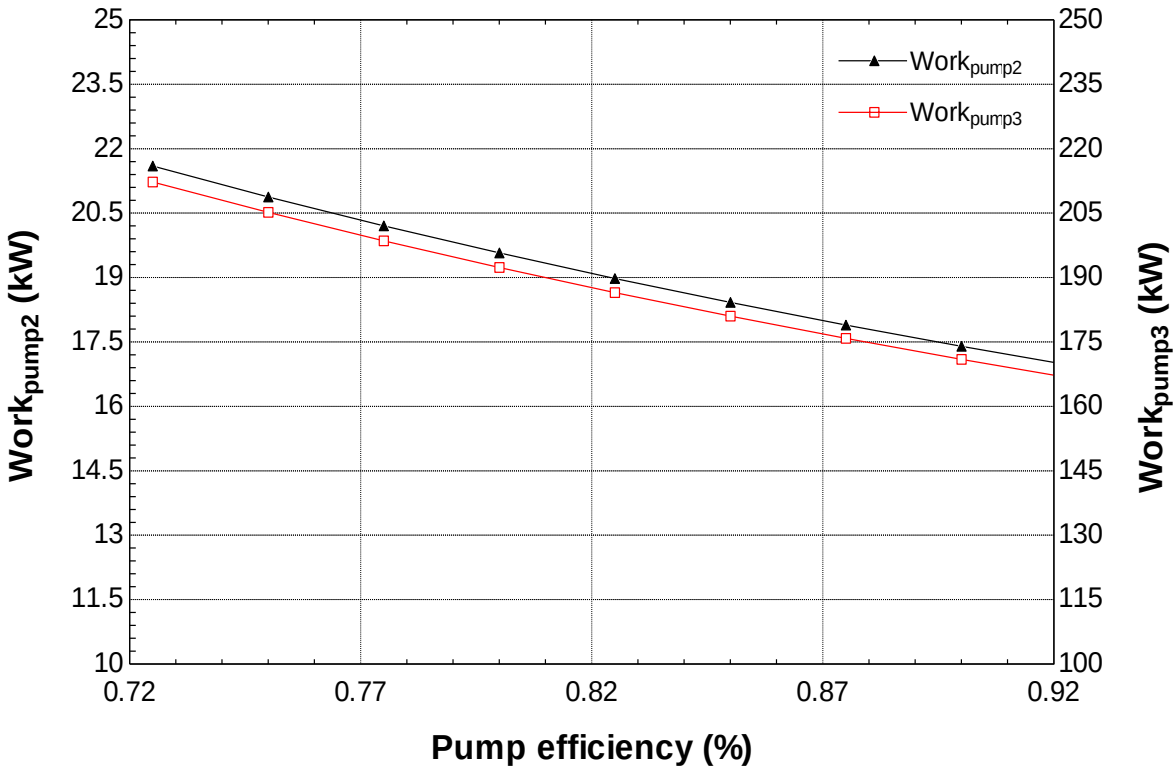

Figure 5.38 Effect of pump efficiency on low pressure and high pressure pump work rate.

The salinity of the sea water is considered as 35000 PPM [87]. The Figure 5.43 presents the effect of sea water salinity on the energy and exergy efficiency of the reverse osmosis desalination system. Figure shows that with the increase in sea water salinity, the energy efficiency of desalination unit increases while the exergy efficiency decreases with the increase in sea water salinity. The reason behind decrease in the exergy efficiency is that with the increase in sea water salinity, the exergy of the sea water increases while exergy of fresh water remains constant. Which results in increasing the overall exergy efficiency of the desalination unit.

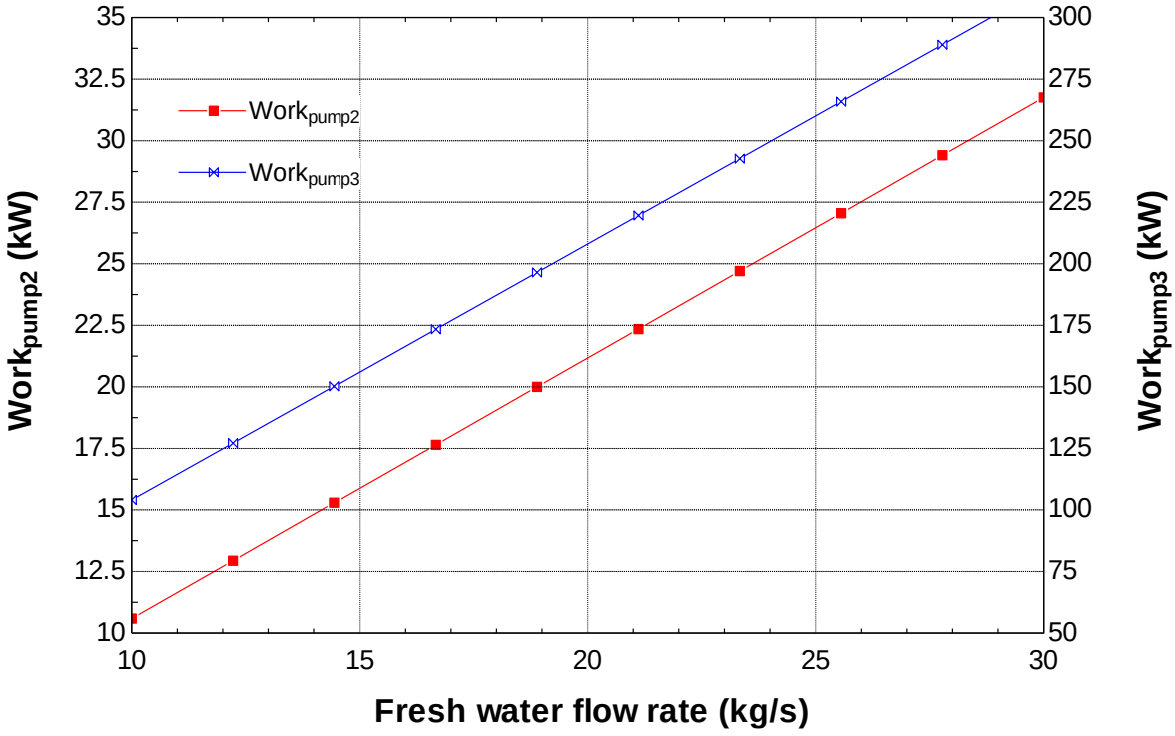

Figure 5.39 Effect of fresh water flow rate on the work rates of low pressure and high pressure pump.

The recovery ratio can be selected in the range of 0.6 to 0.7. A parametric study is established by varying the recovery ratio of the reverse osmosis desalination unit and to see its effect on the energy and exergy efficiency of the system. Figure 5.42 shows the effect of recovery ratio on the energy and exergy efficiency of desalination unit. So with the increase in recovery ratio, both energy and exergy efficiencies of the desalination unit increase.

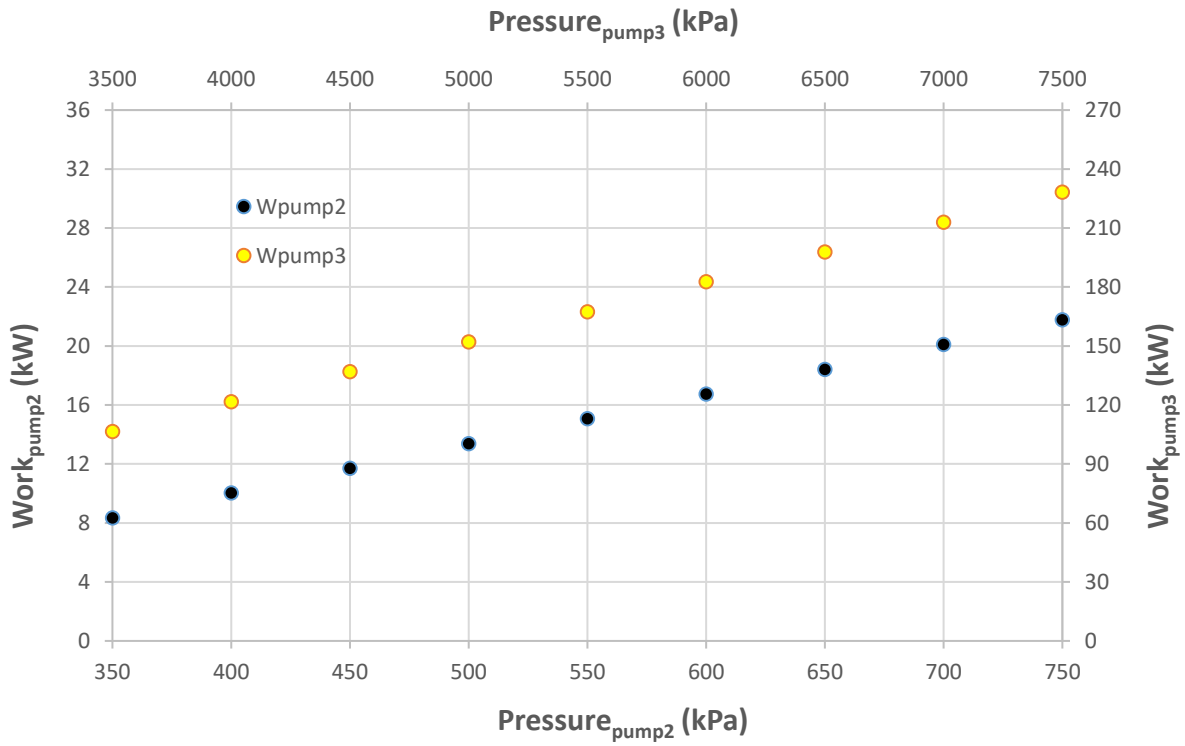

Figure 5.40 Variation in the work rates of pumps by changing the pressure ranges.

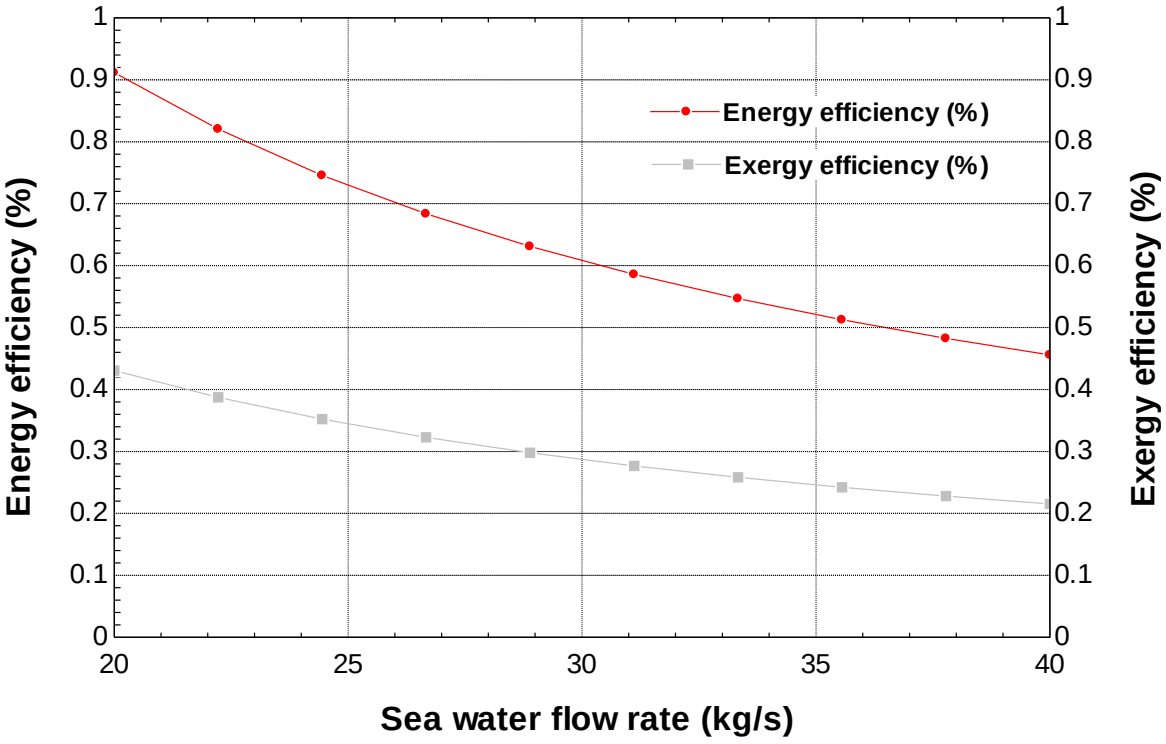

Figure 5.41 Effect of sea water flow rate on energy and exergy efficiency of reverse osmosis desalination unit.

The salinity of the fresh water also effects the overall energy and exergy efficiency of the reverse osmosis desalination unit. The Figure 5.44 represents the effect of fresh water salinity on the energy and exergy efficiency of the desalination unit. The salinity of the produced fresh water is 450 PPM so the range of salinity is considered from 400 to 500. The graph shows that with the increase in fresh water salinity, the exergy efficiency decreases very slightly which can be seen from the graph while energy efficiency decrease more slightly then the exergy efficiency which can be hardly noticed.

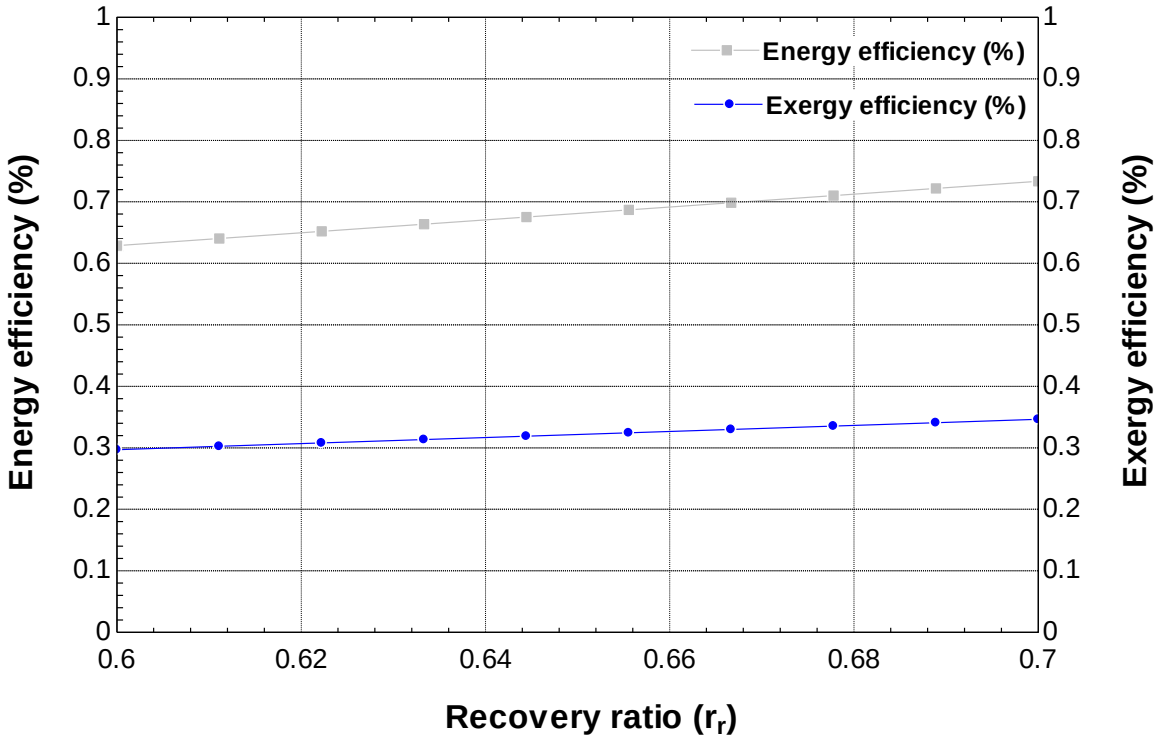

Figure 5.42 Effect of recovery ratio on energy and exergy efficiency of reverse osmosis desalination unit.

Figure 5.45 shows that with an increase in the ambient temperature, the energy efficiency of the reverse osmosis desalination unit remains constant while exergy efficiency decreases with the increase in ambient temperature.

In Figure 5.47, the exergy destruction rate, work rates and exergy efficiency of the work producing or consuming devices are presented [61]. The maximum exergy destruction rate and work rate takes place in pump B4 and maximum exergy efficiency belongs to the third compressor B22. The second highest exergy destruction rate and work rate occurs in third compressor B22 while second highest exergy efficiency belongs to

second compressor B21. The exergy destruction rate, exergy efficiency and work rates of other devices are also presented in Figure 5.47.

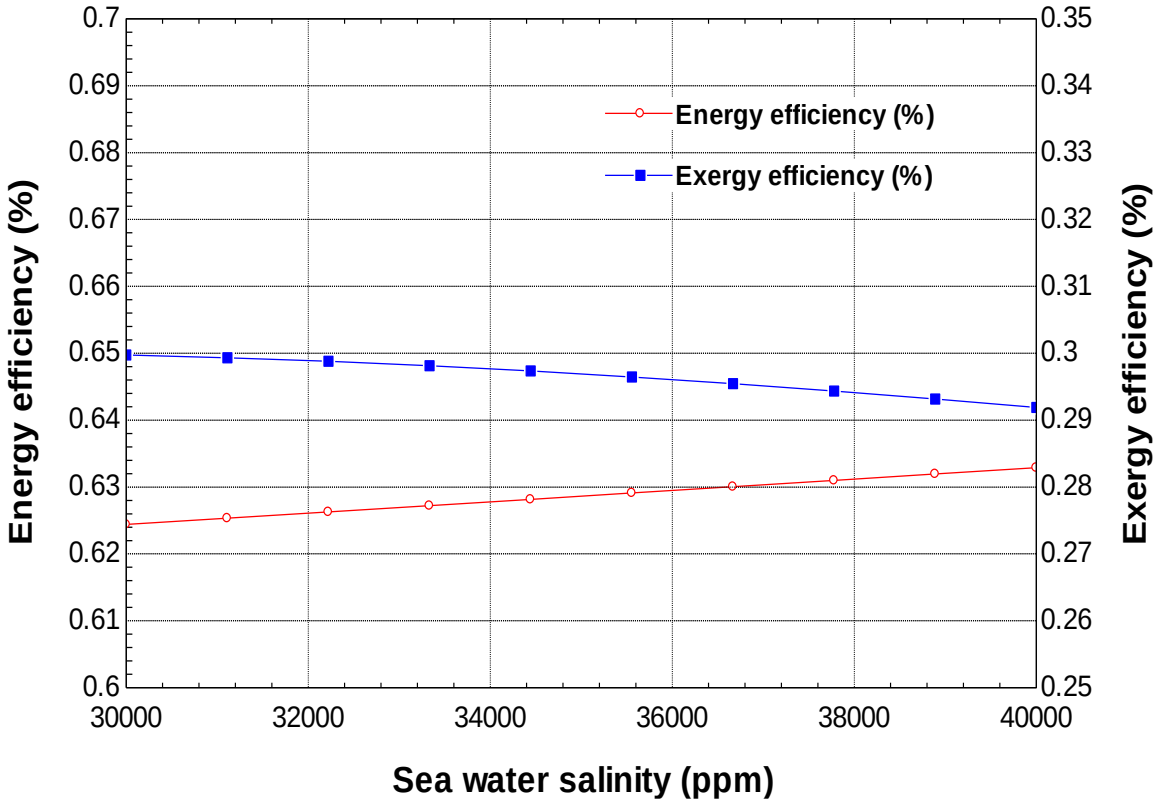

Figure 5.43 Effect of sea water salinity on exergy and exergy efficiency of reverse osmosis desalination unit.

The energy and exergy efficiencies of the subsystems of the proposed system 3 are presented in Figure 5.48. The energy efficiency of the Rankine cycle in system 3 is 28.97% and exergy efficiency is 31.23%. The energy efficiency of the multistage reheat Rankine cycle is 34.9% and exergy efficiency is 39.47%. And the energy efficiency of reverse osmosis desalination unit is 62.86% and exergy efficiency is 29.69%.

The hydrogen production rates of all three designed systems are plotted in Figure 5.49. The maximum hydrogen production is provided by the second system which is 140.8 kg/h. The second highest hydrogen production rate is offered by the first system and the rate is 64.8kg/h. The hydrogen production offered by the third system is 43.2 kg/h. A comparison of all three systems on the basis of hydrogen production is presented in Figure 5.49.

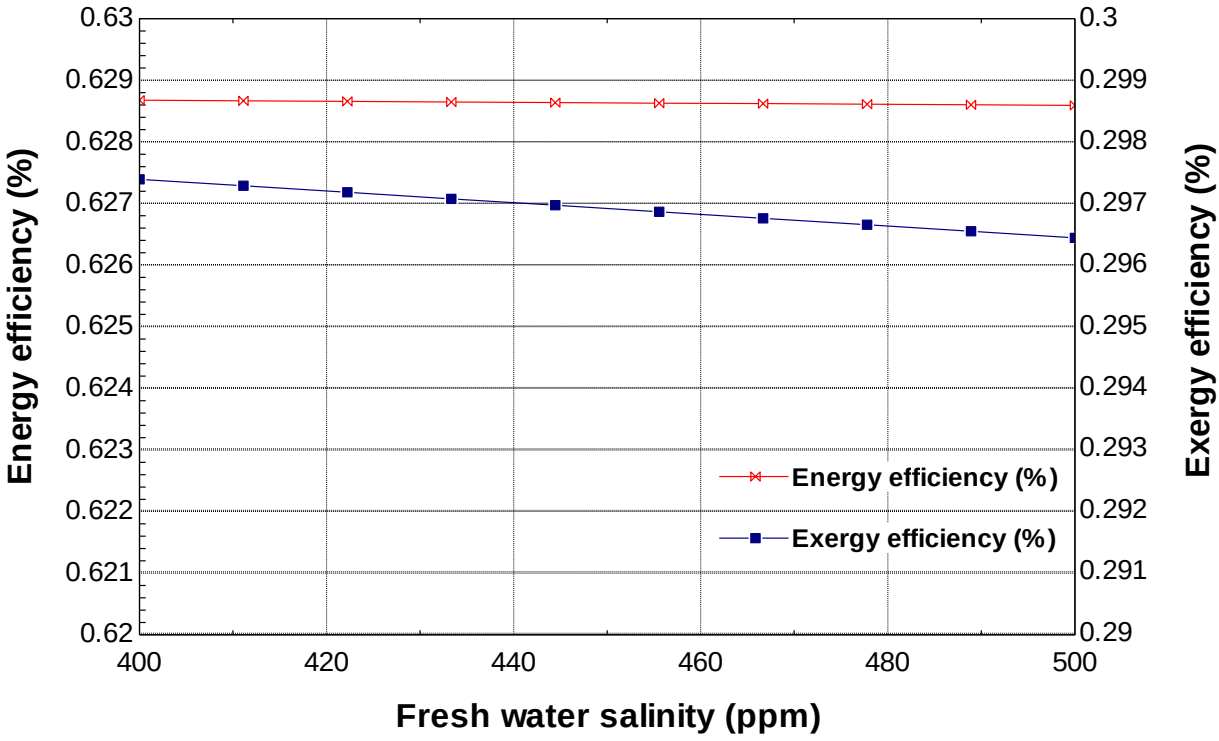

Figure 5.44 Effect of fresh water salinity on exergy and exergy efficiency of reverse osmosis desalination unit.

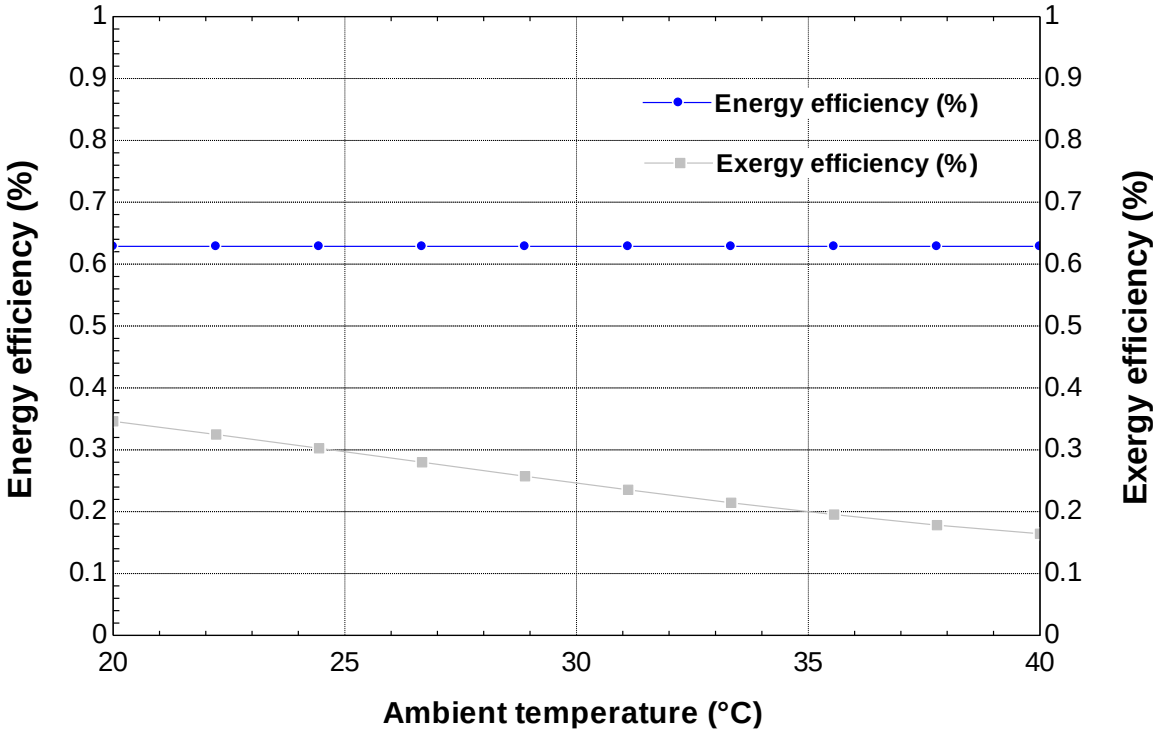

Figure 5.45 Effect of ambient temperature on exergy and exergy efficiency of reverse osmosis desalination unit.

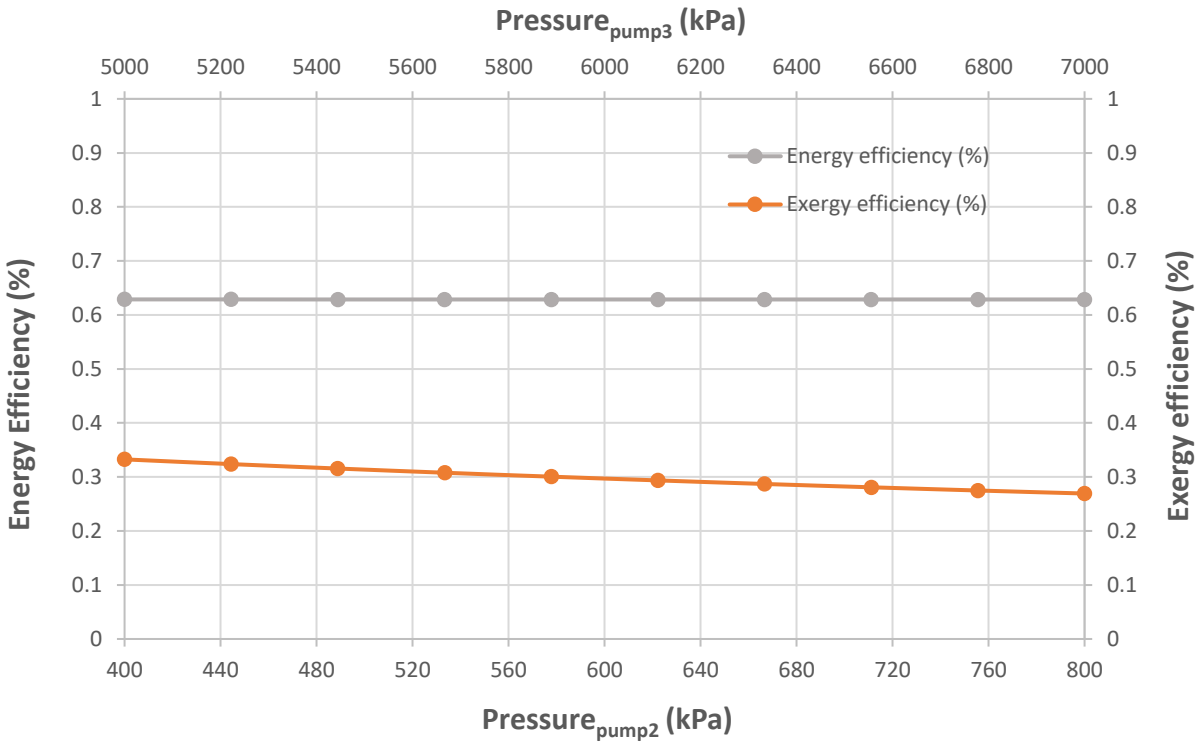

Figure 5.46 Effect of pressures of low pressure and high pressure pump on the energy and exergy efficiency.

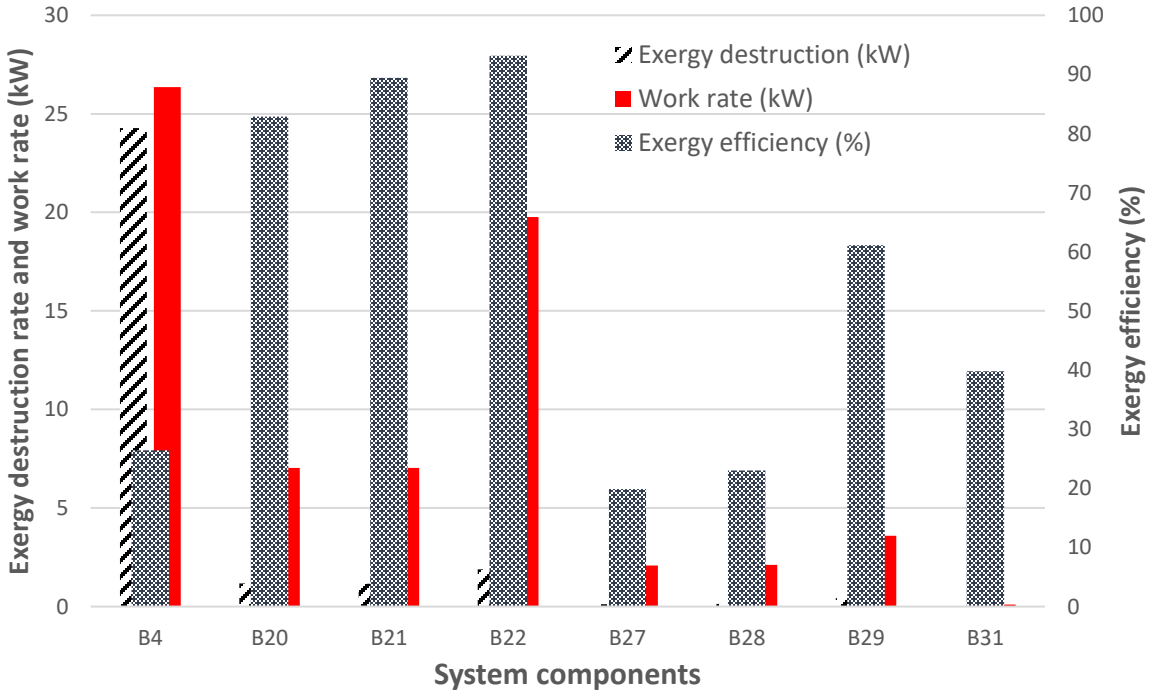

Figure 5.47 Exergy destruction rate, work rate and exergy efficiency of the work producing and consuming devices.

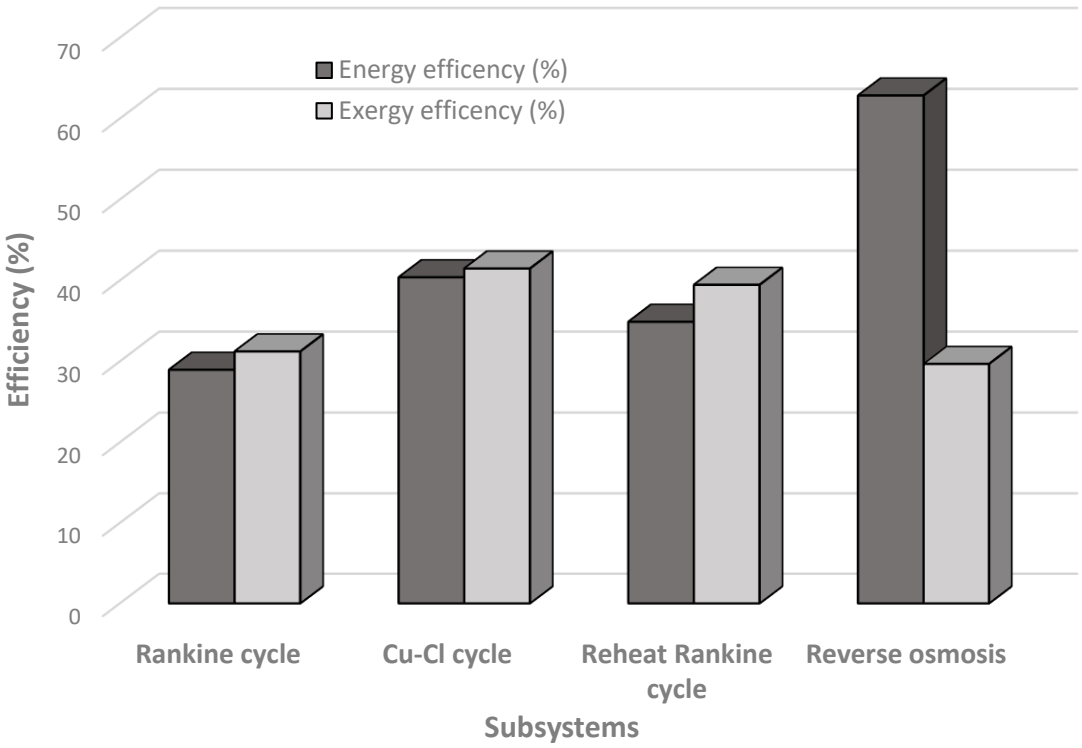

Figure 5.48 Energy and exergy efficiencies of the main subsystems of proposed system 3.

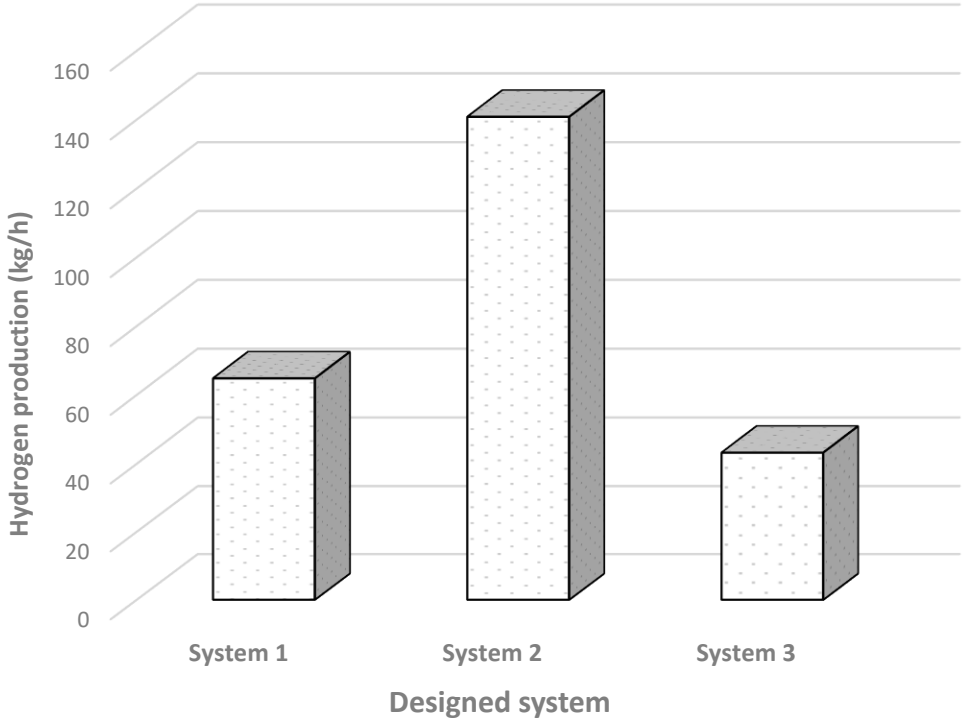

Figure 5.49 Comparison of all three systems on the basis of the hydrogen production.

The overall efficiencies of all the integrated systems are plotted in Figure 5.50. The energy efficiency of system 1 is calculated as 39.8% and the exergy efficiency is 40.5%. The energy efficiency of system 2 is 32.5% and exergy efficiency is 31.82% while the energy efficiency of system 3 is 48.6% and exergy efficiency is found to be 40.2%.

The exhaust heat ejected from the steel, cement and glass production processes is integrated with the Cu-Cl cycle to produce hydrogen. In Ontario, natural gas is commonly used for heating purposes, thus, this industrial heat available is compared with the heat provided by natural gas. The CO_2 emission calculations are conducted for one year of the operating period. In addition, CO_2 emissions are calculated for the amount of heat which is utilized. The CO_2 emissions can be avoided by utilizing this waste heat. The amount of CO_2 emissions which can be avoided by each system is presented in Figure 5.51. The maximum amount of reduced CO_2 emissions is obtained for system 2.

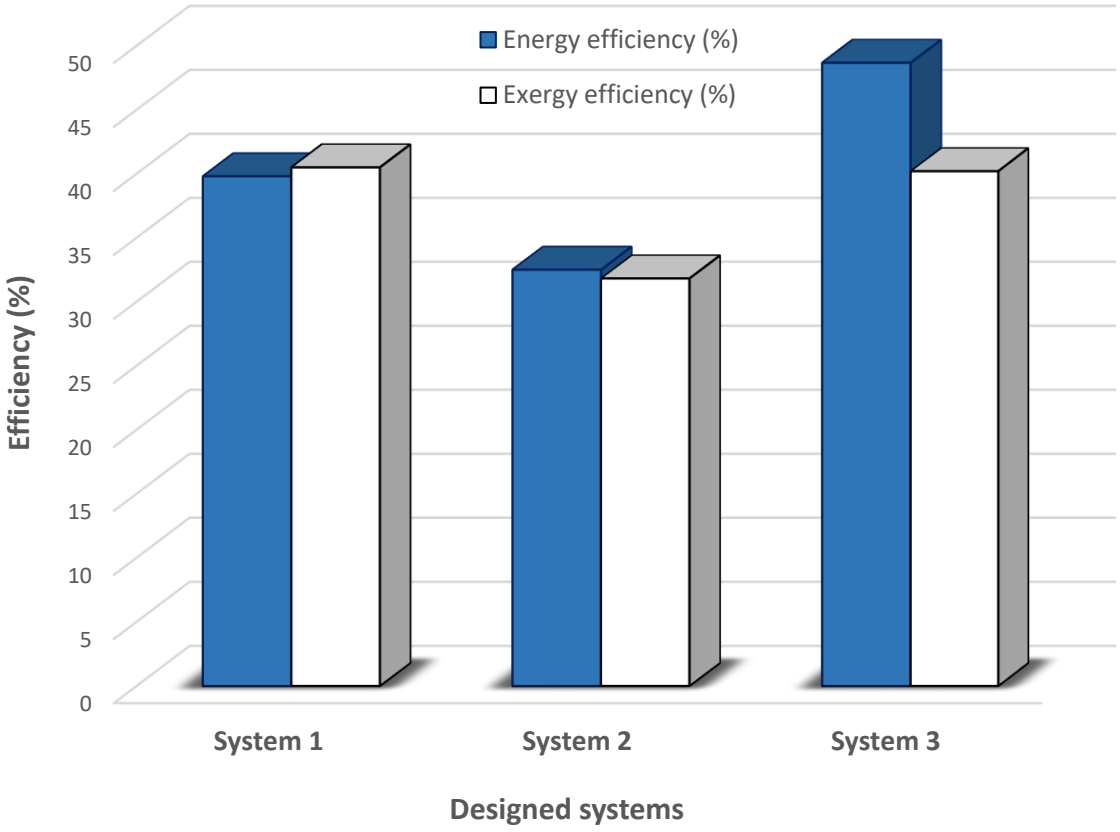

Figure 5.50 Energy and exergy efficiencies of all three hydrogen production systems.

In Ontario, natural gas for heating purposes is assumed to have a cost of 15.9 ¢/m^3. The cost calculations are conducted on a per year basis of the operating period. The industrial exhaust heat is compared with the cost of heat provided by natural gas. In addition, the cost is calculated for the amount of heat which is utilized. This cost can be saved by utilizing waste heat. The cost which can be saved by each system is presented in Figure 5.52. The maximum cost saved is by system 2 and then system 1.

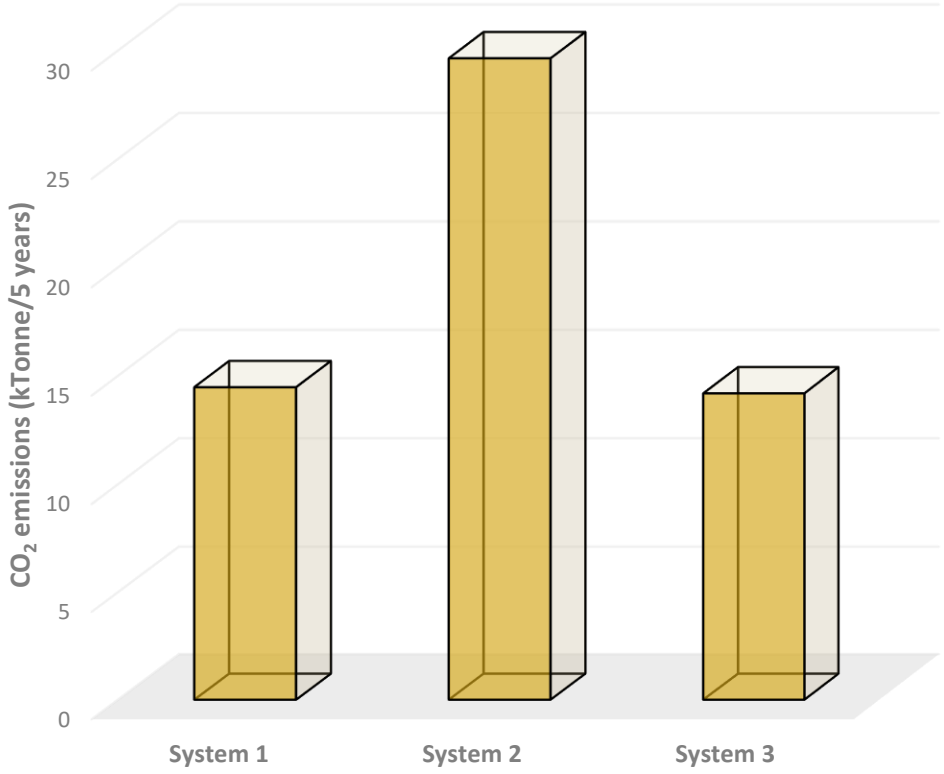

Figure 5.51 CO_2 emissions comparison of all three designed systems.

5.4 Model validation

The designed systems are conceptually validated though the first and second law of thermodynamics. All four (mass, energy, entropy and exergy) balances are applied on each component of the designed systems. No thermodynamic law is violated during the thermodynamic analysis of the designed systems. All the results of the subsystems are compared with the currently available experimental results and validated. Integrated systems recovering the industrial waste heat are designed in Aspen Plus software which is also a kind of validation.

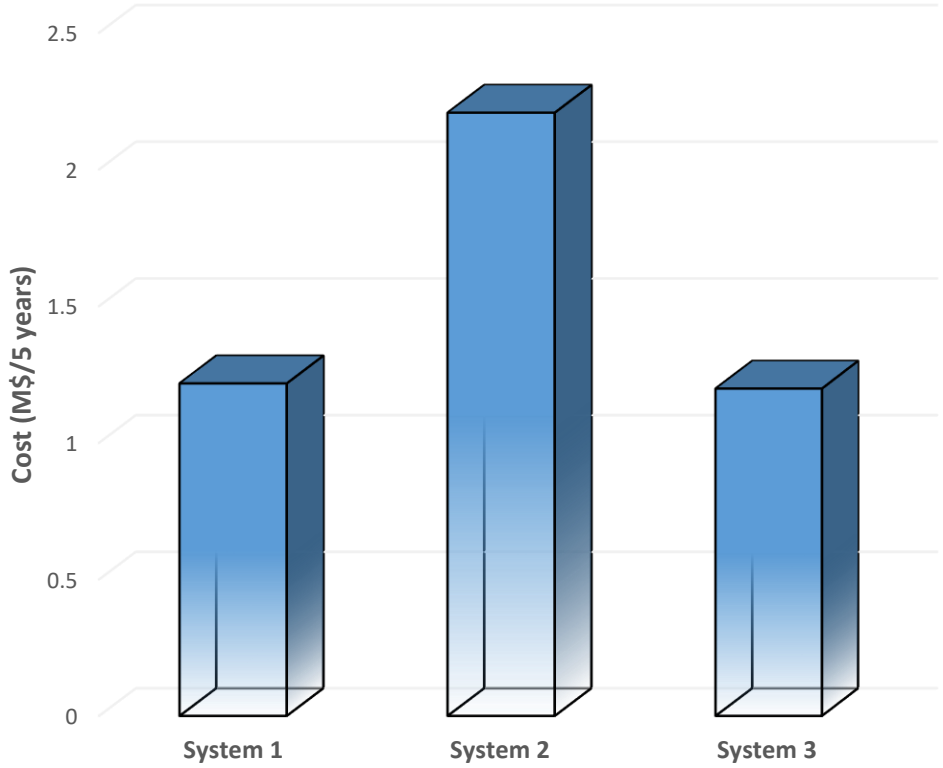

Figure 5.52 Cost comparison of all three designed systems.

The experimental results shows that increasing temperature of hydrolysis reactor results in increasing the production of CuCl as well with the production of Cu2OCl$_2$ by CuCl$_2$ conversion. Therefore, temperatures around 375°C and smaller particles are suggested for increasing the production of Cu$_2$OCl$_2$ by reacting CuCl$_2$ with H$_2$O to for the second generation reactor design. One more result was concluded that with the high flow rates of carrier gas, the formation of CuCl increases but increased mass transfer also results in increasing Cu$_2$OCl$_2$ production. The comparison of the experimental result with this simulated system is provided in Table 5.4.

Table 5.4 Comparison of the Cu-Cl cycle results with the experimental data.

Reference	3-step Cu-Cl cycle		4-step Cu-Cl cycle		5-step Cu-Cl cycle	
	η	ψ	η	ψ	η	ψ
Proposed system			40.4	41		
Lewis et al. (2009)	40.4					
Naterer et al (2009)			43			
Orhan et al. (2008)					43	7.9
Ferrandon et al. (2008)	39					

A comparison of the efficiencies of the thermochemical copper-chlorine (Cu-Cl) is conducted and validated through the previous studies. The thermochemical copper-chlorine cycle used in the designed system is analyzed energetically and exergetically and the overall energy and exergy efficiencies are compared with the past studies.

Chapter 6: Conclusions and Recommendations

Different industrial waste heat sources are integrated with hydrogen production Cu-Cl cycle and this study might help in the industrialization of the hydrogen production Cu-Cl cycle. This study developed, analyzed and evaluated the performance parameters of all three proposed hydrogen production systems utilizing different waste heat sources. Aspen plus modeling software and Engineering Equation Solver (EES) are used in order to perform the simulation and analysis of all three proposed systems. The overall performance assessment of all three hydrogen production systems highly relies on the energy and exergy efficiencies.

6.1 Conclusions

The developed systems are designed and integrated with different systems for hydrogen production, to demonstrate the potential of these designed systems in order to operate in a more environmentally benign manner. This research assessed and developed the performance of three proposed hydrogen production systems integrated with various waste heat sources utilizing the Cu-Cl cycle. The industrial waste heat sources are integrated with the thermochemical Cu-Cl cycle for hydrogen production in this thesis. The performance assessment of all of the three systems was based on the energy and exergy efficiencies. All of the three designed systems were simulated using Aspen Plus modeling software and EES.

The main findings extracted from this study are listed as follows:

- The waste heat of 7,876 kW carried by the flue gas from the steel heating furnace is recovered to produce 64.8 kg/h of hydrogen and 1.3 MW of electricity.
- Waste heat from the cement slag is utilized to produce heating and 140.8 kg/h of hydrogen.
- The exhaust gas from the glass melting furnace transfers 7,855 kW of heat to produce 42.3 kg/h of hydrogen, 1.8 MW of electricity and fresh water for a community of 1,500 houses.

- The overall energy efficiency of the system 1 is 39.8% and overall exergy efficiency is 40.5%.
- The energy efficiency of the system 2 is 32.5% and the exergy efficiency is found to be 31.82%.
- The energy efficiency of the system 3 is 48.6% and the exergy efficiency is found to be 40.2%.
- The compressed hydrogen production capacity of integrated system 1 is 64.8 kg/h, for system 2 it is 140.8 kg/h, and for system 3 it is 43.2 kg/h at 750 bar pressure.

6.2 Recommendations

In this study, three design concepts of hydrogen production system are proposed. All three proposed hydrogen production systems are analyzed, modeled and designed. The industrial waste heat is integrated with thermochemical hydrogen production cycle to produce clean hydrogen. A number of recommendations are made for the industrialization of Cu-Cl cycle on the basis of results of this study:

- Future studies should integrate more than one source of energy with thermochemical hydrogen production Cu-Cl cycle.
- Additional supporting systems in all three proposed systems contain the main part of exergy destruction of the overall systems.
- Some other systems providing the same purpose should be replaced with subsystems of designed systems in order to obtain more performance assessment.
- Further research should be conducted for experimental validation of the systems.
- Optimization of the designed systems should be considered in future studies.
- An exergoeconomic analysis and cost analysis should be conducted for the systems.
- Integrated systems with thermochemical cycle should consider a proper heat delivering and recovering method.
- A complete life cycle assessment should be performed on the systems proposed in this study which will help in the industrialization of thermochemical hydrogen production Cu-Cl cycle.

References

1. Dincer I. 2010. Global warming : engineering solutions. volume 31. Springer, London, New York.
2. Naterer GF, Dincer I, Zamfirescu C. 2013. Hydrogen production from nuclear energy. London, New York: Springer.
3. Dincer I, Zamfirescu C. 2011. Sustainable Energy Systems and Applications. Springer, London, New York.
4. World Energy Council. 2013. World Energy Resources: 2013 survey. World Energy Counc.:11.
5. Dincer I, Rosen M. 2003. Thermal energy storage systems and applications. Wiley second edition. Hoboken, New Jersey.
6. Acar C, Dincer I, Naterer GF. 2016. Review of photocatalytic water-splitting methods for sustainable hydrogen production. Int. J. energy Res.
7. Muradov NZ, Veziroglu TN. 2008. 'Green' path from fossil-based to hydrogen economy: An overview of carbon-neutral technologies. Int. J. Hydrogen Energy. 33:6804–6839.
8. Miller B. 2005. Coal Energy Systems. Elsevier Academic Press, Cambridge, Massachusetts.
9. IEA IEA. 2007. Tracking Industrial Energy Efficiency and CO2 Emissions. Energy Policy. 30:849–863.
10. Marys S, Bowmanville C. 2014. Application and Supporting Documentation for an Environmental Compliance Approval (Air) Amendment with Limited Operational Flexibility (LOF).
11. Choo CW. 1993. Environmental scanning: Acquisition and use of information by chief executive officers in the Canadian telecommunication industry.
12. Landolina S, Fernandez A. 2017. Global Iron & Steel Technology Roadmap.
13. Incorporated B. 2008. Waste Heat Recovery: Technology and Opportunities in U.S. Industry.
14. Canada. 2009. Canadian Cement industry energy benchmarking-Summary report.
15. Banerjee A, Rai A, Mohanty B, Varun A. 2017. Simulation of Combustion Space Heat Transfer of Glass Melting Furnace. Heat Transf. - Asian Res. 46:569–584.
16. Kumar S, Energy T. Waste Heat Recovery : Case study of Indian Glass Industry Sector (TERI), New Delhi , India Energy Consumption Pattern in India.
17. Jang JH, Lee DE, Kim MY, Kim HG. 2010. Investigation of the slab heating characteristics in a reheating furnace with the formation and growth of scale on the slab surface. Int. J. Heat Mass Transf. 53:4326–4332.

18. Taylor SW, Wang S. 2009. Overheating steel in an annealing furnace. AIP Conf. Proc. 1168, pp 1457–1460.

19. Brandt C, Schüler N, Gaderer M, Kuckelkorn JM. 2014. Development of a thermal oil operated waste heat exchanger within the off-gas of an electric arc furnace at steel mills. Appl. Therm. Eng. 66:335–345.

20. Pansuwan A, Smerpitak K, Ukakimaparn P. 2009. Temperature Estimation of Liquid Steel in Induction Furnace. Proceeding Int. MultiConference Eng. Comput. Sci. 2009. 2, pp 5–9.

21. Kim MY. 2007. A heat transfer model for the analysis of transient heating of the slab in a direct-fired walking beam type reheating furnace. Int. J. Heat Mass Transf. 50:3740–3748.

22. Gunarathne DS, Mellin P, Yang W, Pettersson M, Ljunggren R. 2016. Performance of an effectively integrated biomass multi-stage gasification system and a steel industry heat treatment furnace. Appl. Energy. 170:353–361.

23. Camdali U, Tunc M. 2006. Steady State Heat Transfer of Ladle Furnace During Steel Production Process. J. Iron Steel Res. Int. 13.

24. Si M. 2011. The feasibility of waste heat recovery and energy efficiency assessment in a steel plant.

25. Arzbaecher C, Fouche E, Parmenter K, Partners GE. 2007. Industrial Waste-Heat Recovery : Benefits and Recent Advancements in Technology and Applications Definition of Waste Heat for This Paper Quantity , Quality and Temporal Availability of Waste Heat Heat-Recovery Potential in US Manufacturing Industry.:1–13.

26. Luo S, Feng Y. 2016. The production of hydrogen-rich gas by wet sludge pyrolysis using waste heat from blast-furnace slag. Energy. 113:845–851.

27. Zhang Z, Chen L, Yang B, Ge Y, Sun F. 2015. Thermodynamic analysis and optimization of an air Brayton cycle for recovering waste heat of blast furnace slag. Appl. Therm. Eng. 90:742–748.

28. Dal Magro F, Savino S, Meneghetti A, Nardin G. 2017. Coupling waste heat extraction by phase change materials with superheated steam generation in the steel industry. Energy. 137:1107–1118.

29. Zhang H, Wang H, Zhu X, Qiu YJ, Li K, Chen R, Liao Q. 2013. A review of waste heat recovery technologies towards molten slag in steel industry. Appl. Energy. 112:956–966.

30. Esfahani S. 2016. Crystallization of Synthetic Blast Furnace Slags Pertaining to Heat Recovery Crystallization of Blast Furnace Slags Pertaining to Heat.

31. De Schutter G, Taerwe L. 1995. General hydration model for portland cement and blast furnace slag cement. Cem. Concr. Res. 25:593–604.

32. Reddy AS, Pradhan RK, Chandra S. 2006. Utilization of Basic Oxygen Furnace (BOF) slag in the production of a hydraulic cement binder. Int. J. Miner. Process. 79:98–105.

33. Han F, Zhang Z, Wang D, Yan P. 2015. Hydration heat evolution and kinetics of blended cement containing steel slag at different temperatures. Thermochim. Acta. 605:43–51.

34. Lin KL, Lin DF. 2006. Hydration characteristics of municipal solid waste incinerator bottom ash slag as a pozzolanic material for use in cement. Cem. Concr. Compos. 28:817–823.

35. Wang KS, Lin KL, Huang ZQ. 2001. Hydraulic activity of municipal solid waste incinerator fly-ash-slag-blended eco-cement. Cem. Concr. Res. 31:97–103.

36. Lin KL, Wang KS, Tzeng BY, Lin CY. 2003. The reuse of municipal solid waste incinerator fly ash slag as a cement substitute. Resour. Conserv. Recycl. 39:315–324.

37. Collier NC, Milestone NB, Gordon LE, Ko SC. 2014. The suitability of a supersulfated cement for nuclear waste immobilisation. J. Nucl. Mater. 452:457–464.

38. Lee TC, Wang WJ, Shih PY, Lin KL. 2009. Enhancement in early strengths of slag-cement mortars by adjusting basicity of the slag prepared from fly-ash of MSWI. Cem. Concr. Res. 39:651–658.

39. Barati M, Esfahani S, Utigard TA. 2011. Energy recovery from high temperature slags. Energy. 36:5440–5449.

40. Yoshida H, Nara Y, Nakatani G, Anazi T, Sato H. 1984. 'The technology of slag heat recovery at NKK,' presented at the SEAISI Conference of Energy Utilization in the Iron and Steel Industry.

41. Liu J, Yu Q, Zuo Z, Yang F, Duan W, and Qin Q. 2017. Blast furnace slag obtained from dry granulation method as a component in slag cement. 131.

42. Qin Y, Lv X, Bai C, Qiu G, Chen P. 2012. Waste heat recovery from blast furnace slag by chemical reactions. Jom. 64:997–1001.

43. Vilaplana AS, Ferreira VJ, Lopez-sabiron AM, Lausin-gonzalez C, Berganza-conde C. 2015. Utilization of Ladle Furnace slag from a steelwork for laboratory scale production of Portland cement. 94.

44. Neto JBF, Fredericci C, Faria JOG, Chotoli FF, Tiago R, Malynowskyj A, Silva ANL, Quarcioni VA, Lotto AA. 2016. Modification of Bof Slag for Cement Manufacturing.:847–854.

45. Praznik D. Manitoba , Canada Float Glass Project Feasibility Study.

46. Tapasa K, Jitwatcharakomol T. 2012. Thermodynamic calculation of exploited heat used in glass melting furnace. Procedia Eng. 32, pp 969–975.

47. Li Z, He X, Wang Y, Zhang B, He H. 2014. Design of a flat glass furnace waste heat power generation system. Appl. Therm. Eng. 63:290–296.

48. Butler JH, Hooper P. 2011. Glass Waste. Waste., pp 151–165.

49. Cassiano J, Heitor M V., Silva TF. 1994. Combustion tests on an industrial glass-melting furnace. Fuel. 73:1638–1642.

50. Mueller JR, Boehm MW, Drummond C. 2012. Direction of CRT waste glass processing: Electronics recycling industry communication. Waste Manag. 32:1560–1565.

51. Sardeshpande V, Gaitonde UN, Banerjee R. 2007. Model based energy benchmarking for glass furnace. Energy Convers. Manag. 48:2718–2738.

52. Buchholz A, Rodseth J. 2011. Investigation of Heat Transfer Conditions in a Reverberatory Melting Furnace by Numerical Modeling. Light Met. 2011., pp 1179–1184. doi:10.1002/9781118061992.ch199.

53. Mandal AK, Sen S, Mandal S, Guha C, Sen R. 2015. Energy Efficient Melting of Glass for Nuclear Waste Immobilization Using Microwave Radiation. Int. J. Green Energy. 12:1280–1287.

54. Katou K, Asou T, Kurauchi Y, Sameshima R. 2001. Melting municipal solid waste incineration residue by plasma melting furnace with a graphite electrode. Thin Solid Films. 386:183–188.

55. M. Costa J. Baltasar And M. G. Carvalho UV. 1996. Combustion measurements in an industrial glass-melting furnace. J. Inst. Energy.:80–86.

56. Dzyuzer VY, Minin SA, Alikina K V. 2017. Fume Heat Recovery Efficiency in High-Capacity Glassmaking Furnaces. Glas. Ceram. 74:165–168.

57. Sokolov BA, Abakin DA. 2017. Use of the Heat of Molten Glass Aided by Circulating Furnace Gases. Glas. Ceram. 74:278–281.

58. Yazawa K, Shakouri A, Hendricks TJ. 2017. Thermoelectric heat recovery from glass melt processes. Energy. 118:1035–1043.

59. Suleman F. 2014. Comparative Study of Various Hydrogen Production Methods for Vehicles . Available from http://ubc.summon.serialssolutions.com/2.0.0/

60. Gupta RB. 2009. Hydrogen Hydrogen. Fuel. Taylor & Francis Group, LLC, London New York.

61. Dincer I, Zamfirescu C. 2016. Sustainable hydrogen production. Elsevier, Amsterdam, Netherlands.

62. Al-Zareer M, Dincer I, Rosen MA. 2018. Assessment and analysis of hydrogen and electricity production from a Generation IV lead-cooled nuclear reactor integrated with a copper-chlorine thermochemical cycle. Int. J. Energy Res. 42:91–103.

63. Naterer GF, Dincer I, Zamfirescu C. 2013. Hydrogen Production from Nuclear

Energy. Springer Verlag, London New York.

64. Cetinkaya E, Dincer I, Naterer GF. 2012. Life cycle assessment of various hydrogen production methods. Int. J. Hydrogen Energy. 37:2071–2080.

65. Naterer GF, Suppiah S, Stolberg L, Lewis M, Wang Z, Dincer I, Rosen MA, Gabriel K, Secnik E, Easton EB, Pioro I, Lvov S, Jiang J, Mostaghimi J, Ikeda BM, Rizvi G, Lu L, Odukoya A, Spekkens P, Fowler M, Avsec J. 2013. Progress of international hydrogen production network for the thermochemical Cu-Cl cycle. Int. J. Hydrogen Energy. 38:740–759.

66. Ghandehariun S. 2012. Thermal Management of the Copper-Chlorine Cycle for Hydrogen Production: Analytical and Experimental Investigation of Heat Recovery From Molten Salt.

67. Orhan MF, Dincer I, Rosen MA. 2008. Thermodynamic analysis of the copper production step in a copper-chlorine cycle for hydrogen production. Thermochim. Acta. 480:22–29.

68. Dincer I, Naterer GF. 2014. Overview of hydrogen production research in the Clean Energy Research Laboratory (CERL) at UOIT. Int. J. Hydrogen Energy. 39:20592–20613.

69. Naterer GF, Suppiah S, Stolberg L, Lewis M, Ahmed S, Wang Z, Rosen MA, Dincer I, Gabriel K, Secnik E, Easton EB, Lvov SN, Papangelakis V, Odukoya A. 2014. Progress of international program on hydrogen production with the copper-chlorine cycle. Int. J. Hydrogen Energy. 39:2431–2445.

70. Ozbilen A, Dincer I, Rosen MA. 2016. Development of a four-step Cu-Cl cycle for hydrogen production - Part I: Exergoeconomic and exergoenvironmental analyses. Int. J. Hydrogen Energy. 41:7814–7825.

71. Naterer G, Suppiah S, Lewis M, Gabriel K, Dincer I, Rosen MA, Fowler M, Rizvi G, Easton EB, Ikeda BM, Kaye MH, Lu L, Pioro I, Spekkens P, Tremaine P, Mostaghimi J, Avsec J, Jiang J. 2009. Recent Canadian advances in nuclear-based hydrogen production and the thermochemical Cu-Cl cycle. Int. J. Hydrogen Energy. 34:2901–2917.

72. Naterer GF, Suppiah S, Stolberg L, Lewis M, Wang Z, Daggupati V, Gabriel K, Dincer I, Rosen MA, Spekkens P, Lvov SN, Fowler M, Tremaine P, Mostaghimi J, Easton EB, Trevani L, Rizvi G, Ikeda BM, Kaye MH, Lu L, Pioro I, Smith WR, Secnik E, Jiang J, Avsec J. 2010. Canada's program on nuclear hydrogen production and the thermochemical Cu-Cl cycle. Int. J. Hydrogen Energy. 35:10905–10926.

73. Wang ZL, Naterer GF, Gabriel KS, Gravelsins R, Daggupati VN. 2009. New Cu-Cl thermochemical cycle for hydrogen production with reduced excess steam requirements. Int. J. Green Energy. 6:616–626.

74. Naterer GF. 2008. Second Law viability of upgrading waste heat for thermochemical hydrogen production. Int. J. Hydrogen Energy. 33:6037–6045.

75. Orhan MF, Dincer I, Rosen MA. 2011. Design of systems for hydrogen production

based on the Cu-Cl thermochemical water decomposition cycle: Configurations and performance. Int. J. Hydrogen Energy. 36:11309–11320.

76. Wang ZL, Naterer GF, Gabriel KS, Gravelsins R, Daggupati VN. 2009. Comparison of different copper-chlorine thermochemical cycles for hydrogen production. Int. J. Hydrogen Energy. 34:3267–3276.

77. Ozbilen A, Dincer I, Rosen MA. 2011. A comparative life cycle analysis of hydrogen production via thermochemical water splitting using a Cu-Cl cycle. Int. J. Hydrogen Energy. 36:11321–11327.

78. Balashov VN, Schatz RS, Chalkova E, Akinfiev NN, Fedkin M V., Lvov SN. 2011. CuCl Electrolysis for Hydrogen Production in the Cu–Cl Thermochemical Cycle. J. Electrochem. Soc. 158:B266.

79. Ozbilen A, Dincer I, Rosen MA. 2012. Life cycle assessment of hydrogen production via thermochemical water splitting using multi-step Cu-Cl cycles. J. Clean. Prod. 33:202–216.

80. Naterer G, Suppiah S, Lewis M, Gabriel K, Dincer I, Rosen MA, Fowler M, Rizvi G, Easton EB, Ikeda BM, Kaye MH, Lu L, Pioro I, Spekkens P, Tremaine P, Mostaghimi J, Avsec J, Jiang J. 2009. Recent Canadian advances in nuclear-based hydrogen production and the thermochemical Cu-Cl cycle. Int. J. Hydrogen Energy. 34:2901–2917.

81. Zamfirescu C, Naterer GF, Dincer I. 2011. Vapor compression CuCl heat pump integrated with a thermochemical water splitting cycle. Thermochim. Acta. 512:40–48.

82. Jaber O, Naterer GF, Dincer I. 2010. Heat recovery from molten CuCl in the Cu-Cl cycle of hydrogen production. Int. J. Hydrogen Energy. 35:6140–6151.

83. Ferrandon MS, Lewis MA, Tatterson DF, Gross A, Doizi D, Croizé L, Dauvois V, Roujou JL, Zanella Y, Carles P. 2010. Hydrogen production by the Cu-Cl thermochemical cycle: Investigation of the key step of hydrolysing CuCl2to Cu2OCl2and HCl using a spray reactor. Int. J. Hydrogen Energy. 35:992–1000.

84. Jaber O, Naterer GF, Dincer I. 2010. Heat recovery from molten CuCl in the Cu-Cl cycle of hydrogen production. Int. J. Hydrogen Energy. 35:6140–6151.

85. Al-Zareer M, Dincer I, Rosen MA. 2017. Performance analysis of a supercritical water-cooled nuclear reactor integrated with a combined cycle, a Cu-Cl thermochemical cycle and a hydrogen compression system. Appl. Energy. 195:646–658.

86. Naterer GF, Gabriel K, Wang ZL, Daggupati VN, Gravelsins R. 2008. Thermochemical hydrogen production with a copper-chlorine cycle. I: oxygen release from copper oxychloride decomposition. Int. J. Hydrogen Energy. 33:5439–5450.

87. Siddiqui O, Dincer I. 2018. Examination of a new solar-based integrated system for desalination, electricity generation and hydrogen production. Sol. Energy. 163:224–

234.

88. Khalid F, Dincer I, Rosen MA. 2016. Analysis and Assessment of a Gas Turbine-Modular Helium Reactor for Nuclear Desalination. J. Nucl. Eng. Radiat. Sci. 2:31014.

89. Islam S, Dincer I, Yilbas BS. 2018. Development of a novel solar-based integrated system for desalination with heat recovery. Appl. Therm. Eng. 129:1618–1633.

90. Orhan MF. 2011. Conceptual design analysis and optimization of nuclear-based hydrogen production via cupper-chlorine thermochemical cycles.

91. Ozturk M, Dincer I. 2013. Thermodynamic assessment of an integrated solar power tower and coal gasification system for multi-generation purposes. Energy Convers. Manag. 76:1061–1072.

92. Glasser FP 1997. 1997. Fundamental aspects of cement solidification and stabilization. J. Hazard. Mater. 52: 151 – 170. 52:1997.

93. Hosseini M, Dincer I, Naterer GF, Rosen MA. 2012. Thermodynamic analysis of filling compressed gaseous hydrogen storage tanks. Int. J. Hydrogen Energy. 37:5063–5071.

94. Al-Zareer M. 2016. Conceptual Development and Analysis of Multiple Integrated Hydrogen Production Plants with Cu-Cl Cycle.

95. Cengel YA, Boles MA. 2015. Thermodynamics: an Engineering Approach 8th Edition. McGraw-Hill.

96. Almahdi M. 2016. Integrated Heat Pump Options for Heat Upgrading in Cu-Cl Cycle for Hydrogen Production.

97. Al-Zareer M, Dincer I, Rosen MA. 2017. Development of an integrated system for electricity and hydrogen production from coal and water utilizing a novel chemical hydrogen storage technology. Fuel Process. Technol. 167:608–621.

98. Ozbilen AZ. 2013. Development, analysis and life cycle assessment of integrated systems for hydrogen production based on the copper-chlorine (Cu-Cl) cycle. Univ. Ontario Inst. Technol.:PhD Thesis. doi:10.1073/pnas.0703993104.

99. Nguyen-Schäfer H. 2012. Rotordynamics of Automotive Turbochargers. Springer.

100. JM C. 1984. Gas Conditioning and Processing: The equipment modules. Campbell Petroleum Series.

101. Dincer I, Rosen MA. 2013. Exergy: Energy, Environment And Sustainable Development. second edition. Elsevier, Amsterdam, Netherlands.